Distribution Agreement

In presenting this thesis of dissertation as a partial fulfillment of the requirements for an advanced degree from Emory University, I hereby grant to Emory University and its agents the non-exclusive license to archive, make accessible, and display my thesis or dissertation in whole or in part in all forms of media, now or hereafter known, including display on the world wide web. I understand that I may select some access restrictions as part of the online submission of this thesis or dissertation. I retain all ownership rights to the copyright of the thesis or dissertation. I also retain the right to use in future works (such as articles or books) all or part of this thesis or dissertation.

Signature:

_____   _____
Seyed A. Safavynia   Date

Spatiotemporal organization of muscle activity throughout human postural responses

By

Seyed A. Safavynia
Doctor of Philosophy

Graduate Division of Biological and Biomedical Science
Neuroscience

Lena H. Ting, Ph.D.
Advisor

Ron Calabrese, Ph.D.
Committee Member

T. Richard Nichols, Ph.D.
Committee Member

Randy Trumbower, P.T., Ph.D.
Committee Member

Steve Wolf, P.T., Ph.D.
Committee Member

Accepted:

Lisa A. Tedesco, Ph.D.
Dean of the Graduate School

Date

Spatiotemporal organization of muscle activity throughout human postural responses

By

Seyed A. Safavynia
B.S., Georgia Institute of Technology, 2002

Advisor: Lena H. Ting, Ph.D.

An abstract of
A dissertation submitted to the Faculty of the Graduate School of Emory
University in partial fulfillment of the requirements for the degree of
Doctor of Philosophy

Graduate Division of Biological and Biomedical Science
Neuroscience

2012

Abstract

Spatiotemporal organization of muscle activity throughout human postural responses

By Seyed A. Safavynia

Falls are the leading cause of morbidity and mortality among the elderly and result from a failure of the nervous system to appropriately coordinate muscles to maintain balance. Because muscle activity represents the output of the nervous system, examining muscle activation may reveal differences in neural mechanisms underlying falls; however, there is enormous spatial and temporal variability in muscle activation patterns, making them difficult to functionally interpret. Recent work has demonstrated that the spatial and temporal features of muscle activity can be functionally yet separately explained by muscle synergies and task-level feedback, respectively. The spatial coordination of muscles has been functionally characterized in a variety of motor tasks using muscle synergies, or groups of muscles with fixed ratios of coactivation. However, the temporal recruitments of such muscle synergies as well as the underlying neural mechanisms have largely been uninvestigated. Conversely, temporal activation of individual muscles throughout postural responses has been functionally characterized using task-level feedback of center of mass (CoM). However, CoM feedback has only been applied to perturbations where the body starts from rest and CoM kinematics (displacement, velocity, acceleration) are highly correlated.

I hypothesize that the nervous system continuously uses task-level feedback of CoM to recruit muscle synergies throughout standing balance tasks. Here, I unified the

muscle synergy hypothesis with task-level feedback to functionally explain the spatiotemporal features of muscle activity throughout human postural responses. I first demonstrated that the temporal recruitment of muscle synergies throughout discrete sagittal perturbations could be well-reconstructed using delayed feedback of CoM. I then developed complex perturbations to test the robustness of delayed CoM feedback on muscle activity and muscle synergy recruitment. Delayed feedback of CoM was shown to robustly modulate muscle activity throughout continuous sagittal perturbations that decouple CoM kinematics in magnitude. Moreover, delayed feedback of CoM was shown to robustly modulate muscle synergy recruitment throughout multidirectional discrete and biphasic perturbations that decouple CoM kinematics from each other in direction. These results suggest that a consistent spatial and temporal structure of motor outputs exists across static and dynamic states. Such an organization may aid in functionally identifying pathologic strategies for maintaining balance.

Spatiotemporal organization of muscle activity throughout human postural responses

By

Seyed A. Safavynia
B.S., Georgia Institute of Technology, 2002

Advisor: Lena H. Ting, Ph.D.

A dissertation submitted to the Faculty of the Graduate School of Emory University in partial fulfillment of the requirements for the degree of Doctor of Philosophy

Graduate Division of Biological and Biomedical Science
Neuroscience

2012

Acknowledgements

The work presented in this dissertation would not have been possible had it not been for the unfaltering support of a number of people. First, I would like to thank my advisor, Lena H. Ting, for teaching me what it means to be a true scientist. She has taught me how to formulate scientific questions, design experiments, and think independently and critically. Lena has always been a generous mentor; she has always made time to discuss science with me, motivated me to succeed independently, and supported my scientific, professional, and personal pursuits. I can't thank her enough for the education she has given me, and I have greatly appreciated her guidance and friendship. I would also like to thank the members of my thesis committee, Ron Calabrese, T. Richard Nichols, Randy Trumbower, and Steve Wolf, for their outstanding mentorship throughout my graduate career. In particular, I would like to thank Richard Nichols and Steve Wolf for their guidance in formulating an appropriate scientific question for my thesis. I have truly appreciated their expertise as it has greatly strengthened the quality of my work.

I thank the current and former members of my lab for generously devoting their time to help me succeed in my graduate career. I thank Nate Bunderson, Julia Choi, Kyla Ross, Hongchul Sohn, and Keith van Antwerp for their insightful comments and suggestions for data analysis. I thank Gelsy Torres-Oviedo and Torrence D. J. Welch for their role in developing the muscle synergy analysis and the feedback model, respectively; I have used their outstanding work as a foundation to build my PhD dissertation upon. I thank J. Lucas McKay for guiding me along the scientific process and helping me see the merit in my work, even when I didn't think I could continue. I cannot thank Jeff Bingham enough for helping me solve any technical problem I have ever had in the lab and for helping me understand a variety of complex mathematical techniques. A lot of experiments and analyses went smoother thanks to the help of an undergraduate student, D. Joseph Jilk; it has truly been a pleasure to mentor him and watch him grow as a researcher. Lastly, I thank Stacie Chvatal for her unending support as a researcher and as a friend. She has always led me to answer more interesting questions and has helped me hone my scientific intuitions. Her insight, determination, and work ethic have both humbled me and inspired me to be a better scientist.

I have been fortunate enough to have an abundance of mentors outside of the laboratory. I thank Marie Csete for being everything a mentor should be – someone whom I aspire to emulate professionally and personally. She has taught me that it is possible to be an outstanding scientist, clinician, administrator, entrepreneur, and musician. She has constantly pushed me to improve myself in every challenge I have faced, whether scientific, artistic, or ethical. I am grateful for her generous support and honored to have a teacher and friend with such strong character. I also thank Tris Parslow and Carolyn Katzen for their guidance, advice, and friendship throughout my graduate career. They have kept me aware of my ideals, focused on my aspirations, and have been supportive of all of my endeavors.

Aside from my scientific work, I would also alike to thank a group of compassionate individuals who have encouraged me to continue my musical interests. I thank Gail Starr

for pushing me to compose, even when I thought I didn't have time; she has kept me well-balanced and fulfilled throughout many challenging times. I thank Stephen Slater for introducing me to a plethora of great musicians and for constantly promoting my work in new circles. I cannot thank Justin Bruns enough for believing in my musical abilities and for giving me unparalleled musical outlets to express myself. He has always treated me as an equal, and I have felt nothing less than esteemed in his presence. Our conversations have enriched and improved my artistry to a level that I did not think was possible while pursuing a graduate career in science. Lastly, I thank the tireless and selfless efforts of my former composition professor, John Anthony Lennon. He has always pushed me to think creatively and expressively, helping me see my compositional ideas to realization. He has always given me the best of advice, and his meticulous attention to detail has constantly improved my musical work.

I owe a great deal of happiness and sanity to all of my close friends with whom I started my medical education. I thank Adam Prater for many study sessions and clinical discussions; he has helped me think like an engineer and kept my clinical knowledge up while in my graduate career. I don't know where I would be without the support of Jason Lake, Melody Lao, Ria Pitts, and Katie Shields. I thank them for listening to my scientific ideas, discussing the clinical relevance of my dissertation, and reminding me of why I went to graduate school. As a collective, they have always known what I have needed, whether it has been a hand of support, a difficult conversation, or a respite from my work. They have stayed behind me for years, and I look forward to having them as colleagues in the future.

There are a few individuals who have supported me before I even considered graduate school, and whose families I have regarded as my own over the past decades. I thank Julie and Adam Hord and their wonderful family for opening up their arms to me. I owe a great deal of confidence and tenacity to Julie, and I would never have taken so many risks had it not been for her constant support and encouragement. I thank Kerry Allan and Ray Patton for ensuring that I stayed passionate about all of my endeavors. Whether indulging me in lengthy conversations about my graduate work, finding ways to express my scientific interests artistically, or editing countless manuscripts, they have fostered my intellectual growth and supported my successes more than they have realized. All of these wonderful people have shown me that deep friendships are among the most fulfilling and important aspects of life. Their two families have been nothing short of magnanimous with me, and they have unconditionally cared for me throughout my adult life. I am honored to be a part of their families, and I am forever indebted to their kindness.

Lastly, I thank members of my family, without whom I would not be the person I am today. I would like to thank my brothers, Mohammad and Mehdi, and my sister, Sarah, for allowing me to look after them and learn responsibility at an early age. I thank my grandparents, Filiberto and Mercedes Romero, for teaching me to be accountable for my actions and for showing me the value of hard work. I thank my parents for doing their best to prepare me for my future. They have given me the all of the opportunities that they possibly could have throughout my life, and I am still in awe of the sacrifices they

have made to ensure that I could receive a great education. I love them both dearly and will always have an overwhelming sense of respect and gratitude for their altruism.

Lastly, I would like to thank George Nicholson for making my life nothing less than wonderful. He has brought so much happiness and calmness to my life that mediocre times are enjoyable, and difficult times bearable. He has always treated me with kindness, understanding, and patience, and has given me the strength I needed to finish my graduate work. I am inspired daily by his character, as he has helped me become a kinder, more understanding and more tolerant person. I am so fortunate to have him and all of the aforementioned people in my life, and I will never forget their contributions.

TABLE OF CONTENTS

LIST OF FIGURES

LIST OF TABLES

CHAPTER 1: INTRODUCTION

Parts of this chapter were originally published as an article in *Topics in Spinal Cord Injury and Rehabilitation*:

Safavynia SA, Torres-Oviedo G, Ting LH. Muscle synergies: implications for clinical evaluation and rehabilitation of movement. *Top Spinal Cord Inj Rehabil.* 2011 Summer; 17(1):16-24.

1.1 LIMITATIONS OF CLINICAL ASSESSMENT OF MOTOR FUNCTION AND CONTROL

Falls are the leading cause of morbidity and mortality among the elderly (CDC 2011) and cause great expense to the US healthcare system (Stevens 2005). While falls generally result from a failure to coordinate muscles to maintain balance, the specific deficits in motor coordination contributing to falls are often musculoskeletal manifestations of a variety of pathologic changes in the nervous system. For example, altered interlimb coordination during locomotion is a major contributor to falls and is exhibited in a wide range of neural pathologies including Parkinson's disease (Nevitt et al. 1989), peripheral neuropathy (Richardson and Hurvitz 1995), cerebellar ataxia (Van de Warrenburg et al. 2005), multiple sclerosis (Cattaneo et al. 2002), and stroke (Moroz et al. 2004). While the neural changes underlying motor deficits are often disparate and complex, the entire motor output of the nervous system is manifested in the muscle activation patterns of the musculoskeletal system. Thus, it is prudent to evaluate changes in the neural control of movement at the musculoskeletal level. Moreover, it is crucial to
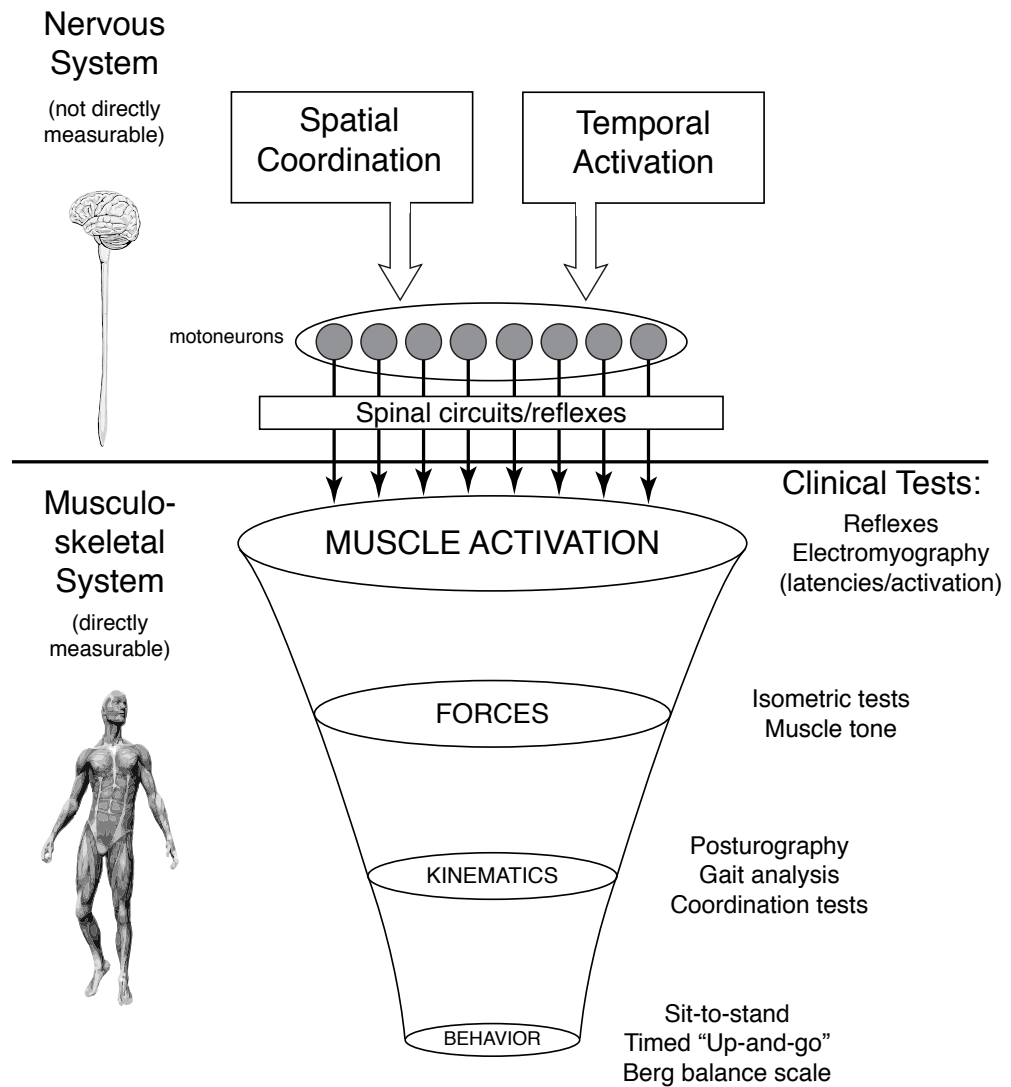
Figure 1.1. Conceptual model of muscle coordination. Although there are many competing influences and complex circuits governing spatial coordination and temporal activation of muscles in the nervous system, motoneurons represent the motor output of the nervous system and directly activate the musculature. The existing muscle activation patterns give rise to a smaller set of producible forces, which in turn produce a smaller set of kinematics and, ultimately, an even smaller set of motor behaviors. Clinical motor tests mainly focus on these musculoskeletal outcomes, as the nervous system is not directly measurable.

determine the appropriate musculoskeletal variables of interest that will provide sufficient

information about the underlying neural deficits.

In diagnosis of motor disease and rehabilitation of movement, clinical tests

mainly focus on behavioral or kinematic outcomes (Horak et al. 1997) at the

musculoskeletal level; while such assessments are descriptive of the overall motor

behavior, they provide only ambiguous information about the underlying neural deficits

due to muscular redundancy (Figure 1.1). For example, behavioral tests like sit-to-stand,

Timed Up and Go, and the Berg Balance Scale offer global and/or descriptive

information about the behavior, such as the time for a person to complete or maintain a

task (Berg et al. 1995; Horak et al. 1997; Tinetti 2003). Similarly, kinematic measures

from gait analysis and posturography (Berg and Norman 1996; Camicioli et al. 1997; Gill

et al. 2001; Norris et al. 2005) provide a more detailed and quantitative description of

behaviors. While motor deficits may be observable at the behavioral or kinematic level,

an altered behavioral or kinematic outcome (e.g., walking slowly) could be the result of

multiple distinct neural or musculoskeletal abnormalities, and thus does not distinguish

between specific neural deficits or dissociate neural from musculoskeletal deficits.

Furthermore, neural pathologies may be masked at the kinematic level by compensatory

strategies, as similar movements may be produced through different neuromuscular

mechanisms. While it is possible to evaluate forces due to the neural activation of

muscles through muscle tone and force production tests during isometric tasks (Dewald et

al. 1995; Gladstone et al. 2002), such measures may have limited relevance to dynamic

production of movement due to the activation of different neural pathways. Additionally,

the same endpoint force and resulting movement can be achieved by many different muscle coordination patterns (Bernstein 1967). Because muscle activity represents the output of the nervous system, the direct examination of muscle activation may reflect differences in the flexibility and adaptability of neural mechanisms in patients with motor disorders, leading to differences in kinetic and kinematic strategies for movement.

Furthermore, in rehabilitation of motor function following neural injury, it is difficult to distinguish between restitution versus compensation of motor function, which has different implications at the neural level. Currently, following neural injury and rehabilitation treatments, motor function is assessed periodically using endpoint performance based measures such as the Fugl-Meyer Scale (FMS) or the Wolf Motor Function Test (WMFT) (Fugl-Meyer 1980; Gladstone et al. 2002; Levin et al. 2009; Morris et al. 2001); however, these indices do not make distinctions at the neuronal level. Thus, while a variety of rehabilitation therapies have been shown to improve performance based impairment indices (Raghavan et al. 2010; Woodbury et al. 2009), they cannot differentiate between restitution (i.e. reparation of previously damaged structures) versus compensation (i.e. recruitment or development of alternative pathways) of motor function. Indeed, as opposed to a restitution of motor function, humans and animals often improve motor performance following stroke using compensatory strategies with abnormal limb kinematics and impairments of each phase of movement (Metz et al. 2005; Raghavan et al. 2010). Moreover, abnormal compensatory patterns do not generalize to a variety of movements. The difference between restitution and compensation may explain why not all patients benefit from specific rehabilitative interventions; for example, only 50% of fallers significantly reduce their fall risk

following balance training (Wolf et al. 1996). Because the underlying neural strategies for producing coordinated movements remain unknown, it is difficult to determine why specific interventions work (Levin et al. 2009), or develop prognostic measures to determine which populations would benefit from a rehabilitation treatment (Kwakkel 2009). Thus, it is unknown how to specifically rehabilitate motor deficits to produce a restitution of motor function.

Although muscle activity during movements is measurable via electromyographic (EMG) signals during motor tasks, it has been difficult to interpret the functional implications of such measurements as a result of the spatial and temporal variability of EMG. Due to the overabundant musculature of the body, the range of possible muscle activation patterns is larger than the range of possible motor behaviors (Figure 1.1). This can result in highly variable spatial patterns of muscle coordination between repeated measurements and highly variable temporal patterns in single EMG recordings (Ting 2007), both of which pose experimental problems with averaging data. This variability does not necessarily indicate dysfunction: for example, in postural control, EMG patterns are normally variable due to a range of factors such as attention (Woollacott and Shumway-Cook 2002), body configuration (Horak and Moore 1993), and emotional state (Hillman et al. 2004). Furthermore, functional motor behaviors require coordination between different joints, and motor pathologies generally feature abnormal patterns of multi-segmental coordination (Cruz and Dhaher 2008). Although it may be prudent to assess EMG of multiple muscles spanning body segments, multi-muscle EMG recordings result in very large datasets with even more variability. Thus, simply using expensive and sophisticated equipment to simultaneously record multiple EMG signals may not be

sufficient to functionally interpret the spatial and temporal features of EMG during movements. Instead, it is necessary to develop tools to address the temporal and spatial variability of EMG in a functional framework.

In this work, I investigate the spatiotemporal organization of muscle activity using recent advances in functional characterization of EMG. Previously, the spatial activation of muscles has been functionally characterized by identifying *muscle synergies*, defined as groups of muscles with fixed ratios of coactivation. Concurrently, the functional significance of temporal activation of muscles has been characterized using feedback control of task-level variables. To evaluate the functional significance of muscle activity, I tested the robustness of the muscle synergy concept and task-level feedback separately, and ultimately unified the muscle synergy concept with task-level feedback during human standing balance control.

1.2 SPATIAL COORDINATION OF EMG: MUSCLE SYNERGY CONCEPT

Recent work has shown that the spatial coordination of muscles exhibited in a variety of natural movements can be explained by flexibly combining a few motor modules called muscle synergies. The analysis makes it possible to determine the functional groupings of muscles within a highly variable set of muscle activation patterns. Traditionally, the term "synergy" has been used clinically to describe the pathologic co-activation of muscles as seen in stroke (Bourbonnais et al. 1989) leading to dysfunctional coordination across joints. However in recent years, the concept of a muscle synergy has reemerged in neuroscience as a proposed mechanism for neural control of normal movement (Saltiel et al. 2001; Ting and McKay 2007; Torres-Oviedo

and Ting 2007; Tresch et al. 1999). Specifically, it has been suggested that muscle synergies in healthy subjects represent functional muscle coordination patterns used to reliably produce motor functions during natural motor behaviors (Ivanenko et al. 2005; Torres-Oviedo and Ting 2007). This suggests that the existence of muscle synergies in the production of movements may not be restricted to pathology, but may reflect a general principle of neural control.

It has been hypothesized that muscle synergies represent a library of motor subtasks, which the nervous system can flexibly combine to produce complex and natural movements (d'Avella and Bizzi 2005; Overduin et al. 2008; Torres-Oviedo and Ting 2007). In this formulation, a muscle synergy is defined as a consistent ratio of muscle co-activation necessary to coordinate body segments to perform a motor subtask (Ting 2007; Ting and Macpherson 2005). Thus, a single neural command can recruit a muscle synergy to reliably produce the motor subtask. In contrast to the more traditional concept of synergies in stroke (Bourbonnais et al. 1989), in normal function it is hypothesized that muscle synergies can be comprised of any number of muscles and individual muscles can belong to multiple muscle synergies. Moreover, multiple synergies can be simultaneously recruited in different proportions, giving rise to a wide range of possible movements. Using component analysis algorithms on EMG data, low-dimensional sets of muscle synergies have been identified in a range of movements and in many different tasks, including walking, reaching, and postural control (Cheung et al. 2005; Chvatal et al. 2011; d'Avella and Bizzi 2005; Hart and Giszter 2004). Thus, muscle synergy analysis is robust enough to reveal an underlying neural organization even when there are multiple influences on muscle activity, including local circuits and descending voluntary

commands. Moreover, a muscle synergy organization has been proposed to exist in a variety of contexts and behaviors with different neural control schemes, including central pattern generators (CPGs) (Drew et al. 2008), short- and long-loop reflexes (Honeycutt and Nichols 2010a; Torres-Oviedo and Ting 2007), and descending cortical commands (Overduin et al. 2008), suggesting a common neural substrate for producing movement.

In contrast, it has been proposed that the nervous system achieves motor goals by controlling task-relevant variability of individual muscles. Although low-dimensional patterns of muscle coordination have been identified from a variety of movements (Chvatal et al. 2011; Hart and Giszter 2004; Saltiel et al. 2001; Torres-Oviedo et al. 2006; Tresch and Bizzi 1999), others have argued that low dimensionality arises from the fact that certain tasks can only be achieved in a few ways due to experimental and biomechanical constraints (Bunderson et al. 2008; Tresch and Jarc 2009; Valero-Cuevas et al. 2009). Instead, it has been proposed that the nervous system controls only the variability in EMG that is relevant to the performance of the task and does not address task-irrelevant variability (Kurtzer et al. 2006; Kutch et al. 2008; Latash et al. 2002; Scholz and Schoner 1999; Valero-Cuevas et al. 2009). Known as the *uncontrolled manifold* or *minimum intervention* hypothesis, the nervous system can choose a variety of muscle activation patterns independently to control a low-dimensional set of task-relevant variables. Whether or not the nervous system controls muscles individually based on task-relevant variability, the underlying neural mechanism unknown. Because muscle synergies can transform task-level goals into execution level motor outputs, the two hypotheses need not be in complete conflict. In fact, the patterns of muscle coordination identified from the uncontrolled manifold hypothesis often match the structure of muscle

synergies (Krishnamoorthy et al. 2004). Even if the nervous system does not implement muscle synergies as many have identified previously, muscle synergy analysis may still be useful as it provides functional information about muscle coordination. For example, in healthy individuals, differences in motor strategies can be explained by differences in the structure of muscle synergies (Torres-Oviedo and Ting 2007); similarly, differences in the number of muscle synergies in the impaired leg of hemiparetic post-stroke subjects can explain the differences in functional performance measures (Clark et al. 2010). Nevertheless, questions still remain as to how the nervous system actually encodes muscle synergies or controls task-relevant variability.

The ability of muscle synergy structures to explain detailed features of experimentally recorded EMG provides additional evidence for the muscle synergy hypothesis. For example, during postural responses to perturbations, the variability in muscle activation patterns across perturbation directions can be explained by the recruitment of muscle synergies (Figure 1.2). In response to support-surface perturbations, muscles are tuned to a small range of perturbation directions (Macpherson 1988). For illustrative purposes, tuning curves for three hypothetical muscles with different spatial tunings are shown (Figure 1.2). Muscle 1 is tuned to backward perturbations, muscle 2 is tuned to leftward perturbations, and muscle 3 is tuned to backward-leftward perturbations. By recruiting two muscle synergies (W1 and W2), each with their own spatial tuning (C1 and C2), it is possible to reconstruct muscle activity over all directions. Because W1 has a large contribution of muscle 1 (w_{11}) and a moderate contribution of muscle 3 (w_{13}), a single neural command C1 reproduces muscle 1 and muscle 3 activity in backward-leftward directions. By contrast, W2 is composed of all
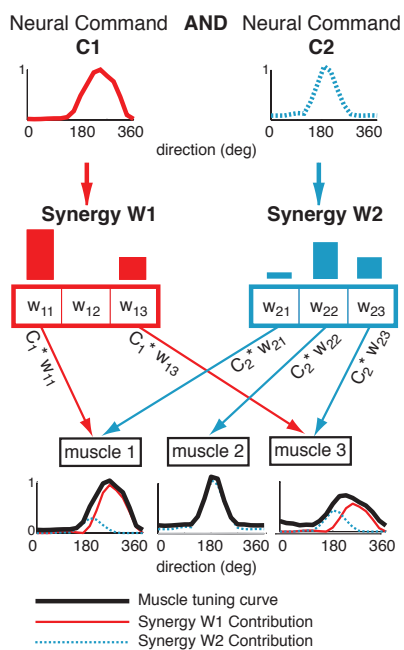
Figure 1.2. Muscle synergy concept. In this formulation, neural commands (C) that vary spatially across perturbation directions recruit muscle synergies (W) that define spatial patterns of muscle activation across multiple muscles. Muscle synergies are represented by specific ratios of activity. Note that any muscle can belong to multiple muscle synergies. The resulting spatial patterns of muscle activity are due to the net activation of each muscle by all of the recruited muscle synergies. A perturbation direction of 0° indicates rightward platform movement; angle of perturbation increases in a counterclockwise manner so that forward movement corresponds to 90° and leftward movement corresponds to 180°.

three muscles, with a small contribution of muscle 1, a large contribution of muscle 2 and a moderate contribution of muscle 3. Neural command C2 thus reconstructs the activity of muscles 1-3 over leftward directions.

A muscle synergy organization allows the nervous system to produce consistent biomechanical functions that are shared across motor tasks. Walking muscle synergies are recruited at specific times in the gait cycle related to functional, task-level variables (Cappellini et al. 2006; Ivanenko et al. 2004) such as standing leg stabilization, forward propulsion, swing initiation, and leg deceleration during swing to stance transitions. Similar relationships to a particular phase of movement requiring different biomechanical functions have been identified in muscle synergies for reaching (d'Avella et al. 2008; Yakovenko et al. 2011). More precise relationships to biomechanical outputs have been found between muscle synergies used during standing balance control, in which recruitment of each muscle synergy is proportional to the production of a particular force vector at the foot (Chvatal et al. 2011; McKay and Ting 2008; Ting and Macpherson 2005). Moreover, the relationships between muscle synergy activation and endpoint force are preserved across stance widths (Torres-Oviedo et al. 2006; Torres-Oviedo and Ting 2010), suggesting that muscle synergies represent a consistent mapping between a desired task-level outcome and an execution-level muscle activation pattern.

While muscle synergies can identify robust spatial patterns of coordination with functional outputs, little is known about how muscle synergies may be temporally recruited. Some people have suggested that muscle synergies represent fixed patterns of temporal coordination in feedforward tasks (Cappellini et al. 2006; Ivanenko et al. 2005; Ivanenko et al. 2004); others have suggested feedback control of muscle synergies in

reactive movements (Chvatal et al. 2011; Kargo et al. 2010). In either case, it is unknown how the nervous system maps sensory inputs to motor outputs in order to recruit muscle synergies during a task. Because muscle synergies produce task-level motor outputs, it is likely that task-level variables mediate their recruitment; however, task-level recruitment of muscle synergies has yet to be explicitly tested. I first address the ability of muscle synergy recruitment to be described by task-level feedback in Chapter 2.

1.3   TEMPORAL ACTIVATION OF EMG: FEEDBACK CONTROL OF TASK-LEVEL VARIABLES

Much evidence suggests that control of task-level goals is a common neural principle for motor control. Defined as motor intentions that cannot be directly mapped to any particular sensory input or unique motor output, task-level goals require that multiple sensory signals be integrated to estimate. Such task-level variables cannot be inferred directly from local anatomical variables such as joint angles, save for the simplest of cases. Moreover, as opposed to independently controlling muscles, joint torques, or joint angles, task-level variables must coordinate the muscles and joints in a task-specific manner. For example, in reactive arm movements, EMG activity of arm muscles has been shown to be modulated not in response to local-level joint angle changes of the arm, but rather to the task-level variable of whole limb position (Kurtzer et al. 2008). In postural control, maintaining the body center of mass (CoM) over the base of support is an established task-variable in maintaining balance (Massion 1994). Similarly, a number of studies have modeled joint torques of the lower limb using task-level feedback of center of mass (CoM) kinematics in balance (Kuo 1995) as well as postural sway (Peterka 2000; van der Kooij and de Vlugt 2007). As opposed to low-level variables providing

information about individual joints, task-level variables such as CoM integrate many local sensory inputs (Peterka 2002), encapsulate the net motion of the body, and are most reliably correlated to muscle activity (Gollhofer et al. 1989; Szturm and Fallang 1998).

In balance control, it has been recently shown that temporal patterns of EMG during postural responses can be predicted with high fidelity using delayed feedback of CoM kinematics (Lockhart and Ting 2007; Welch and Ting 2009; 2008); this model was developed on the assumption that CoM kinematic signals are linearly combined to activate muscles (Welch and Ting 2009; 2008). By assigning unique feedback gains for sagittal CoM displacement, velocity, and acceleration for each muscle at a common delay, EMG activity was reconstructed throughout postural responses to sagittal support-surface perturbations (Figure 1.3). The results were consistent with previous studies that have reported changes in muscle activity that scale with changing perturbation velocities and accelerations (Brown et al. 2001; Carpenter et al. 2005; Diener and Dichgans 1988; McIlroy and Maki 1994).

In contrast to task-level control of muscle activity, it has long been hypothesized that local-level changes in muscles and joints are responsible for modulating motor outputs via spinal pathways. This hypothesis is supported by the fact that the nervous system can modulate individual muscle activity via a variety of local neural pathways. For example, muscle activity can be modulated at short latencies via monosynaptic stretch reflexes (Liddell and Sherrington 1924); muscle spindles embedded within the muscle respond to muscle lengthening and activate the homonymous muscle (via Ia afferent fibers) as well as heterogenic muscles with similar functions (Nichols and Houk 1976; Sinkjaer et al. 1996). Afferent fibers from Golgi tendon organs (Ib), joint receptors,

and cutaneous receptors can dynamically modulate muscle activity throughout tasks via Ib inhibitory neurons (Prochazka 1996). Moreover, the action of muscle spindles can be modified in specific tasks by gamma motoneurons (Matthews 1981), and Ib afferents from Golgi tendon organs can have opposite effects on muscle activation, a process known as state-dependent reflex reversal (Pearson and Collins 1993). While all of these connections exist in the nervous system, little is known about the functional effects that such connections have on temporal patterns of muscle activation or spatial patterns of muscular coordination during motor behaviors. Presumably, the documented neural pathways exist to satisfy biomechanical functions during movements, which in turn produce task-relevant motor outputs; however, it is unknown whether task-dependent EMG activity can be produced by feedback from individual local segments.
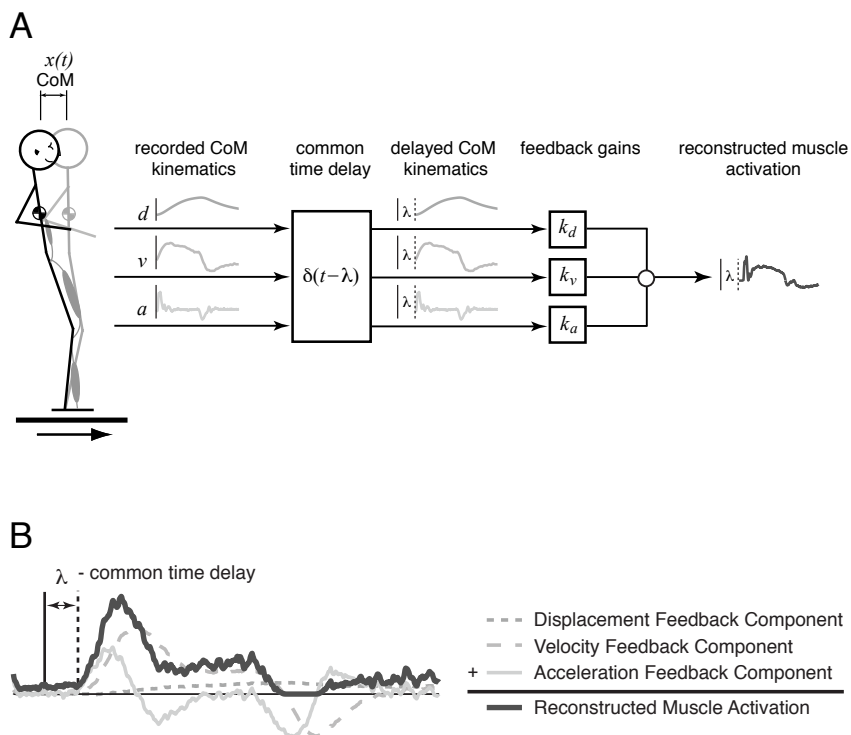
Figure 1.3. Feedback model concept. Recorded center of mass (CoM) kinematics are used to reconstruct muscle activation patterns throughout postural responses to perturbations. Each component of CoM motion (**d**, **v**, **a**) is multiplied by a feedback gain (k_d, k_v, k_a) and linearly added to reconstruct muscle activity. d: displacement; v: velocity; a: acceleration.

Although delayed feedback of CoM has been explicitly shown to predict the temporal activation of muscle activity throughout postural responses, task-level versus local-level control of muscle activity has not been explicitly compared. Previously, delayed CoM feedback has been used to predict muscle activity throughout discrete and double one-dimensional support-surface perturbations (Lockhart and Ting 2007; Welch and Ting 2009; 2008). Such perturbations elicit stereotypically coordinated kinematics with similar temporal features of EMG (Horak and Macpherson 1996; Welch and Ting 2009). As a result, task-level CoM kinematics are often correlated with local-level joint kinematics, making it difficult to dissociate task-level versus local-level control of muscle activity. Moreover, CoM kinematic components (displacement, velocity, acceleration) are coupled in discrete perturbations, limiting the utility of the feedback model to states where task-level control of CoM is predictable. It is thus unknown whether more complex and behaviorally relevant perturbations can still be explained using task-level feedback of CoM. I address local- versus task-level control of EMG as well as the robustness of task-level feedback on EMG activity in Chapter 3.

Another limitation of previous studies is that delayed feedback of CoM has only been used to reconstruct individual EMG activity in perturbations that are applied when the body is in a quasi-static state. The feedback model by Welch and Ting (2009) was robust enough to reconstruct the entire time course of postural responses of multiple muscles of the leg and trunk, suggesting that the nervous system uses task-level feedback to activate muscles throughout a balance challenge. However, the model was applied independently for each muscle in each perturbation direction, yielding a unique set of feedback gains for each muscle in every perturbation direction. As a result, interpreting

functional activity at the level of EMG requires a larger number of feedback gains than muscles, limiting the utility of the model. Moreover, the model has only been applied to one-dimensional perturbations that start from rest; thus it remains unknown whether task-level feedback of EMG can be generalized across more dynamic states. In chapter 4, using muscle synergies to reduce the dimensionality of EMG, I evaluate the robustness of task-level feedback on muscle synergy recruitment across multiple perturbation directions, as well as in dynamic perturbations that change direction.

1.4   THESIS OVERVIEW
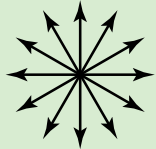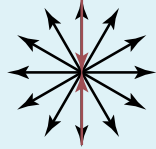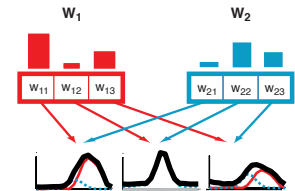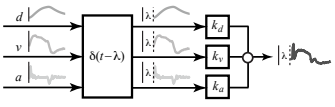
I hypothesize that the nervous system continuously uses task-level feedback of CoM to recruit muscle synergies throughout standing balance tasks. By combining the muscle synergy hypothesis (Torres-Oviedo and Ting 2007) with the feedback model (Welch and Ting 2009), I predicted that a delayed feedback model based on CoM kinematics would reconstruct spatial and temporal patterns of muscle activity throughout balance challenges. I used posture and balance as a model to study the functional determinants of muscle activity: by recording muscle activity via an EMG telemetry system, kinematics via optical tracking of reflective markers on the body, and external forces via force plates, it is possible to assess the functional significance of muscle activity (Figure 1.4).

To test the robustness of task-level feedback of CoM on muscle synergy recruitment, I developed a series of support-surface perturbations of increasing kinematic complexity (Figure 1.5). Compared to discrete perturbations, continuous perturbations dissociated the magnitude of CoM components from each other in the sagittal plane;
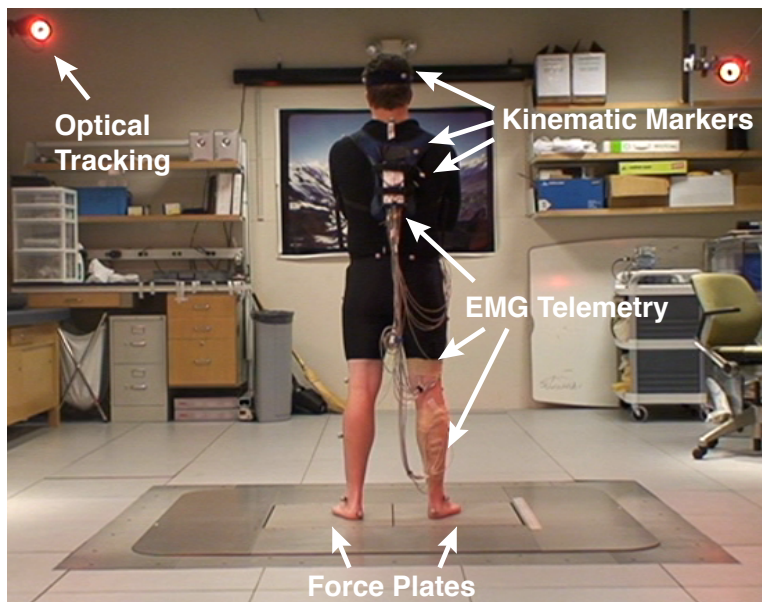
Figure 1.4. Human postural perturbation experimental paradigm. Subjects stand and maintain their balance on a custom platform that translates in the horizontal plane. EMG activity is measured via EMG electrodes and telemetered via transmitters worn in a backpack. Kinematics are captured via reflective markers that are recorded by an 8-camera Vicon optical tracking system. Ground reaction forces are measured via two embedded force plates (one under each foot).

	Study 1	**Study 2**	**Study 3**
Perturbations	Discrete	Continuous	Biphasic
Muscle Synergy Analysis	Compare muscle synergy structure throughout perturbations		Compare muscle synergy structure across perturbation types
Feedback Model	Reconstruct muscle synergy recruitment from CoM feedback	Reconstruct muscle activation from CoM feedback	Predict muscle synergy recruitment from CoM feedback

Figure 1.5. Overall study design. The spatial and temporal determinants of muscle activity were evaluated using muscle synergy analysis and a delayed feedback model, respectively. Perturbations of increasing kinematic complexity were administered from Studies 1-3. Muscle synergy analysis was combined with the feedback model in Study 1. These two methods were used independently in Studies 2 and 3.

biphasic perturbations dissociated CoM components in both magnitude and direction. In **Study 1**, I validated the hypothesis that muscle synergies are recruited by task-level feedback by reconstructing the temporal recruitment of muscle synergies throughout discrete sagittal perturbations using a delayed feedback model of CoM. I then tested the robustness of muscle synergy analysis and the feedback model in continuous and biphasic perturbations where CoM kinematics are decoupled (Studies 2 and 3). In **Study 2**, I explicitly compared task-level versus local level control of the temporal recruitment of muscles. I also determined whether task-level feedback of EMG was robust enough to explain muscle activity evoked in complex continuous perturbations. In **Study 3**, I determined whether the same muscle synergies were used in static and dynamic states by comparing muscle synergies extracted separately from discrete and biphasic perturbations. I also evaluated the robustness of task-level feedback on muscle synergy recruitment in multidirectional biphasic perturbations that change direction while the body is moving. A more detailed description of each study is offered below.

1.4.1   Study 1

In **Study 1**, I investigated the hypothesis that muscle synergies have spatially-fixed structure but are subject to time-varying recruitment. I identified muscle synergies from discrete perturbations in two ways: 1) holding the spatial structure of muscle synergies constant (spatially-fixed or SF muscle synergies), and 2) holding the temporal structure of muscle synergies constant (temporally-fixed or TF muscle synergies). SF muscle synergies produced more consistent and physiologically interpretable results than TF muscle synergies during postural responses to perturbations. Moreover, SF muscle synergy structure was consistent throughout various epochs of the postural response. The

temporal structure of a majority of SF muscle synergies was well-described by task-level feedback of CoM. These results suggest that the nervous system produces motor outputs using a multisensory estimate of task-level variables to modulate SF muscle synergies.

1.4.2   Study 2

In **Study 2**, I determined whether task-level feedback could explain muscle activity in complex dynamic states where CoM kinematics were decoupled in magnitude. I also compared the ability of task-level control of CoM versus local-level control of joint kinematics to reconstruct muscle activity. To this end, I developed continuous perturbations in the sagittal plane that perturbed the body while it was already in motion; these perturbations decoupled CoM kinematic components from each other as well as from joint kinematics. EMG activity was well-reconstructed from delayed feedback of CoM kinematics throughout both discrete and continuous perturbations. Moreover, delayed feedback of CoM kinematics reconstructed EMG activity significantly better than local-level feedback of joint kinematics. These results suggest that CoM feedback may be continuously used by the nervous system when responding to balance challenges. Thus, feedback of CoM kinematics may be a unifying principle of standing balance control.

1.4.3   Study 3

In **Study 3**, I determined whether task-level feedback could explain SF muscle synergy recruitment in complex dynamic states where CoM kinematics were decoupled in magnitude and direction. I developed multidirectional biphasic perturbations that perturbed the body in a variety of directions while it was already moving in the sagittal

plane. The same SF muscle synergies were identified in discrete and biphasic perturbations. SF muscle synergies were consistently tuned to CoM acceleration direction in discrete and biphasic perturbations. SF muscle synergy recruitment patterns across multidirectional perturbations were well-predicted by a fixed set of feedback gains across perturbation directions, and across perturbations that changed direction while the body was moving. These results suggest that the nervous system may continuously use task-level control of SF muscle synergies as a general organization for motor outputs in both static and dynamic states.

CHAPTER 2: TASK-LEVEL FEEDBACK CAN EXPLAIN TEMPORAL RECRUITMENT OF SPATIALLY-FIXED MUSCLE SYNERGIES THROUGHOUT POSTURAL PERTURBATIONS

2.1 INTRODUCTION

A fundamental problem in motor control is how the central nervous system (CNS) chooses among an overabundant set of muscles and joints to execute a movement (Bernstein 1967). Recent evidence in a variety of tasks across species suggests that complex spatiotemporal patterns of muscle activity can be explained using a low-dimensional set of muscle synergies (Cheung et al. 2005; d'Avella and Bizzi 2005; Hart and Giszter 2004; Ivanenko et al. 2005; Krouchev et al. 2006; Saltiel et al. 2001; Ting and Macpherson 2005; Torres-Oviedo and Ting 2007; Tresch et al. 1999). However, previous analyses have either identified low-dimensional structures that constrain the spatial groupings of muscles, leaving temporal patterns unconstrained (Figure 2.1A) (Hart and Giszter 2004; Saltiel et al. 2001; Torres-Oviedo and Ting 2007), or they have

identified low-dimensional structure in the temporal features of muscle activity, leaving

spatial patterns unconstrained (Figure 2.1B) (Cappellini et al. 2006; Ivanenko et al. 2005;

Ivanenko et al. 2004). Although both spatial and temporal constraints on muscle

coordination may be low-dimensional, they likely involve different neural control

mechanisms (Ivanenko et al. 2005; Kargo and Giszter 2000; Kargo et al. 2010; McCrea

and Rybak 2008). Specifically, in postural responses to perturbations, temporal muscle

activation patterns are due to task-level sensorimotor feedback (Welch and Ting 2008), as

opposed to feedforward temporal patterns that may drive locomotor behaviors.

A number of studies have proposed that muscle synergies have spatially-fixed

muscle weightings, but are subject to time-varying temporal recruitment (Clark et al.

2010; Hart and Giszter 2004; Kargo et al. 2010). In this organization, a spatially-fixed

(SF) muscle synergy represents a group of muscles with fixed ratios of activation that can

be recruited by variable temporal neural commands to execute a task in a feedforward or

feedback manner (Figure 2.1A). SF muscle synergies are recruited across a range of

locomotor tasks with varying temporal recruitment patterns (Clark et al. 2010; d'Avella

and Bizzi 2005). For example, changes in the temporal recruitment of SF muscle

synergies can vary from step to step in human walking, as well as systematically across a

range of speeds (Clark et al. 2010). In reactive tasks, altered temporal recruitment

patterns of SF muscle synergies account for many directions of movement and postural

configurations (Hart and Giszter 2004; Kargo et al. 2010; Ting and Macpherson 2005;

Torres-Oviedo et al. 2006; Torres-Oviedo and Ting 2007; 2010). However, in our

previous studies of balance control, analyses of SF muscle synergy recruitment were
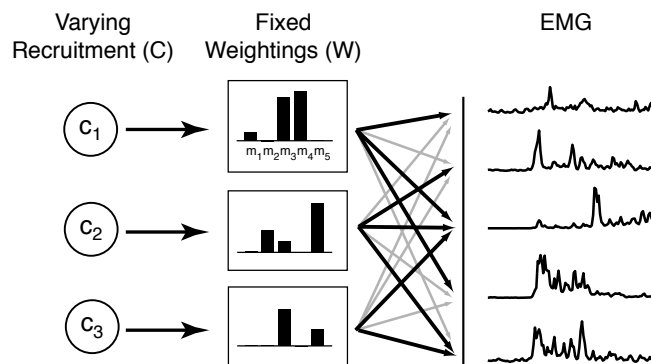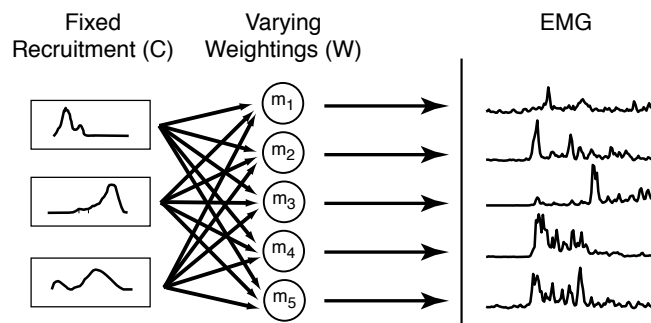
Figure 2.1. Hypotheses and concepts explored in the current study. A, muscle synergies with fixed spatial weightings (SF muscle synergies). Here the nervous system organizes muscle activity spatially. The nervous system can variably recruit SF muscle synergies when a specific muscle combination is desired throughout a task in a feedback or feedforward manner. **B,** muscle synergies with fixed temporal recruitment (TF muscle synergies). In this hypothesis, the nervous system uses fixed temporal sequences to recruit muscles during a task, consistent with feedforward control. When a specific temporal sequence is executed, a set of muscles that can vary across directions and trials is chosen to reproduce EMG activity necessary to achieve the task.

limited to gross variations in a few large time bins (~75 ms) during the initial portion of the postural response. It remains unclear whether SF muscle synergies can account for the finer dynamics of muscle activity throughout the entire postural response, including later periods which are more heavily influenced by ongoing body motion and descending commands.

It has been alternatively proposed that muscle synergies are temporally-fixed patterns of muscle recruitment that are coupled to spatially-varying muscle weightings (Cappellini et al. 2006; Ivanenko et al. 2005; Ivanenko et al. 2004). In a temporally-fixed (TF) muscle synergy organization, rhythmic motor patterns are constructed in a feedforward manner through a set of predefined temporal recruitment patterns that activate variable spatial patterns of muscle activity across conditions (Figure 2.1B). In locomotion, a few temporal patterns can be recruited across step cycles to reproduce electromyographic (EMG) patterns across different walking speeds (Ivanenko et al. 2004) and when walking is combined with other voluntary tasks (Ivanenko et al. 2005). However, it may not be possible to dissociate spatial from temporal organization during cyclical locomotor tasks where temporal and spatial features of muscle activity tend to be correlated.

Recent evidence suggests that low-dimensional temporal patterns may be used to recruit SF muscle synergies. For example, fixed duration temporal pulses are sufficient to explain muscle activation patterns described by SF muscle synergies in frog preparations (Hart and Giszter 2004). Similarly, temporal patterns of muscle activity in postural perturbations during balance are defined by a low-dimensional sensorimotor transformation based on feedback control of center of mass (CoM) motion (Lockhart and

Ting 2007; Welch and Ting 2009; 2008). CoM kinematics are task-level variables that must be estimated from multisensory integration (Peterka 2002), and encapsulate the net motion of the body. By assigning unique feedback gains to CoM displacement, velocity, and acceleration for each muscle at a common delay, the model can reconstruct the entire timecourse of muscle activity in multiple muscles throughout the leg and trunk (Lockhart and Ting 2007; Welch and Ting 2009; 2008). Moreover, the model can explain temporal patterns of muscle activity that vary with perturbation characteristics. While it is unknown whether this model can be used to describe the recruitment of SF muscle synergies, CoM feedback likely recruits SF muscle synergies because SF muscle synergies produce forces necessary for CoM control across a range of postural configurations (Chvatal et al. 2011; McKay and Ting 2008; Ting and Macpherson 2005; Torres-Oviedo et al. 2006). A hierarchical structure in which low-dimensional temporal patterns recruit spatial structures defining muscle activation patterns is also consistent with current theories about locomotor pattern generation (Hart and Giszter 2004; McCrea and Rybak 2008) and trajectory formation (Berniker et al. 2009; Kargo et al. 2010).

Here we hypothesized that during human balance control, low-dimensional temporal feedback mechanisms recruit SF muscle synergies. Specifically, we predicted that SF muscle synergies are modulated by delayed feedback of CoM throughout perturbation responses. To test this hypothesis, we examined muscle synergy structure and recruitment in 10 ms bins throughout postural responses to support-surface translations including later, previously unexplored epochs that extend beyond perturbation deceleration and feature very different combinations of muscle activity and CoM kinematics compared to the initial postural response. We explicitly compared SF

versus TF muscle synergies on their ability to reconstruct EMG activity in reactive

postural responses. We then analyzed the structure and recruitment of SF muscle

synergies extracted from epochs throughout postural responses to perturbations. We

predicted that SF muscle synergies would have consistent structure regardless of the

extraction epoch. Furthermore, we predicted that a feedback model based on CoM

kinematics would be able to reproduce SF muscle synergy recruitment patterns and

reliably reconstruct SF muscle synergy activity throughout postural responses to

perturbations.

2.2 METHODS

2.2.1 Summary

In order to determine the organization and control of muscle synergies throughout

a postural task, we recorded human postural responses to multidirectional ramp-and-hold

translations of the support surface. We investigated different hypotheses on muscle

synergy organization by extracting both SF and TF muscle synergies from the entire

postural response. We compared SF versus TF muscle synergy structure and EMG

reconstructions. We then compared SF muscle synergy structure across epochs to

determine their degree of consistency across the timecourse of postural response. We

investigated task-level control of SF muscle synergies by applying a delayed feedback

model based on CoM kinematics to reconstruct muscle synergy recruitment throughout

anterior-posterior (A-P) perturbations. We compared observed and reconstructed SF

muscle synergy recruitment patterns and examined the ability of the feedback model to

reconstruct trial-by-trial variability in SF muscle synergy recruitment. To ensure that our

models of SF muscle synergy recruitment were adequate to describe actual EMG data, we reconstructed individual muscle activity from reconstructed SF muscle synergy recruitment patterns.

2.2.2   Data collection

Eight healthy subjects (5 male, 3 female; mean age ± SD: 23.5 ± 2 years) were exposed to ramp-and-hold perturbations according to an experimental protocol approved by the Georgia Tech and Emory University Institutional Review Boards. Subjects stood on a platform that translated in 12 directions in the horizontal plane. In order to minimize anticipatory adjustments while maximizing EMG variability, five repetitions were randomly presented over 12 directions for a total of 60 trials. Translations were 12.4 cm in displacement, 35 cm/s in velocity, and 0.5g in acceleration.

EMG activity was recorded from 16 muscles on the right leg and trunk. The muscles include: rectus abdominis (REAB), tensor fascia lata (TFL), tibialis anterior (TA), semitendinosus (SEMT), biceps femoris, long head (BFLH), rectus femoris (RFEM), peroneus (PERO), medial gastrocnemius (MGAS), lateral gastrocnemius (LGAS), erector spinae (ERSP), external oblique (EXOB), gluteus medius (GMED), vastus lateralis (VLAT), vastus medialis (VMED), soleus (SOL), and adductor magnus (ADMG). Raw EMG data were collected at 1080 Hz and then processed according to custom MATLAB routines. Data were high pass filtered at 35 Hz, de-meaned, rectified, and then low pass filtered at 40 Hz. Kinematic and kinetic data were also collected for an estimation of CoM. Kinetic data were collected at 1080 Hz from force plates under the feet (AMTI, Watertown, MA) and kinematic data were collected at 120 Hz using a 6

camera Vicon motion capture system (Centennial, CO) and a custom 25-marker set that included head-arms-trunk (HAT), thigh, shank, and foot segments. CoM displacement and velocity were calculated from kinematic data as a weighted sum of segmental masses (Winter 2005); CoM acceleration was calculated from ground reaction forces (**F**=m**a**).

2.2.3   Data processing

To test whether postural responses could be explained with a SF versus a TF muscle synergy organization, it was necessary to account for muscle activity with high resolution. Therefore, for each trial, EMG data were parsed into 10 ms bins in which mean EMG activity was found. Each muscle was normalized to maximum EMG activity across all epochs and perturbation directions for visualization purposes. A data matrix was assembled for EMG activity during the entire perturbation response (100-800 ms after perturbation onset) over all trials, resulting in (70 time bins $\times$ 12 directions $\times$ 5 repetitions) = 4,200 points for each of 16 muscles. Note that because postural muscle activity begins ~100 ms following a perturbation (Horak and Macpherson 1996), EMG epochs were chosen at a delay of 100 ms with respect to platform motion.

To further test the hypothesis that muscle synergies are spatially invariant, EMG data from the entire perturbation were further analyzed in four smaller epochs corresponding to: platform acceleration (*start*; 100-250 ms following platform onset), maximum platform velocity (*plateau*; 250-450 ms following onset), platform deceleration (*stop*; 450-600 ms), and after deceleration (*stable*; 600-800 ms) (Figure 2.2). We did not include a background epoch because background EMG was < 5% of maximum activity; thus, SF muscle synergies were more likely accounting for noise than relevant features of
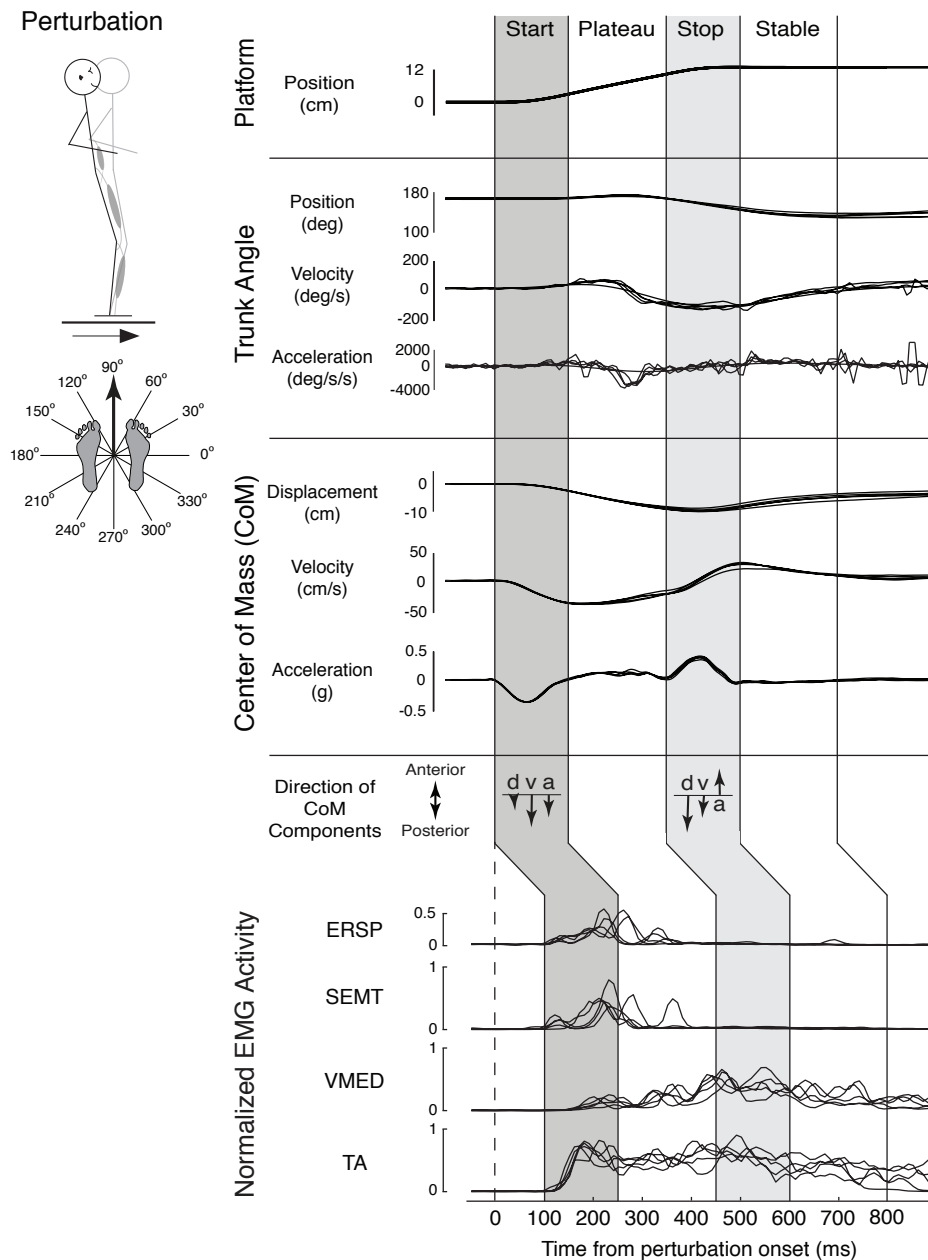
Figure 2.2. Representative postural response to a forward ramp-and-hold perturbation. Subjects exhibit motion of individual joints as well as CoM, and activate muscles over body segments in response to a forward (90°) perturbation. Initially (*start* epoch), CoM kinematics (displacement, velocity, acceleration) were all opposite the direction of platform motion. However, when the platform decelerated (*stop* epoch), CoM acceleration was in the opposite direction of CoM displacement and velocity. Intermuscular coordination patterns also changed throughout the perturbations; the major muscles activated in the *start* epoch (TA, ERSP, SEMT) were different from those activated in the *stop* epoch (TA, VMED). Overlaid muscle traces shown are for individual trials (5 total).

this quiescent dataset. SF muscle synergies from the entire perturbation were able to reconstruct background EMG within 10% of actual EMG.

2.2.4   Muscle synergy extraction

We used non-negative matrix factorization (NNMF) to extract both SF and TF muscle synergies from EMG activity throughout postural responses to perturbations (Lee and Seung 1999; Ting and Chvatal 2011). The NNMF algorithm is a linear decomposition technique that decomposes an original EMG matrix **E** into spatial muscle weightings **W** and temporal recruitment patterns **C**. The NNMF algorithm chooses non-negative matrices **W** and **C** at random initially and modifies their composition to minimize the sum of squared errors between the actual (**E**) and reconstructed (**E***) EMG matrices as shown below:

$$\mathbf{E} = \mathbf{WC} + \text{ error}$$

$$\text{error} = \sum_i \sum_j (\mathbf{E}_{ij} - \mathbf{E}_{ij}^*)^2$$

For a pre-specified number of muscle synergies N_{syn}, the activity of a muscle $\mathbf{M}_i$ is reconstructed by linearly combining muscle weightings $\mathbf{W}_i$ with temporal recruitment patterns **C** according to the equation

$$\mathbf{M}_i = \sum_{j=1}^{N_{syn}} w_{i,j} \mathbf{C}_j$$

For SF muscle synergies, the muscular composition of muscle synergies, **W**, does not change, although their recruitment coefficients, **C**, can vary at each time point for each trial. By contrast, for TF muscle synergies, the temporal recruitment patterns **C** do not change, although their muscular compositions **W** can change across conditions (Figure 2.1).

SF muscle synergies. To test the hypothesis that muscle synergies have fixed spatial weightings with varying temporal recruitment, we used non-negative matrix factorization (NNMF) to extract SF muscle synergies from EMG data matrices as previously used in postural responses (Torres-Oviedo et al. 2006). In this case, the muscular composition of SF muscle synergies **W** is held fixed, and the temporal recruitment coefficients **C** can vary at each time point for each trial. We constructed our EMG data matrix to have the dimensions $m \times s$, where m is the number of muscles and s is the number of samples (bins × directions × repetitions). This ensured that the NNMF algorithm would yield spatially-fixed muscle weightings **W** ($m \times n$ matrix) with varying temporal recruitment coefficients **C** ($n \times s$ matrix). We then scaled the rows of the data matrix to have unit variance, weighting the variance of each muscle equally.

We extracted SF muscle synergies **W** from 60% of trials and reconstructed muscle activity in all trials. Keeping the muscle weightings **W** constant, we varied temporal recruitment coefficients **C** to minimize the sum of squared errors between actual and reconstructed EMG patterns. Although we further extracted SF muscle synergies from individual epochs of trials, we ensured that the same set of trials was used for extraction and validation. In order to compare SF muscle synergy structure across different epochs, we took the unit variance scaling factors from the *start* epoch data

matrix and applied them to all data matrices for a subject. We then ran the NNMF

algorithm; after the algorithm was complete, the scaling of the data matrix was removed,

and each SF muscle synergy was normalized to its maximum muscle composition,

resulting in muscle compositions between 0 and 1.

TF muscle synergies. To compare the results of SF muscle synergies against the

hypothesis that muscle synergies have fixed temporal recruitment patterns with varying

spatial muscle activation, we also extracted TF muscle synergies to yield fixed temporal

recruitment patterns. In this case, the matrix $\mathbf{C}$ specifies the fixed temporal recruitment

patterns, and the weighting coefficients $\mathbf{W}$ can change across conditions. We constructed

our EMG data matrix to have dimension $t \times r$, where t is the number of time points and r

is the number of (muscles $\times$ directions $\times$ trials), so that the NNMF algorithm would yield

temporally-fixed recruitment patterns $\mathbf{C}$ ($t \times n$ matrix) with spatially-varying weightings

$\mathbf{W}$ ($n \times r$ matrix) (Ivanenko et al. 2003). In order to weight the variance of each muscle

equally, we reshaped the data matrix to have individual muscle activity in columns,

scaled the columns of the matrix to have unit variance, and then restored the original

dimensions.

We extracted TF muscle synergies from EMG activity in all directions and trials

throughout postural responses to perturbations. For validation purposes, we extracted TF

muscle synergies from 60% of trials and reconstructed muscle activity in all trials.

Keeping the temporal recruitment patterns $\mathbf{C}$ constant, we varied muscle weighting

coefficients $\mathbf{W}$ to minimize the sum of squared errors between actual and reconstructed

EMG patterns. We ran the NNMF algorithm and subsequently unscaled the data matrix to

remove unit variance. Lastly, we normalized the TF muscle synergies to their maximum level of activation, yielding a value between 0 and 1 for each TF muscle synergy.

2.2.5 Determination of number of muscle synergies

We extracted 1-10 SF and TF muscle synergies throughout postural responses to perturbations in each subject, and further extracted 1-10 SF muscle synergies from individual epochs of the postural response in each subject. For each dataset, goodness-of-fit between actual and reconstructed EMG was quantified using variability accounted for (VAF), defined as 100 × the square of Pearson's uncentered correlation coefficient (Zar 1999). VAF was evaluated both globally and for all active muscles, ensuring the reproduction of relevant features of the data set. While total VAF evaluates the entire data matrix as a whole, muscle VAF evaluates individual muscles over directions, time bins, and repetitions.

We used a combination of global and local criteria (Chvatal et al. 2011; Torres-Oviedo et al. 2006; Torres-Oviedo and Ting 2007; 2010) to determine the fewest number of SF (N_{syn-S}) or TF (N_{syn-T}) muscle synergies needed to faithfully reconstruct the EMG data matrix. For each dataset, we quantified the ability of SF versus TF muscle synergies to account for the variability in the entire dataset (total VAF). We also quantified the ability of SF versus TF muscle synergies to account for the variability in individual muscles (muscle VAF). The number of SF or TF muscle synergies was increased as long as total VAF and VAF across muscles improved. However, additional SF or TF muscle synergies that contributed evenly to the VAF across muscles were not included because they likely represented noise in the data as opposed to variations between trials or

muscles. VAF of N_{syn-S} and N_{syn-T} was $\geq 75\%$ for each subject overall and for the majority

of active muscles (~14 of 16) in all perturbation epochs. A previously established

criterion for choosing the number of TF muscle synergies was to include TF muscle

synergies until the total VAF improved by $< 3\%$ (Ivanenko et al. 2005). When applied to

our dataset, both criteria yielded the same results with the exception of one TF muscle

synergy in 2 subjects. To ensure that N_{syn-S} or N_{syn-T} was appropriately determined, we

also validated N_{syn-S} and N_{syn-T} using factor analysis (FA). 1-10 factors were extracted

and likelihood ratios were computed for the addition of another muscle synergy. We then

graphed the log likelihood versus number of factors; N_{syn-S} and N_{syn-T} were chosen as the

point on the log likelihood plot that had the greatest curvature (Tresch et al. 2006). For

SF muscle synergies, if there was a discrepancy between N_{syn-S} calculated from VAF

versus FA, we examined the spatial tuning curves of the SF muscle synergies themselves.

If the addition of a muscle synergy yielded a flat or nondescript tuning curve, the

additional SF muscle synergy was likely accounting for noise and was not included in

analysis. For TF muscle synergies, there was no discrepancy between N_{syn-T} using either

VAF or FA.

For both SF and TF muscle synergies, we estimated the VAF confidence interval

(CI) for each muscle synergy extraction and ensured that the VAF CIs were non-

overlapping when compared to SF or TF muscle synergies extracted from a shuffled

matrix of the same data (Cheung et al. 2009). Each muscle was shuffled independently,

yielding the same values, range, and variance for muscles with different intermuscular

relationships. The 95% CI for VAF was estimated using bootstrapping. All actual and

shuffled datasets were resampled 500 times with data replacement, and VAF was

calculated from each resampling. VAF values were then ordered; the 95% CI was

represented as the 2.5 and 97.5 percentile of VAF distribution.

2.2.6 *Muscle synergy analysis*

We compared the degree to which SF or TF muscle synergy extractions could

account for total and muscle VAF. We performed a three-way ANOVA (subject ×

extraction method × dataset) on total and muscle VAF for SF and TF muscle synergies

using both actual and shuffled datasets (Zar 1999). We then verified the level of

significance between groups using Tukey-Kramer post-hoc tests ($\alpha = 0.01$).

SF and TF muscle synergies were used to reconstruct EMG patterns for all

perturbations. Measured and reconstructed data were compared over trials, muscles, and

perturbation directions to quantify the ability of SF versus TF muscle synergies to

faithfully reproduce EMG activity throughout perturbations in all subjects. We used r^2

and VAF to quantify the similarity between measured and reconstructed EMG (Torres-

Oviedo et al. 2006; Zar 1999). Both centered (r^2) and uncentered (VAF) Pearson

correlations were necessary: r^2 is high when shapes but not amplitudes of EMG traces are

well matched, while VAF is high when amplitude is high but shapes of traces are noisy.

We further determined the structural consistency of SF muscle synergies across

different epochs of perturbations by calculating correlation coefficients (r) between pairs

of SF muscle synergies. SF muscle synergies from individual epochs were paired with SF

muscle synergies from all epochs pooled together that yielded the highest value of r; this

criterion ensured that only positive correlations between SF muscle synergies were

considered. We considered a pair of SF muscle synergies to have consistent structure if r

> 0.623, which corresponds to the critical value of r^2 for 16 elements at p = 0.01 (r^2 = 0.388). However, because the NNMF algorithm constrains muscle synergies to be non-negative, we expected positive correlations by chance. Therefore, we generated 25,000 random permutations of the elements of SF muscle synergies extracted from the entire perturbation for each subject, yielding a distribution of chance r values with an expected mean (μ) and standard deviation (σ) (Berniker et al. 2009). An r-value of 0.623 corresponded to the 99th percentile of the distribution (p=0.008). Therefore, SF muscle synergy comparisons with r > 0.623 were considered more similar than expected by chance; comparisons with r ≤ 0.623 were considered uncorrelated and labeled as "additional".

2.2.7   Feedback model

To test our hypothesis that SF muscle synergies have time-varying recruitment patterns that are modulated by temporal feedback patterns, we fit SF muscle synergy recruitment patterns in anterior and posterior directions by using a "jigsaw" model based on delayed feedback of CoM kinematics as in previous studies (Welch and Ting 2009) (Figure 2.3). The model assumes that CoM kinematic signals are linearly combined to recruit SF muscle synergies in a feedback manner. Using CoM horizontal displacement (**d**), velocity (**v**), and acceleration (**a**), we reconstructed recruitment patterns C for each SF muscle synergy W_i (C_{W_i}) by assigning feedback gains (k_d, k_v, k_a) at a common time delay (λ), representing neural transmission and processing time, and then half-wave rectifying the muscle synergy recruitment pattern found using the equation below:

$$\mathbf{C}_{W_i} = k_d \mathbf{d}(t - \lambda) + k_v \mathbf{v}(t - \lambda) + k_a \mathbf{a}(t - \lambda)$$

Muscle synergies extracted from pooled perturbation epochs were used to reconstruct EMG activity throughout all A-P trials, yielding temporal recruitment patterns. The recruitment patterns were then interpolated and re-sampled at 1000 Hz for finer resolution. For every A-P trial, all active muscle synergies were included in analysis; an active muscle synergy was defined as a muscle synergy that was recruited at $\geq 20\%$ of maximum activation (determined over all trials) for at least 30 ms. All analyses were performed over a 1-s time interval, beginning 100 ms before platform onset ($t = 0$) to the end of the *stable* epoch of EMG activity following the end of the perturbation (t_{end}; 900 ms following perturbation onset). The initial feedback gains k_i were constrained to be between -5 and 5; this range was about an order of magnitude larger than the range of typical feedback gain values. The time delay λ was restricted to be between 90-150 ms, a range encompassing physiological delays of muscle activity to postural responses (Horak and Macpherson 1996). For each muscle synergy, three feedback gains (k_i) and a common time delay (λ) were identified that best reproduced the SF muscle synergy recruitment patterns according to the cost function

$$\min\left\{\mu_s \int_0^{t_{end}} e_m^2 dt + \mu_k \max\left(\left|e_m\right|\right)\right\}$$

The first term penalized the squared error (e_m) between recorded and simulated muscle synergy recruitment patterns throughout the perturbation with weight μ_s. The second

term penalized maximum error between simulated and recorded data at any point in time with weight μ_k. The ratio of $\mu_s{:}\mu_k$ was 10:1. Temporal patterns of recruitment for each SF muscle synergy were determined independently, yielding an independent set of feedback gains in response to the same CoM kinematics for a given trial. Feedback gains were then averaged over all trials and used to reconstruct SF muscle synergy recruitment patterns for active muscle synergies.

We also quantified the similarity between SF muscle synergy recruitment patterns obtained from experimental data and those predicted from the delayed feedback model. Recruitment patterns were considered well-reconstructed when mean $r^2 \geq 0.5$ or mean VAF $\geq 75\%$ for all trials in an active SF muscle synergy. The reconstructed SF muscle synergy recruitment patterns were also used to reconstruct observed EMG throughout A-P perturbations; r^2 and VAF were used to quantify the similarity between recorded and reconstructed EMG.
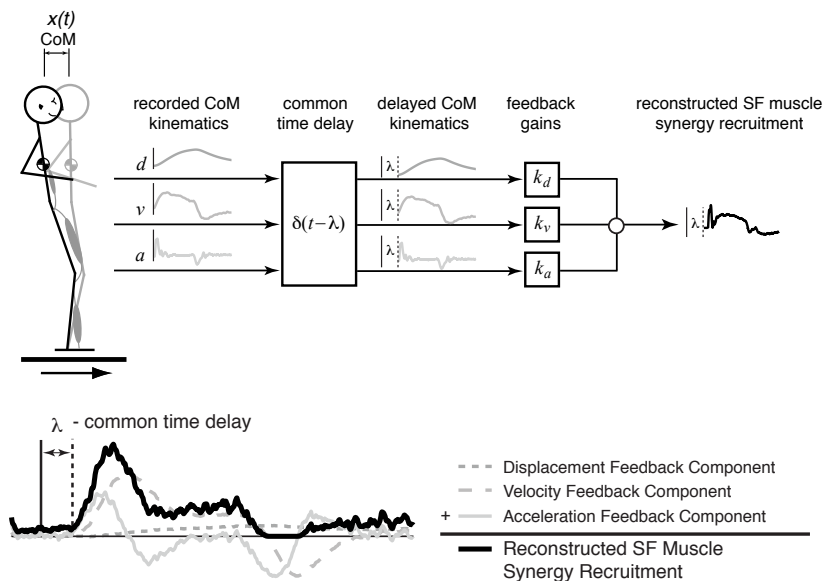
Figure 2.3. Delayed feedback model. Recorded CoM kinematics from A-P perturbations are used to reconstruct SF muscle synergy recruitment patterns throughout a perturbation. Each component of CoM motion is multiplied by a feedback gain at a common time delay and linearly added to produce a reconstructed SF muscle synergy recruitment pattern.

2.3   RESULTS

2.3.1   Summary

For each subject, a small number of both SF and TF muscle synergies was able to explain the majority of the variability in muscle activity throughout the timecourse of postural responses to perturbations. A small number of SF muscle synergies (≤ 7) accounted for significantly more EMG variability than a small number of TF muscle synergies. In each subject, a consistent set of SF muscle synergies was found across different epochs of postural responses. Furthermore, in anterior and posterior perturbations, SF muscle synergies exhibited variable recruitment patterns across trials, which were sufficient to explain differences in EMG patterns across trials and in different perturbation epochs. Temporal patterns of SF muscle synergy recruitment in anterior and posterior perturbations were well-reconstructed by delayed feedback of CoM kinematics in all subjects. Trial-by-trial variations in SF muscle synergy recruitment patterns were accounted for by trial-by-trial differences in CoM kinematics and a fixed set of feedback gains (k_d, k_v, k_a). Thus, EMG patterns measured throughout A-P perturbations could be reconstructed by a low-dimensional delayed feedback model that recruits SF muscle synergies based on CoM kinematics.

2.3.2   Postural responses throughout perturbations

CoM kinematics and intermuscular coordination patterns differed across perturbation epochs in postural responses to ramp-and-hold perturbations (Figure 2.2). During the *start* epoch, CoM kinematic vectors (**d**, **v**, **a**) were all oriented in the same direction, opposite that of platform acceleration. During the *stop* epoch, the platform decelerated to a final position, such that the resulting CoM acceleration vector was

opposite the direction of platform acceleration as well as opposite to the CoM position

and velocity vectors (Figure 2.2). Similarly, some muscles (e.g. ERSP, SEMT) had bursts

mainly in the *start* epoch in a matter resembling CoM acceleration. Other muscles (e.g.

VMED) showed increased activity later in the perturbation, similar to CoM displacement.

Another subset of muscles (e.g. TA) showed an initial burst of activity followed by

sustained activity throughout the perturbation. In addition, some muscles exhibited large

bursts of activity at inconsistent times during the postural response; these were largely

proximal muscles that moved the trunk, consistent with the "hip" strategy. These types

of responses were seen over all perturbation directions for all subjects.

2.3.3   EMG reconstructions using SF versus TF muscle synergies

We quantified the ability of SF versus TF muscle synergies to reconstruct EMG

variability (VAF) throughout a postural task. However, because SF versus TF muscle

synergy analyses impose different constraints, we evaluated EMG reconstructions of SF

versus TF muscle synergies in three ways to avoid biasing results toward either an SF or

TF muscle synergy organization. We first quantified total and muscle VAF using

previously established criteria for the number of SF muscle synergies (N_{syn-S}). We then

compared total VAF, muscle VAF, and individual EMG reconstructions using N_{syn-S} SF

muscle synergies to reconstructions using different numbers of TF muscle synergies

found by 1) previously established criteria for identifying TF muscle synergies (N_{syn-T}),

2) using the same number of components as SF muscle synergies (N_{syn-S}), and 3) roughly

matching the total number of parameters present in the model with N_{syn-S} SF muscle

synergies (N_{syn-P}).

SF muscle synergies reproduced postural EMG variability better than TF muscle synergies using either similar criteria or the same number of components (Figure 2.4A). Across all subjects, more SF muscle synergies (N_{syn-S}: 5-7) were identified compared to TF muscle synergies (N_{syn-T}: 2-4). N_{syn-S} SF muscle synergies accounted for significantly more total VAF than N_{syn-T} TF muscle synergies across all subjects (Figure 2.4A; N_{syn-S} total VAF = 85-92%, mean VAF $\pm$ SD=88 $\pm$ 2%; N_{syn-T} total VAF = 75-85%, mean VAF $\pm$ SD = 79 $\pm$ 3%; F[3,63] = 81.57, p < 10^{-16}; p < 0.01 using Tukey-Kramer post-hoc analysis). Moreover, N_{syn-S} SF muscle synergies accounted for more muscle VAF than N_{syn-T} TF muscle synergies in all subjects at α=0.01 (N_{syn-S} muscle VAF = 31-100%, 85 $\pm$ 13%; N_{syn-T} muscle VAF = 75-85%, 79 $\pm$ 3%; F[3,1023] = 79.25; p < 10^{-16}; p < 0.01 using Tukey-Kramer post-hoc analysis). To ensure that the observed differences in VAF were not due to the smaller number of TF muscle synergies, we quantified VAF using N_{syn-S} TF muscle synergies. The total VAF of the dataset using N_{syn-S} TF muscle synergies was still significantly lower than that of N_{syn-S} SF muscle synergies (Figure 2.4A; N_{syn-S} TF VAF = 85 $\pm$ 2%; p < 0.01).

We also evaluated EMG reconstructions using SF versus TF muscle synergies to match the total number of parameters present in the two methods of analysis (N_{syn-P} TF versus N_{syn-S} SF muscle synergies). A much larger number of TF muscle synergies was necessary (N_{syn-P}: 20-29) in order to incorporate roughly the same number of parameters for TF and SF muscle synergy extractions. However, using N_{syn-P} TF muscle synergies, both total VAF and muscle VAF were significantly higher than using N_{syn-S} SF muscle synergies (Figure 2.4A; N_{syn-P} TF total VAF = 95 $\pm$ 1%, p < 0.05; N_{syn-P} TF muscle VAF = 95 $\pm$ 1%, p < 0.01).

A Total and Muscle VAF - All Subjects

B Total VAF - Subject 1

TF muscle synergies: —— Actual data ----- Shuffled data
SF muscle synergies: —— Actual data ----- Shuffled data
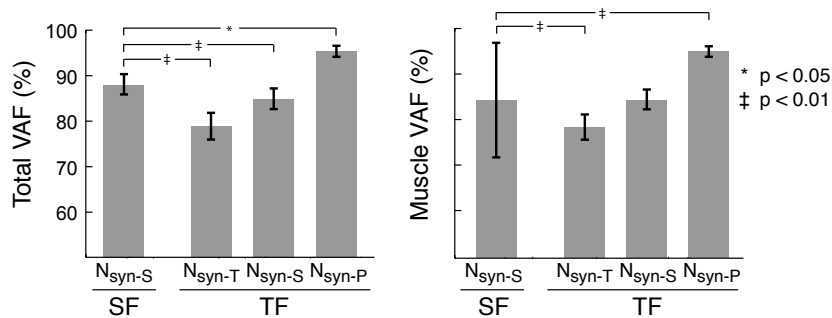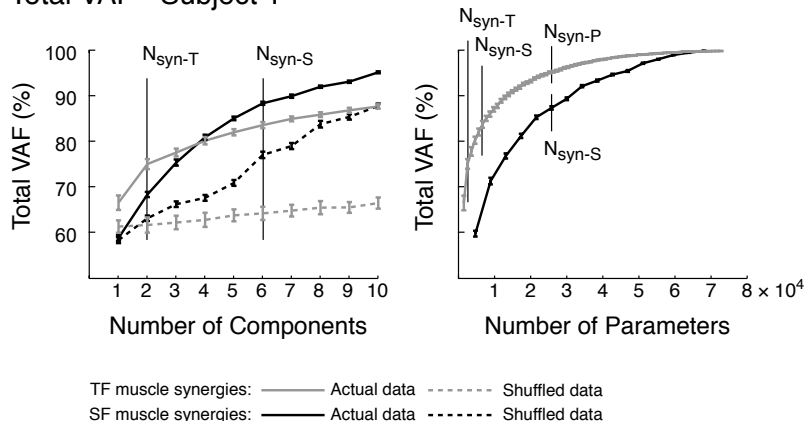
Figure 2.4. Variability accounted for (VAF) comparisons using TF versus SF muscle synergies. A, total and muscle VAF for all subjects. N_{syn-S} SF muscle synergies explain a significantly larger portion of the dataset than N_{syn-T} or N_{syn-S} TF muscle synergies, but significantly less variability than N_{syn-P} TF muscle synergies. Error bars represent standard deviation of the mean. * - $p < 0.05$, ‡ - $p < 0.01$, ANOVA, Tukey-Kramer post-hoc tests. **B,** total VAF for subject 1. *Left panel: total VAF versus number of components.* Total VAF with N_{syn-S} SF muscle synergies is higher than VAF with N_{syn-T} or N_{syn-S} TF muscle synergies. Both methods of synergy extraction account for significantly more variability than with shuffled muscle synergies. *Right panel: total VAF versus number of parameters incorporated into the muscle synergy extraction.* VAF of TF muscle synergies was always higher than SF muscle synergies. However, many more TF muscle synergies (25) were needed to incorporate the same number of parameters as SF muscle synergies (6). Error bars represent the estimated 95% confidence interval of VAF.

The differences in total VAF between SF and TF muscle synergies were found in each subject. For example, in a representative subject (subject 1), six SF muscle synergies were needed to meet the criteria for EMG reconstruction. By contrast, only two TF muscle synergies were needed to meet the criteria (Figure 2.4B – left panel). On average, the lower limit of the 95% confidence interval (CI) for total VAF of N_{syn-S} SF muscle synergies was 4.0 CIs higher than the upper limit of the 95% CI for N_{syn-T} TF muscle synergies. In our representative subject, the lower limit of the 95% confidence interval (CI) for total VAF of N_{syn-S} SF muscle synergies was 1.8 CIs higher than the upper limit of the 95% CI for N_{syn-S} TF muscle synergies (Figure 2.4B). When comparing VAF as a function of the number of parameters, VAF was always higher for TF versus SF muscle synergies (Figure 2.4B – right panel). However, 25 TF muscle synergies were needed to incorporate the same number of parameters as N_{syn-S} SF muscle synergies.

SF muscle synergy structure was different than TF muscle synergy structure, and TF muscle synergy structure varied depending on the criteria used (Figure 2.5A). Because SF muscle synergies fractionated muscle activity spatially, each SF muscle synergy corresponded to a specific muscle coordination pattern. Note that muscles with multiple actions (i.e. RFEM) can belong to more than one SF muscle synergy with presumably different functions (e.g. W4 – RFEM/TA; W6 – RFEM/quadriceps). Moreover, antagonistic muscles such as TA and MGAS are not grouped in the same SF muscle synergy. In contrast, TF muscle synergies fractionated muscle activity by time (Figure 2.5A – right columns). Each TF muscle synergy was activated in a localized region in time; this time-localized region became shorter and shorter as the number of TF muscle synergies increased.
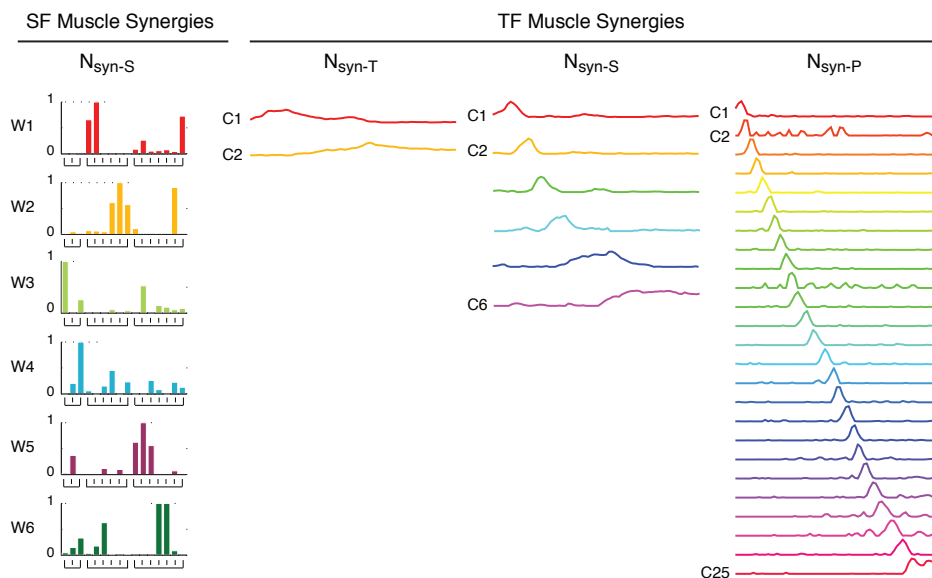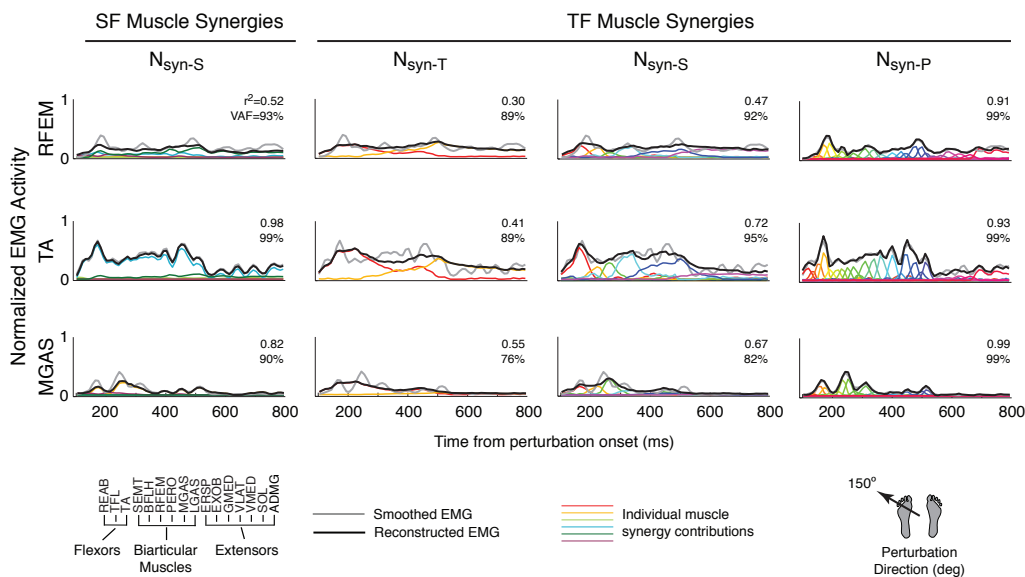
Figure 2.5. Comparison of SF versus TF muscle synergy structure and muscle reconstructions. A, muscle synergy structure. SF muscle synergies organize muscle activity into groups of muscles that have common spatial activation patterns (left column). TF muscle synergies organize muscle activity into consistent temporal patterns (right columns). As the number of TF muscle synergies increases, temporal patterns of activation become more localized in time. Data are shown for subject 1. **B,** muscle reconstructions during a forward-leftward (150°) perturbation. A small subset of SF muscle synergies was recruited to reconstruct each muscle (left column). Note that multiple SF muscle synergies contributed to the reconstruction of muscles with multiple actions (i.e. W4 and W6 for REFM), and separate SF muscle synergies were recruited in antagonistic muscle pairs (W4 for TA, W2 for MGAS). In contrast, a majority of TF muscle synergies was recruited to reconstruct each muscle (right columns). The same TF muscle synergies were used to recruit antagonistic muscle pairs. Grey lines: smoothed EMG. Black lines: reconstructed EMG. Colored lines: individual muscle synergy contributions.

Individual muscle reconstructions were fundamentally different when using SF versus TF

muscle synergies (Figure 2.5B). For example, in individual muscle reconstructions for a

forward-leftward (150°) perturbation using SF muscle synergies, RFEM was

reconstructed using W4 and W6. Moreover, antagonistic muscles TA and MGAS were

reconstructed using different SF muscle synergies W4 and W2, respectively (Figure 2.5B

– left column). In contrast, regardless of the number of components used, the majority of

TF muscle synergies were used to reconstruct any one muscle. For example, both C1 and

C2 were used to reconstruct RFEM, as well as antagonistic muscles TA and MGAS when

using N_{syn-T} TF muscle synergy components (Figure 2.5B). Although muscle

reconstructions improved when using N_{syn-S} or N_{syn-P} TF muscle synergies, a majority of

TF muscle synergies were still used to reconstruct all muscles. Moreover, the increased

localization of the TF muscle synergies approached the time resolution of the EMG

signals.

When reconstructing EMG data across perturbation directions, SF muscle

synergies had more consistent temporal recruitments than the spatial weightings of TF

muscle synergies (Figure 2.6). Because muscle activity is tuned to certain spatial

directions, SF muscle synergies are recruited only in a subset of directions. For example

in subject 1, W2 comprised mainly of calf muscles had large temporal patterns of

recruitment in backward and backward-leftward perturbations (210° – 300°) that caused

dorsiflexion (Figure 2.6A). Although TF muscle synergies are recruited across all

perturbation directions, the muscle weightings varied considerably. TF muscle synergy

C1 was mainly active in the initial postural response (Figure 2.6B), activating mainly TA

in forward-rightward perturbations (0° – 60°), TA with proximal muscles (EXOB,

A SF muscle synergies - varying temporal recruitment by direction
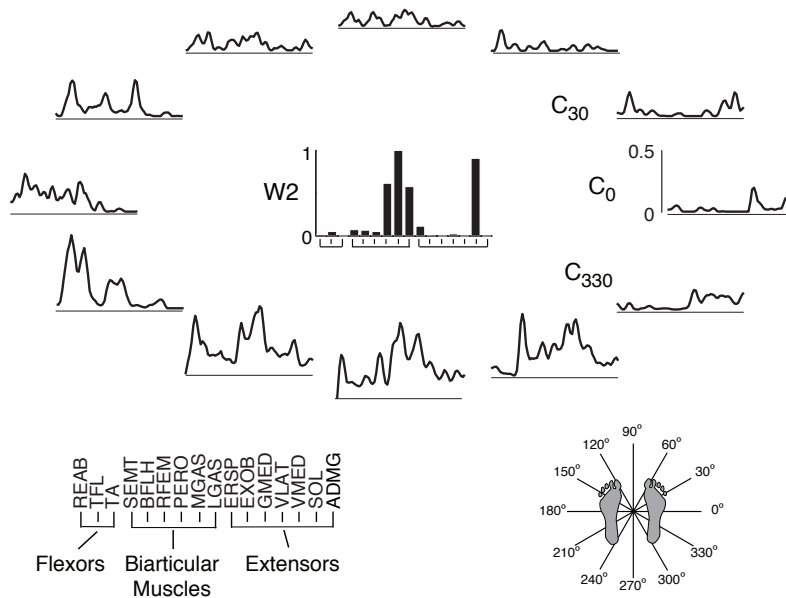
B TF muscle synergies - varying spatial recruitment by direction
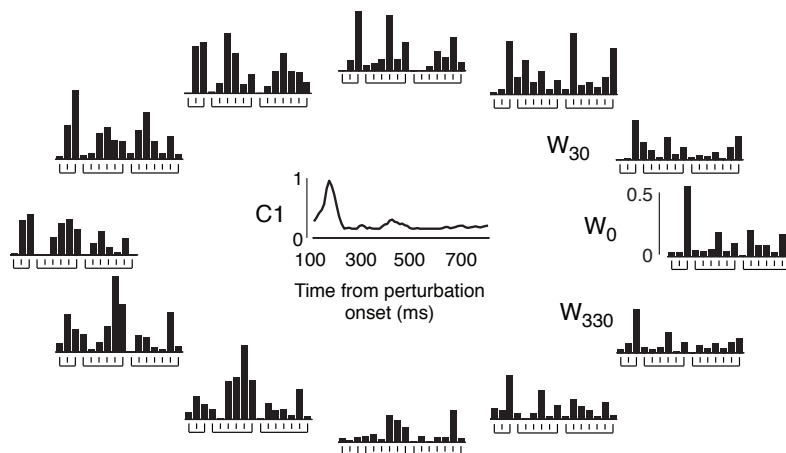
Figure 2.6. Variable SF muscle synergy recruitment versus variable TF muscle synergy weighting across multidirectional perturbations. A, SF muscle synergies. SF muscle synergy recruitment was variable over directions but consistently recruited in backward and leftward (210° – 300°) perturbations. **B,** TF muscle synergies. TF muscle synergy weightings changed considerably over directions and trials and included antagonistic pairs of muscles. Data are shown for the same subject as in Figure 2.5 (subject 1).

GMED, TFL) in forward-leftward perturbations ($120° - 180°$), and TA with calf muscles (PERO, MGAS, LGAS, SOL) in backward-leftward perturbations ($210° - 270°$). Because a single TF muscle synergy describes the muscle activity of a small time bin, the resulting muscle weightings describe the EMG pattern during that time bin.

2.3.4 SF muscle synergies have similar structure across perturbation epochs

A small number of SF muscle synergies independently extracted from different perturbation epochs could equally explain the total EMG variability of postural responses. Only 3-7 SF muscle synergies were necessary to reconstruct the activity of 16 muscles during postural perturbations in all subjects, regardless of the extraction epoch (cf. Figure 2.2). 4-6 SF muscle synergies accounted for EMG activity in *start* (total VAF = $87 \pm 2\%$) and *plateau* ($86 \pm 4\%$) epochs, consistent with previous studies on human balance (Torres-Oviedo and Ting 2007). In addition, 3-6 SF muscle synergies were able to account for EMG activity in previously unexamined *stop* ($88 \pm 4\%$) and *stable* ($88 \pm 1\%$) epochs using 10 ms bins. 5-7 SF muscle synergies were necessary to reproduce EMG activity from the entire perturbation ($87 \pm 3\%$).

In all subjects, a subset of SF muscle synergies extracted from individual epochs had consistent structure when compared to SF muscle synergies extracted from the entire perturbation. 2-4 SF muscle synergies per subject were consistent across all epochs at $p < 0.01$ ($0.62 \le r \le 1.0$; $r = 0.88 \pm 0.10$). Moreover, 1-5 SF muscle synergies per subject were not identified in every epoch but were consistent whenever they were found ($0.66 \le r \le 1.0$, $r = 0.90 \pm 0.10$). Six of eight subjects had at least one additional SF muscle synergy; these SF muscle synergies were most often found in the *start* and

plateau epochs and were most often composed of proximal muscles that acted at the hip joint.

The level of consistency in SF muscle synergy structure across epochs was robust for all subjects. For example, subject 7 had the highest comparisons between SF muscle synergy pairs (Figure 2.7A). In subject 7, four of the six SF muscle synergies (W1, W2, W3, W6) were consistent across every epoch ($0.76 \leq r \leq 1.0$, $r = 0.92 \pm 0.073$). W4 and W5 were consistent across epochs where they were identified ($0.68 \leq r \leq 0.99$, $r = 0.90 \pm 0.15$). Subject 5 had the lowest level of consistency between SF muscle synergy pairs (Figure 2.7B). For subject 5, all six SF muscle synergies from the entire perturbation (*all*) had consistent structure with SF muscle synergies from various epochs ($0.67 \leq r \leq 0.99$, $r = 0.86 \pm 0.10$). However, three additional SF muscle synergies (W7, W8, W9) were identified. Of the additional SF muscle synergies, W7 was composed primarily of ankle flexors TA and PERO, W8 consisted mainly of RFEM, a biarticular muscle that aids in hip flexion, and W9 was composed mainly of hamstring muscles (BFLH, SEMT) as well as muscles that acted at the hip and trunk (EXOB, ERSP, GMED).

2.3.5   *Consistent SF muscle synergies across subjects*

Although different subjects had different numbers of SF muscle synergies, the muscular composition of SF muscle synergies was similar across subjects (Figure 2.8). Ten different SF muscle synergies were found across all subjects. Two SF muscle synergies (W2, W6) were found in all 8 subjects ($0.71 \leq r \leq 0.96$, $r = 0.87 \pm 0.072$) and had muscles spanning the ankle and knee, respectively. Three additional SF muscle synergies (W1, W2, W5) were found in 7 of 8 subjects ($0.62 \leq r \leq 0.95$, $r = 0.83 \pm 0.11$),
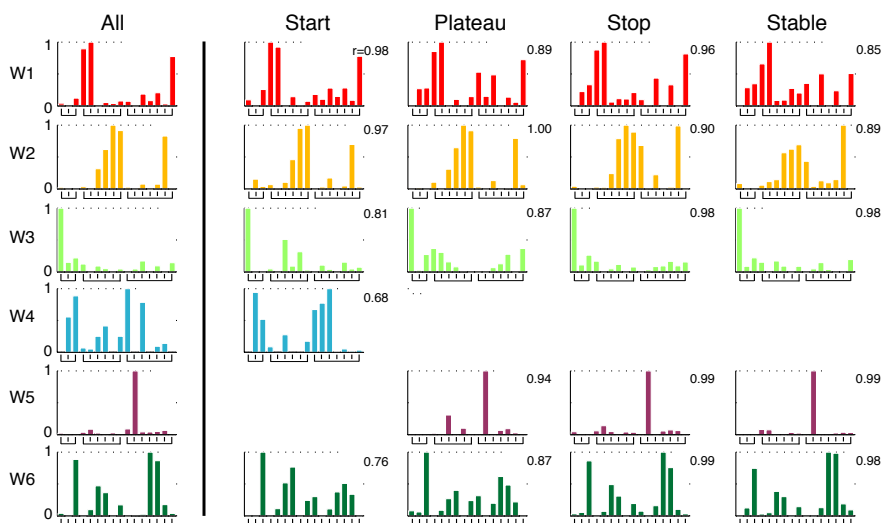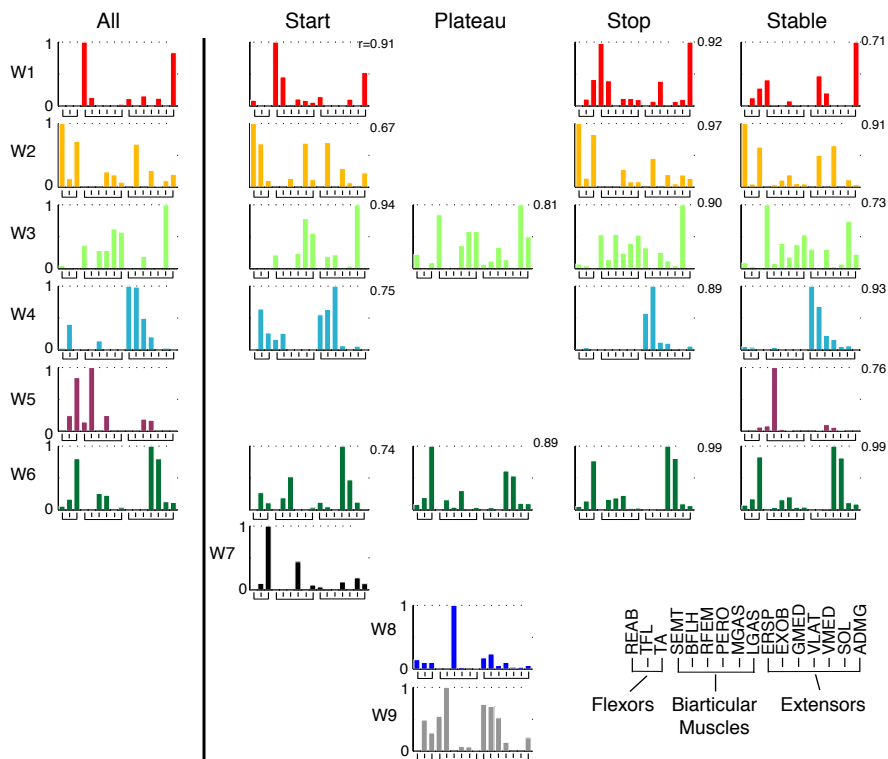
Figure 2.7. Comparison of SF muscle synergy structure across various epoch throughout a perturbation. A, comparisons for a subject with high structural consistency (subject 7). SF muscle synergies extracted independently from *start*, *plateau*, *stop*, and *stable* epochs were similar to those extracted from all epochs pooled together (*all*). W1, W2, W3, and W6 were identified in every epoch, while W4 and W5 were only identified in some epochs. **B,** comparisons for a subject with low structural consistency (subject 5). W3, and W6 were identified in every epoch, while W1, W2, W4, and W5 were only identified in some epochs. Three SF muscle synergies were uncorrelated at $p < 0.01$ ($r < 0.623$) and were considered "additional". W7 was mainly composed of ankle muscles TA and PERO, W8 was mainly composed of RFEM, a biarticular muscle that aids in hip flexion, and W9 had large involvement of hamstrings (BFLH, SEMT) and muscles with actions at the trunk and hip (EXOB, ERSP, GMED).
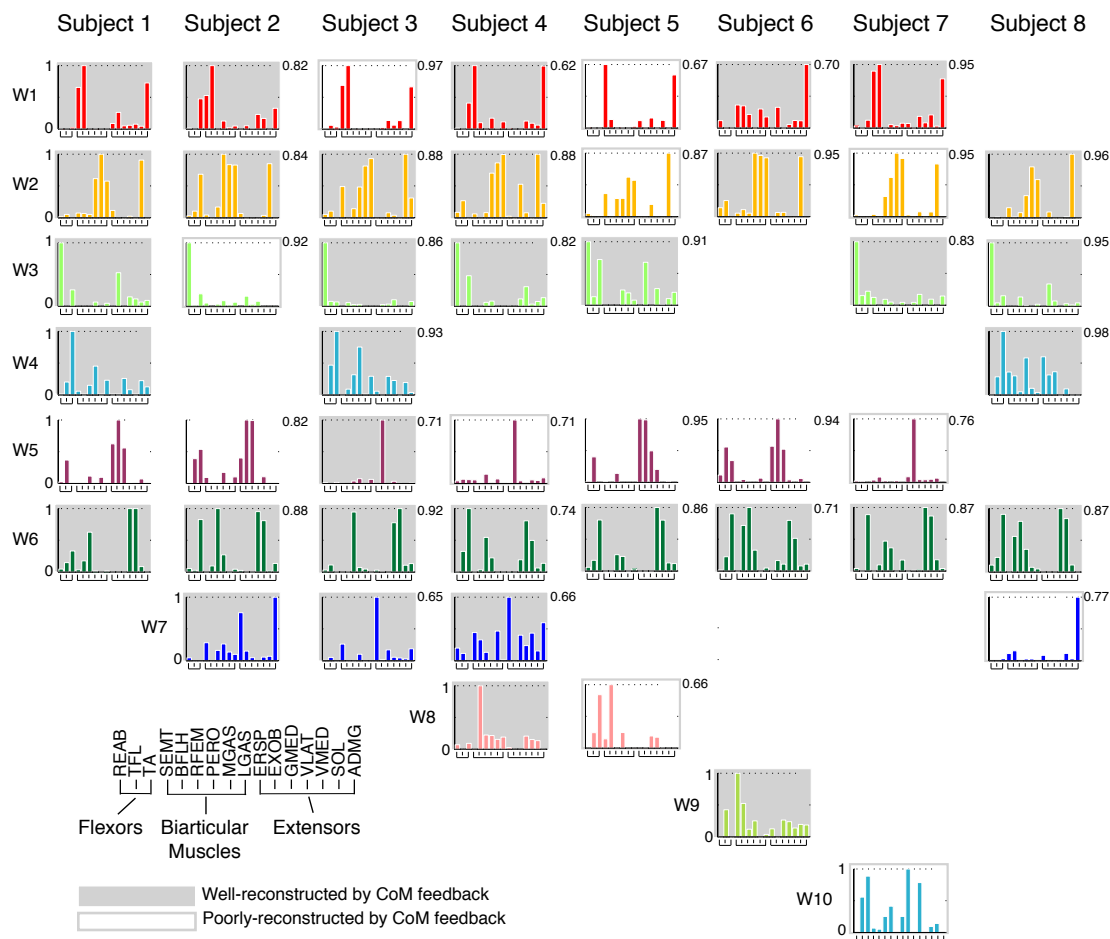
Figure 2.8. SF muscle synergies extracted from the entire timecourse of perturbations for all subjects. Five of ten SF muscle synergies (W1, W2, W3, W5, W6) were similar in at least 7 of 8 subjects. Of the remaining SF muscle synergies, W8 and W9 had large contributions from the hamstrings (BFLH, SEMT), biarticular muscles that aid in hip extension. W10 had large contributions from trunk muscles. Grey shaded and outlined SF muscle synergies were active during A-P perturbations (n = 44). For active SF muscle synergies, shaded muscle synergies were well-reconstructed using a delayed feedback model based on CoM motion across A-P trials (34/44). Outlined muscle synergies (10/44) were poorly-reconstructed by the feedback model. Of these ten SF muscle synergies, eight had major contribution of mono- and biarticular muscles acting at the hip. Numbers indicate r values for comparisons.

having actions of hamstring and trunk muscles. Three of the remaining four SF muscle synergies (W4, W7, W8) were found in only 2-4 subjects; W4 was composed mainly of calf muscles, W7 of hip muscles, and W8 of hamstrings. Two SF muscle synergies (W9 and W10) were statistically different than all of the other SF muscle synergies and had a large hamstring or trunk muscle contribution.

2.3.6   *CoM kinematic feedback reconstructs SF muscle synergy recruitment*

SF muscle synergies exhibited time-varying recruitment patterns across directions with considerable trial-to-trial variability (Figure 2.9). For each perturbation direction, a subset of SF muscle synergies was recruited to maintain balance. Each SF muscle synergy was recruited in response to a subset of perturbation directions. For example, data from a representative subject (subject 2) are shown for one forward and one backward trial (Figure 2.9A). In this subject, four muscle synergies (W1, W3, 54, W6) were active (recruited at $\geq$ 20% of maximum activity for at least 30 ms) in forward (90°) perturbations; W2 and W5 were active in backward (270°) perturbations. In contrast, W4 was active in mediolateral (0°/180°) perturbations. Within a given perturbation direction, active SF muscle synergies were recruited at different times during the perturbation. For forward perturbations, W1, W5, and W6 had bursts of activity in the start epoch. While W6 was mainly active during the *start* epoch alone, W1 and W5 had continued activity extending through the *stop* epoch. W5 remained active during the *stable* epoch. W3 was active in the *plateau* through *stable* epochs, peaking during the *stop* epoch. For backward perturbations, W2 was active in the *start* and *plateau* epochs. W5 was active during the

start epoch. SF muscle synergy recruitment patterns also varied from trial-to-trial; for example, W1 was recruited differently across five anterior perturbations (Figure 2.9B).

For each subject, a subset (2-7) of active SF muscle synergy recruitment patterns was well-reconstructed in A-P perturbations. We only considered the recruitment of active SF muscle synergies, which had ≥ 20% of maximum activity for at least 30 ms in a trial. In a subject representative of our average results (subject 2), four of six SF muscle synergies (W1, W2, W5, W6) were well-reconstructed (Figure 2.9A, shaded boxes). While W5 was also defined as active in the backward direction by our criteria, it was not well-reconstructed for backward perturbations (Figure 2.9A, outlined box). We defined a well-reconstructed SF muscle synergy recruitment pattern to have an average $r^2 \geq 0.50$ or VAF ≥ 75% over all trials. This threshold was well above the reconstruction of SF muscle synergy recruitment patterns using shuffled CoM kinematics ($r^2 = 0.02 \pm 0.027$; VAF = 31 ± 16%). W1 responded similarly to backward position, velocity, and acceleration, W2 responded mainly to forward velocity, W5 responded mainly to backward position, and W6 responded mainly to backward acceleration. Time delays were between 100-120 ms for all trials, consistent with postural delays described in the literature. Although the feedback model reconstructed most of the contour of the recruitment patterns, it often did not account for short bursts in the start epoch of individual trials (data not shown). However, these short bursts were seen in perturbations of many directions and likely represented co-contraction of muscles in response to the onset of perturbation.
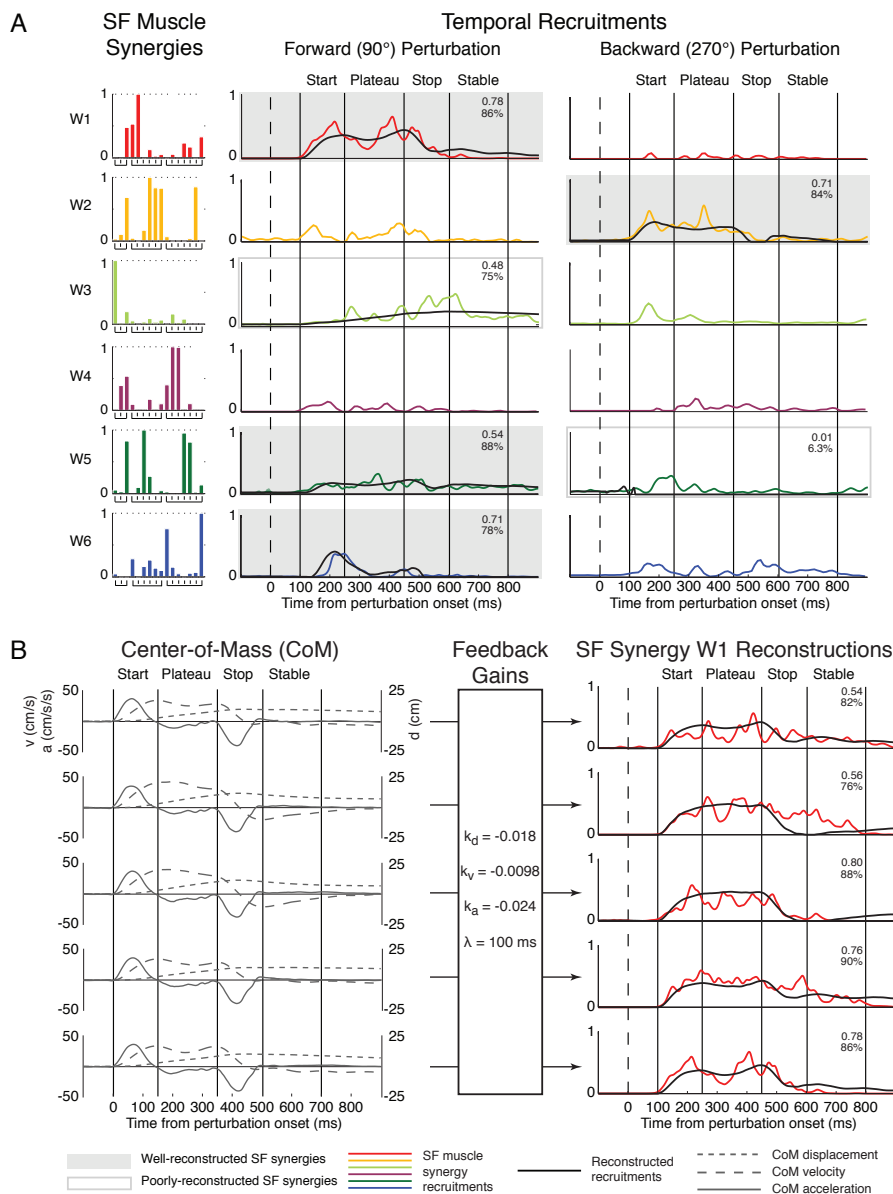
Figure 2.9. Feedback model reconstruction of SF muscle synergy recruitment patterns. Data are shown for subject 2. **A,** reconstruction of recruitment patterns in a forward and backward perturbation. SF muscle synergies (W1-W6) are differentially recruited throughout A-P perturbations. Active SF muscle synergies (shaded) were reconstructed using a delayed feedback model based on CoM motion. W1, W2, and W6 were well-reconstructed across trials (mean $r^2 \geq 0.5$ or mean VAF $\geq 75\%$ for all trials). W2 was poorly-reconstructed over trials. W5 was well-reconstructed in forward perturbations, but poorly-reconstructed in backward perturbations. Both W1 and W6 have major contributions from mono- and biarticular muscles affecting the trunk (REAB, RFEM, GMED). Reconstructions are only shown for one trial for ease of interpretation. Colored lines: SF muscle synergy recruitment patterns; black lines: feedback model reconstructions. **B,** reconstruction of muscle synergy W1 for all forward trials. Inter-trial differences in SF muscle synergy recruitment can be accounted for by differences in CoM kinematics. Using a single set of feedback gains, the feedback model can account for trial-by-trial variability in recruitment for SF muscle synergies. Numbers indicate r^2 (top) and VAF (bottom) values for reconstructions. Grey lines: CoM kinematics; colored lines: muscle synergy recruitment patterns; black lines: feedback model reconstructions.

Using the feedback model, a fixed set of feedback gains (k_d, k_v, k_a) could reconstruct trial-by-trial variability in SF muscle synergy recruitment patterns (Figure 2.9B), but could not account for the timecourse of TF muscle synergies. While W1 was recruited differently over all five forward perturbations, the differences in W1 recruitment could be reconstructed by the differences in CoM kinematics for each trial. For example, CoM velocity peaked twice in trials 4, and 5; these peaks were seen in the actual and reconstructed recruitment of W1 for these trials. Similarly, CoM displacement remained high throughout trials 1 and 4, resulting in continued W1 recruitment (actual and reconstructed) in the *stable* epoch for these trials. While CoM feedback on SF muscle synergies did not predict all bursts in SF muscle synergy recruitment (e.g. *stop* and *stable* epochs in trial 2), CoM feedback on TF muscle synergies could not account for any trial-by-trial variability, as the temporal commands were fixed across trials for a given time epoch by definition. Furthermore, a given TF muscle synergy exhibited the same pattern of recruitment for all directions of perturbation, resulting in inconsistent feedback gains for every direction of perturbation.

A delayed feedback model based on CoM kinematics reproduced a majority of SF muscle synergy recruitment patterns throughout A-P perturbations across all subjects. Across all subjects, the recruitment patterns of 34 of 48 SF muscle synergies were well-reconstructed by the feedback model (Figure 2.8, shaded boxes). For all SF muscle synergies, the model used a delay (λ) of 100-130 ms, consistent with previously described postural delays (Horak and Macpherson 1996; Nashner 1976). 14 of the 48 SF muscle synergies across subjects were poorly-reconstructed by the feedback model in A-P perturbations (Figure 2.8, outlined boxes). These SF muscle synergies had

unpredictable and/or inconsistent recruitment patterns (e.g. Figure 2.9A, W3). 12 of the

14 poorly-constructed SF muscle synergies involved hip and hamstring muscles. Two

more poorly-reconstructed SF muscle synergies had a major contribution of RFEM, a

biarticular muscle that aids in hip flexion. In addition, two subjects had SF muscle

synergies with inconsistent feedback gains between A-P perturbations (four SF muscle

synergies total). These SF muscle synergies also had large contribution of mono- and

biarticular muscles that acted at the hip. To determine if hip angle kinematics could be

responsible for SF muscle synergy recruitment patterns in the poorly-reconstructed SF

muscle synergies, we qualitatively compared the hip angle kinematics to muscle synergy

recruitment. While the hip angle kinematics were different than CoM kinematics,

changes in hip kinematics were not seen until after the onset of SF muscle synergy

recruitment patterns, making hip angle kinematics an unlikely candidate for driving the

recruitment of SF muscle synergies with actions at the hip.

*2.3.7   SF muscle synergies recruited by CoM feedback reproduce temporal variations in
muscle activity*

By flexibly combining SF muscle synergies with time-varying recruitment

patterns, a small set of SF muscle synergies reconstructed muscle activity throughout

postural responses to A-P perturbations (Figure 2.10, left column). Of 16 surface EMGs,

5-7 SF muscle synergies were needed to reproduce muscle activation patterns in all

subjects. These SF muscle synergies were able to reproduce bursts of activity seen in

start and *stop* epochs, as well as continuing muscle activity seen in *plateau* and *stable*

epochs for all A-P trials ($r^2 = 0.78 \pm 0.16$; VAF = $91 \pm 9\%$). Notice that the recruitment

patterns of individual SF muscle synergies (colored lines) were scaled differently for each

muscle; the scaling corresponds to the muscular contribution of each SF muscle synergy (see figure 2.9 muscle synergy composition and recruitment). Also note that multiple SF muscle synergies can contribute to a temporal EMG pattern. For example, in forward perturbations, EMG activity of ADMG during the *start* epoch is mainly reconstructed with W6 (blue). In the late *plateau* and *stop* epochs, W1 (red) is the major contributor to ADMG activity. Similarly, the initial burst of PERO in backward perturbations is reconstructed with W2 (orange) with a contribution of W6 (blue) to reconstruct later activity.

Feedback model reconstructions of SF muscle synergy recruitment patterns were also able to reconstruct muscle activity throughout postural responses to perturbations (Figure 2.10, right column). By replacing SF muscle synergy recruitment patterns determined by NNMF with feedback model recruitment patterns, EMG activity was reconstructed throughout A-P perturbations in all trials for all subjects ($r^2 = 0.65 \pm 0.22$; VAF = $85 \pm 11\%$). However, correlation values were significantly lower than those for EMG reconstructed from NNMF recruitment patterns ($p < 0.01$ for r^2 and VAF). This discrepancy may be due to the low frequency signal of feedback model recruitment patterns being unable to reproduce higher frequency oscillations seen in EMG patterns. Alternatively, high frequency oscillations in SF muscle synergy recruitment patterns may represent high frequency coupling of muscles due to either a slightly different form of feedback or the superposition of CoM feedback with other concurrent feedback mechanisms. Nevertheless, N_{syn-S} SF muscle synergies with feedback model recruitment patterns still reconstructed EMG activity significantly better than TF muscle synergies in

all subjects using either $N_{syn\text{-}T}$ ($r^2 = 0.35 \pm 0.17$; VAF $= 78 \pm 11\%$; $p < 0.01$ for r^2 and

VAF) or $N_{syn\text{-}S}$ ($r^2 = 0.51 \pm 0.17$; VAF $= 84 \pm 8\%$; $p < 0.01$ for r^2) TF muscle synergies.

A Reconstructed Muscle Activity - Forward Perturbation

Unconstrained SF Synergy Recruitments

Feedback SF Synergy Recruitments
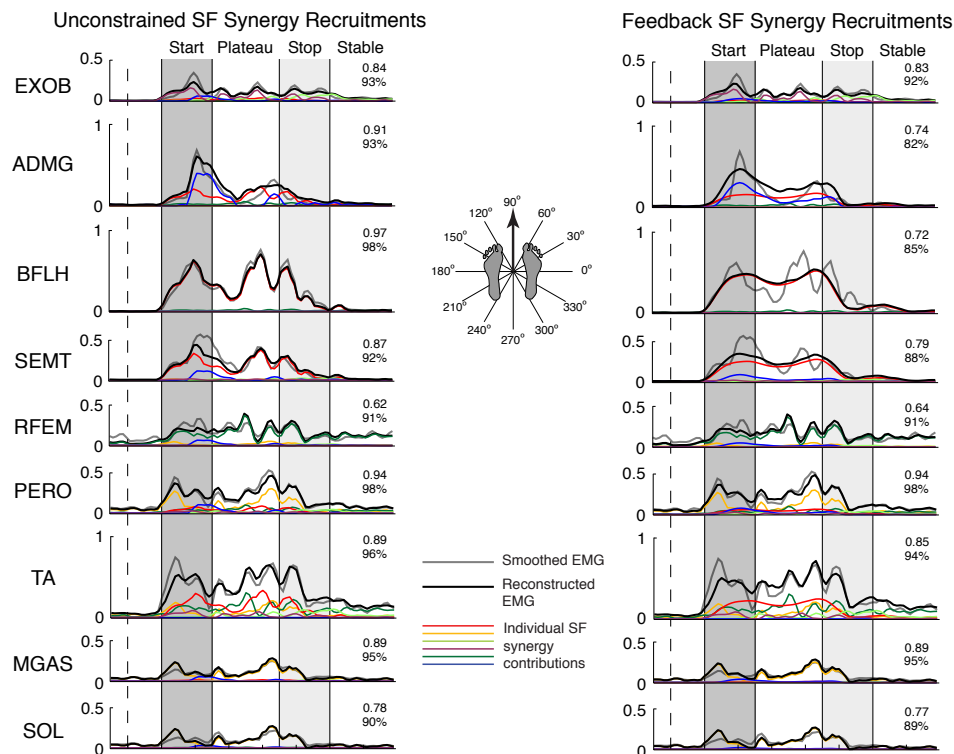
B Reconstructed Muscle Activity - Backward Perturbation

Time from perturbation onset (ms)

Time from perturbation onset (ms)
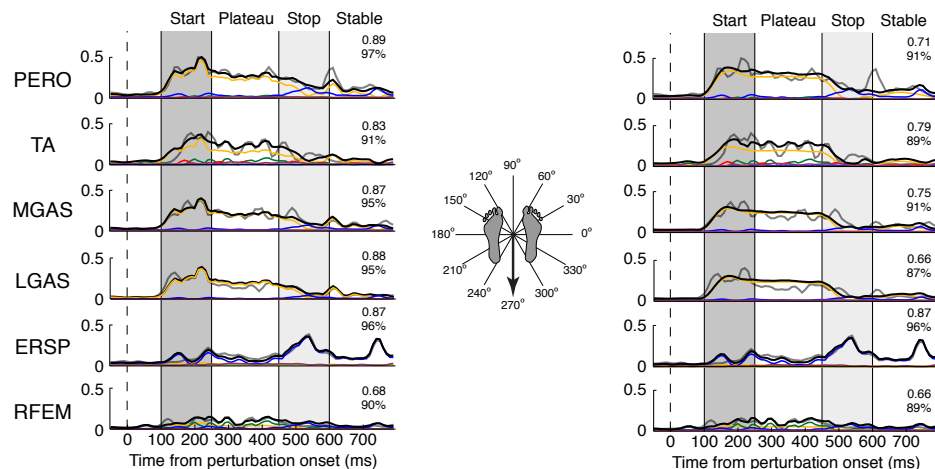
Figure 2.10. Reconstruction of individual muscle activity using SF muscle synergy recruitment patterns determined from NNMF (unconstrained, left) and the feedback model (right) for a forward (A) and backward (B) perturbation. Data are shown for subject 2. Although recruitment patterns determined from NNMF explain the variability better than recruitment patterns determined from the feedback model, both methods of extraction have high correlation values for active muscles in A-P perturbations. Both SF muscle synergy recruitment patterns reconstructed muscle activation patterns significantly better than when using N_{syn-T} (p < 0.01 for r^2 and VAF) or N_{syn-S} (p < 0.01 for r^2) TF muscle synergy recruitment patterns (data not shown). Grey lines: smoothed EMG; black lines: reconstructed EMG; colored lines: individual SF muscle synergy contributions.

2.4 DISCUSSION

2.4.1 Summary

Taken together, our results suggest that the nervous system produces motor outputs using a multisensory estimate of task-level variables to modulate SF muscle synergies. SF muscle synergies provide a low-dimensional sensorimotor transformation whereby task-level variables can be mapped to execution-level variables that define the spatiotemporal patterns of muscles. For standing balance control, many of the identified SF muscle synergies were recruited throughout postural perturbations by delayed feedback on the task-level variables defined by CoM kinematics. Thus, the low-dimensional organization of temporal and spatial features of muscle coordination are independent during postural responses to perturbations. These results are consistent with a hierarchical neural control scheme where a low-dimensional feedback structure recruits SF muscle synergies.

2.4.2 Feedback control of SF muscle synergies for standing balance

Our results support the idea that the temporal modulation of SF muscle synergies is a general neural mechanism for producing a wide range of both feedforward and feedback movements. Here, we showed that SF muscle synergies are modulated on a much finer timescale (10 ms) than prior studies (Torres-Oviedo et al. 2006; Torres-Oviedo and Ting 2010), and that the same SF muscle synergies are recruited throughout the entire timecourse of muscle activity that extends beyond the end of the perturbation. In contrast, prior studies only investigated SF muscle synergies in a few coarse (75 ms) time bins during the initial postural response and did not include deceleration epochs that have more variable spatial and temporal patterns of muscle activation (Carpenter et al.

2005). We studied the entire timecourse of postural stabilization and found that despite the differences in body configuration and dynamics in later epochs, SF muscle synergies nonetheless had consistent structure across perturbation epochs, but could be recruited differently from trial to trial, consistent with previous studies (Torres-Oviedo and Ting 2007). Similarly, SF muscle synergies have been shown to be modulated throughout voluntary tasks that alter limb configuration, including upper limb reaching movements (Cheung et al. 2009; Muceli et al. 2010). SF muscle synergies are also shared across motor tasks with different dynamics (Cheung et al. 2005; d'Avella and Bizzi 2005; Kargo et al. 2010). Moreover, SF muscle synergies are preserved after the removal of sensory feedback but the temporal recruitment of muscle synergies is altered (Cheung et al. 2005). Similarly, in post-stroke hemiparesis, the timing of SF muscle synergy recruitment during gait is impaired, but the structure of SF muscle synergies is similar to that found in healthy subjects (Clark et al. 2010).

Our results suggest that the temporal recruitment of SF muscle synergies during human balance control is constrained by low-dimensional task-variables. Previously, constraints have been identified in the temporal structure of muscle activity using TF muscle synergies (Cappellini et al. 2006; Ivanenko et al. 2005; Ivanenko et al. 2004); alternatively, no constraints on temporal structure have been applied when using SF muscle synergies (Hart and Giszter 2004; Saltiel et al. 2001; Torres-Oviedo and Ting 2007). Here we demonstrate that the temporal constraints on the recruitment of SF muscle synergies are decoupled from the spatial constraints in human postural control, as also shown in corrective movements in frog (Kargo and Giszter 2000) and deletions during fictive locomotion in decerebrate cats (McCrea and Rybak 2008). Recently,

delayed feedback of CoM was shown to reconstruct the temporal activity of several individual muscles in unidirectional postural responses (Lockhart and Ting 2007; Welch and Ting 2009; 2008). We extend this work to show that SF muscle synergy recruitment is also modulated by task-level feedback both throughout and across trials, providing a hierarchical, low-dimensional organization of temporal features of muscle coordination. Our formulation is particularly useful in postural control, where the temporal recruitment patterns of muscle synergies are modifiable from trial to trial.

2.4.3 SF versus TF muscle synergies

We found that SF muscle synergies produced better data reconstructions when using a small number of components and yielded more physiologically interpretable results than TF muscle synergies. Because SF muscle synergies have different preferred directions of activation, only a subset of SF muscle synergies was necessary to reconstruct muscle activity for any given perturbation direction. Similarly, directional tuning is seen in many populations of cells in the nervous system (Georgopoulos et al. 1982; Hubel and Wiesel 1962; Weinstein et al. 1991). By contrast, a majority of TF muscle synergies were necessary to reconstruct muscle activity for any given perturbation direction, regardless of the number of muscle synergies extracted (Figure 2.5B). Increasing the number of TF muscle synergies resulted in components that were more finely localized in time yet were still recruited across all perturbation directions and muscles, ultimately achieving the resolution of the EMG signal. Because the same temporal commands are recruited across perturbation directions, the muscles recruited by TF components must be rearranged to account for the trial-by-trial variations in muscle recruitment both across and within perturbation directions (Figure 2.6B). As a result, in a

postural task, TF muscle synergies can only reveal muscle patterns at an instant in time. Thus, it is difficult to interpret the functional significance of temporal components in balance control. In contrast, SF muscle synergies can account for muscle activation patterns across trials and direction by relatively modest changes in their temporal recruitment patterns (Figure 2.6A). Because SF muscle synergies can be variably recruited across trials and directions, SF muscle synergies reveal muscle coactivation patterns across a variety of timescales.

TF muscle synergies have been previously identified during feedforward tasks in which there may not have been sufficient dissociation of spatial and temporal features to identify the underlying structure of motor outputs. For example, the stereotyped cyclical motor patterns in locomotion make it difficult to dissociate spatial and temporal control of movement in walking tasks. Although aspects of locomotion are under feedback control (Kuo 2002; Lam et al. 2006; Reisman et al. 2005), the basic pattern of muscle activity is produced in a feedforward manner (Winter and Yack 1987). As such, muscle groups are activated at consistent phases of gait across walking speeds and gait patterns (Nilsson et al. 1985). Thus, the data can appear to have either a fixed temporal or fixed spatial structure. For example, the variability in EMG during locomotor tasks can be equally explained using TF (Ivanenko et al. 2004; Krouchev et al. 2006; Monaco et al. 2010) or SF (Clark et al. 2010) muscle synergies. Moreover, muscle activity during other voluntary tasks such as primate grasping or frog kicking, swimming, and jumping can be explained using muscle synergies with co-varying spatiotemporal structure (d'Avella and Bizzi 2005; Overduin et al. 2008). In contrast to walking, perturbations separate and resolve such covariations (Kargo and Giszter 2000; Kargo et al. 2010); postural responses

allow for the dissociation of spatial and temporal features of muscle coordination which have similar temporal structure but recruit different muscles (Nashner 1976) across perturbation directions (Henry et al. 1998; Macpherson 1988). Moreover, very different temporal patterns can be elicited by varying perturbation characteristics, which can still be explained by CoM feedback (Lockhart and Ting 2007).

2.4.4   *Neural substrates for the recruitment and structure of muscle synergies*

The mapping of task-variables to muscle activity via SF muscle synergies is consistent with divergence in hierarchical neural structures. In order to produce desired motor outputs, multiple joints must be coordinated (Zajac and Gordon 1989). By coordinating muscles across joints, SF muscle synergies produce biomechanical functions to achieve motor outputs. The multi-joint coordination patterns seen in SF muscle synergies mirror central nervous system structure: corticomotoneuronal, reticulospinal, and spinal cord interneurons are known to have divergent projections to multiple motoneurons (Jankowska 1992; Turton et al. 1993). Moreover, interneurons have been shown to project in patterns that match the structure of SF muscle synergies (Hart and Giszter 2010). Depending on the task, muscle synergies have been hypothesized to be encoded at different levels of the central nervous system, including motor cortex for grasping (d'Avella et al. 2008; Overduin et al. 2008), brainstem for postural control (Torres-Oviedo et al. 2006; Torres-Oviedo and Ting 2007), and spinal cord for locomotion (Drew et al. 2008) and other voluntary and reactive tasks (Bizzi et al. 1991; Giszter et al. 1993; Hart and Giszter 2010; Saltiel et al. 2001). Because the same muscle synergies can be used across tasks, it is likely that they can be accessed using multiple neural control schemes in a hierarchical fashion, regardless of their location in the

nervous system.

The representation of global task-variables such as CoM requires multisensory integration to estimate and reflects convergence in hierarchical neural structures. To estimate CoM, it is necessary to know the configuration of all body segments and their associated masses; Thus, CoM must be estimated by integrating proprioceptive information across body segments with vestibular and/or visual information (Peterka 2002). Many diverse postural paradigms have suggested that CoM governs muscle activity during standing balance in a feedback manner (Gollhofer et al. 1989; Kuo 1995; Peterka 2000; 2002; van der Kooij and de Vlugt 2007). As a global task-level variable, CoM is more tightly regulated in postural control than local variables such as joint angles (Allum et al. 2003; Brown et al. 2001; Gollhofer et al. 1989; Krishnamoorthy et al. 2003; Scholz and Schoner 1999). Task-level feedback is implicated in electrophysiological studies as well: in primate motor cortex, pyramidal neurons are found to respond to task-level variables during voluntary reaching such as movement direction, velocity and endpoint force (Georgopoulos et al. 1992; Georgopoulos et al. 1986). Limb length and orientation can be assembled from afferent signals in both the dorsal root ganglia (Weber et al. 2007) and the dorsal spinocerebellar tract (Bosco et al. 1996).

Task-level variables provide a low-dimensional neural control scheme that may be mapped to individual muscles via low-dimensional muscle synergies. It has been proposed that the nervous system could make use of sensory feedback to estimate the body's state and achieve a desired movement trajectory through low-dimensional control (Todorov 2004). By using task-level feedback to recruit SF muscle synergies, it may be possible for the nervous system to reliably control task-level variables. Using SF muscle

synergies, low-dimensional control has been demonstrated to be sufficient to simulate effective locomotion (Neptune et al. 2009). Kargo and Giszter (2010) showed that simulations of frog wiping trajectories are more accurate when using feedback modulation of SF muscle synergies than without proprioceptive feedback. Berniker et al. (2009) also suggested that neural commands would be driven by task-level variables; simulations of SF muscle synergy recruitment using low-dimensional, task-level control provided a more accurate prediction of frog hindlimb muscle activity than with other control schemes. In cat reaching, pyramidal tract neurons are found to discharge in a manner related to task dynamics and muscle synergy recruitment (Yakovenko et al. 2011).

2.4.5   Competing influences on muscle activation during standing balance control

Aside from CoM, our results suggest that other task-variables such as orientation may also be important for recruiting SF muscle synergies that had actions at the hip. Trunk orientation has been proposed as a competing task-variable on postural responses (Kluzik et al. 2005; Macpherson et al. 1997; Massion 1994). Similarly, neurons in the reticular formation have been shown to respond to task-level variables such as orientation (Deliagina et al. 2008) or equilibrium (Schepens et al. 2008; Stapley and Drew 2009). Moreover, sensory feedback and descending control may have a greater influence on muscle activity at the hip due to the biomechanics of bipedal stance. However, muscle synergies with hip involvement were recruited in a manner inconsistent with changes in hip angle kinematics or vertical deviation. Thus, local control of hip angle is unlikely to account for SF muscle synergy recruitment. As opposed to local variables, the nervous system may be integrating and responding to a combination of joint kinematics. Because

joint torques are coupled across body segments during postural responses (Alexandrov et al. 1998), it is likely that the combinations of joint kinematics are integrated into a task-level variable, such as maintaining a vertical orientation of the lower limb or minimizing the overall bending of the joints.

In addition to recruiting SF muscle synergies, there may be other neural influences underlying muscle activation in human postural control. Despite the consistency of SF muscle synergies throughout perturbations, SF muscle synergy structure was slightly less consistent in later epochs versus earlier epochs. While SF muscle synergies may reflect an underlying neural structure for producing motor outputs, observed muscle activity is the result of a superposition of a variety of commands in the nervous system (Horak et al. 1997; Ting 2007). Later muscle activity could be due to descending cognitive influences that act at longer latencies, possibly via corticospinal loops and/or brainstem interactions (Jacobs and Horak 2007). Sensory feedback via local and/or global circuits may also affect muscle activity, since postural control is an ongoing task that is dependent on sensory cues for an estimate of body position and orientation (Macpherson et al. 1997; Massion 1994). Altered sensory feedback of multiple modalities has been known to modulate muscular patterns in postural responses (Honeycutt and Nichols 2010b; Stapley et al. 2002; Stapley et al. 2006), and sensory feedback has been shown to slightly alter the composition of SF muscle synergies (Cheung et al. 2005).

The deviations in our predictions from actual data may be explained in part by inherent methodological limitations of our analyses. Using NNMF, we performed SF muscle synergy analysis on 16 EMG signals during small epochs throughout the postural response. Because component analysis algorithms such as NNMF are used to parse out

salient features of muscle coordination, more robust muscle synergies can be identified when the EMG variability is high. When the extraction epoch is reduced, the dataset contains less EMG variability; as a result, SF muscle synergies identified from these smaller epochs can reflect smaller variations in EMG. Interestingly, additional SF muscle synergies were most often identified when extracted from early epochs that have most often been studied in postural responses (Henry et al. 1998; Macpherson 1988; Ting and Macpherson 2005; Torres-Oviedo and Ting 2007). Some of these previously identified SF muscle synergies may reflect smaller variations during these epochs and may be less indicative of the actual spatial structure of muscle coordination patterns. Additionally, the reconstructions of high-frequency oscillations in EMG activity and SF muscle synergy recruitment patterns were limited because we used low-frequency kinematic signals as inputs. Nevertheless, our reconstructions were still able to explain the majority of the variability in SF muscle synergy recruitment patterns, suggesting that higher frequency variations in muscle synergy recruitment may not be significant. Lastly, ramp-and-hold perturbations artificially correlate joint and CoM kinematics, making it difficult to establish truly independent correlations with SF muscle synergy activity. In a natural environment, these variables may be decoupled; alternative perturbations that decouple these variables (Kung et al. 2009) may need to be explored to better our understanding of neural control schemes.

CHAPTER 3:   MUSCLE ACTIVITY DURING PERTURBATIONS TO BALANCE CAN BE RECONSTRUCTED BY CONTINUOUS, DELAYED TASK-LEVEL BUT NOT JOINT-LEVEL FEEDBACK

3.1   INTRODUCTION

Mechanical perturbations imposed on the body induce sensorimotor feedback responses in electromyographic (EMG) activity at both short and long latencies, but the functional differences between these responses are unclear. Short-latency responses can be mediated by muscle stretch and/or force changes due to monosynaptic and polysynaptic spinal cord pathways between proprioceptive afferents and motoneurons (Liddell and Sherrington 1924; Nichols and Houk 1976; Prochazka 1996; Sinkjaer et al. 1996). In contrast, long-latency responses are thought to be influenced by multiple mechanisms spanning the neural axis (Jacobs and Horak 2007; Matthews 1981; Pruszynski et al. 2011; Taube et al. 2006). Typically, short- and long-latency responses are both observed in a muscle following a perturbation, however they can be elicited independently under certain conditions in both standing balance and reactive arm movements (Gollhofer et al. 1989; Kurtzer et al. 2008). Evidence suggests that short-latency responses counteract muscle stretch, whereas long-latency responses reflect attainment of task-level goals in both the upper and lower limbs.

In reactive arm movements, long-latency EMG has been shown to respond to task-level goals as opposed to local-level joint changes. Perturbations to the arm elicit

short latency responses in stretched muscles; conversely, long-latency responses can be evoked in muscles that are not stretched, reflecting torques required to stabilize the hand (Kurtzer et al. 2008; Pruszynski et al. 2011). However, such analyses have been limited to mean EMG magnitude during epochs following discrete, transient perturbations. Thus, it is unknown whether long-latency EMG reflects a triggered or preprogrammed response that precedes a voluntary response (Crago et al. 1976), or is due to continuous task-level feedback based on task-level performance.

In reactive postural responses during standing balance, long-latency EMG can be reconstructed by task-level feedback of center of mass (CoM) kinematics. When standing on a tilting platform, short-latency responses are observed in stretched muscles, whereas long latency responses are observed in opposing muscles that act to stabilize the CoM (Allum et al. 2003; Diener et al. 1983; Gollhofer et al. 1989; Nashner 1976). Moreover, EMG responses to perturbations during whole-body reach tasks can be modulated to aid the performance of the reach (Trivedi et al. 2010). Further, the entire time course of responses throughout discrete ramp-and-hold translation perturbations have been reproduced using delayed feedback of CoM kinematics (displacement, velocity, acceleration) (Lockhart and Ting 2007; Welch and Ting 2009; 2008). As CoM and joint kinematics are highly correlated in discrete perturbations applied at rest, it remains uncertain whether task-level CoM feedback is better than local-level joint feedback in describing long-latency EMG responses during dynamic conditions.

We hypothesized that the nervous system uses continuous task-level feedback at long-latencies to modulate EMG responses to perturbations. To test our hypothesis, we developed long (~4.5 s) continuous perturbations that allowed us to impart identical

acceleration pulses during different CoM position and velocity states, which temporally

decoupled CoM from joint kinematics. We predicted that the entire time course of

postural responses would be reconstructed throughout discrete and continuous

perturbations by delayed feedback of CoM kinematics better than joint kinematics.

3.2 METHODS

3.2.1 Summary

To test whether task-level feedback of CoM robustly modulates EMG activity at

long-latencies, we reconstructed EMG evoked throughout postural responses to

perturbations using a delayed feedback model. In addition to discrete ramp-and-hold

perturbations (Torres-Oviedo and Ting 2007; 2010; Welch and Ting 2009; 2008), we

designed long (~4.5 s), continuous perturbations that featured sequences of identical

acceleration pulses delivered during different CoM position and velocity states, and also

decoupled CoM kinematics from joint kinematics. We compared reconstructions of EMG

activity throughout discrete and continuous perturbations using delayed feedback of CoM

kinematics as well as joint kinematics at a variety of latencies.

3.2.2 Experimental design

23 healthy subjects (14 male, 9 female; mean age ± SD: 22 ± 3 years) participated

in an experimental protocol approved by Institutional Review Boards of Emory

University and the Georgia Institute of Technology.

Subjects stood on a moving platform while discrete and continuous perturbations of the

support surface in the horizontal plane were delivered (Figure 3.1). Discrete ramp-and-

hold translations lasted 570 ms and featured two acceleration bursts of equal magnitude (0.5g) but opposite direction, spaced 400 ms apart. These accelerations yielded a total perturbation displacement of 12 cm and peak velocity of 30 cm/s (Figure 3.1 – left panel). Continuous perturbations featured identical acceleration bursts applied at 400 ms intervals in the forward, and then in the backward directions resulting in complex perturbations of stepped velocities in forward followed by backward directions (Figure 3.1 – right panel). This resulted in a position trajectory that initially moved forward and reversed direction half way through the perturbation, returning to the initial position. To ensure that the platform continued to move throughout the perturbation (i.e. did not have zero velocity), the first and last acceleration bursts were set at half the magnitude (0.1g) of the other acceleration bursts (0.2g). Continuous perturbations lasted 4 s with total perturbation excursion of 15 cm, and had stepped velocities with a maximum of 15 cm/s (Figure 3.1 – right panel). All perturbations were administered using a custom 2-axis perturbation platform commanded with a Baldor NextMove ESB controller (Fort Smith, AR) through a custom MATLAB interface.

Subjects were subject to 3 sets of perturbations, of which two were analyzed for the current study. First a set of 60 discrete translations was randomly presented over 12 directions in the horizontal plane (5 trials per direction) as in previous studies (Chvatal et al. 2011; Torres-Oviedo and Ting 2007). Only forward and backward trials were used for analysis (Figure 3.1). Next, a set of 120 horizontal-plane perturbations which changed direction were randomly presented; these trials were used for a separate study and were not included in current analysis. Finally, ten identical continuous perturbations were administered, which were the analyzed in the current study.
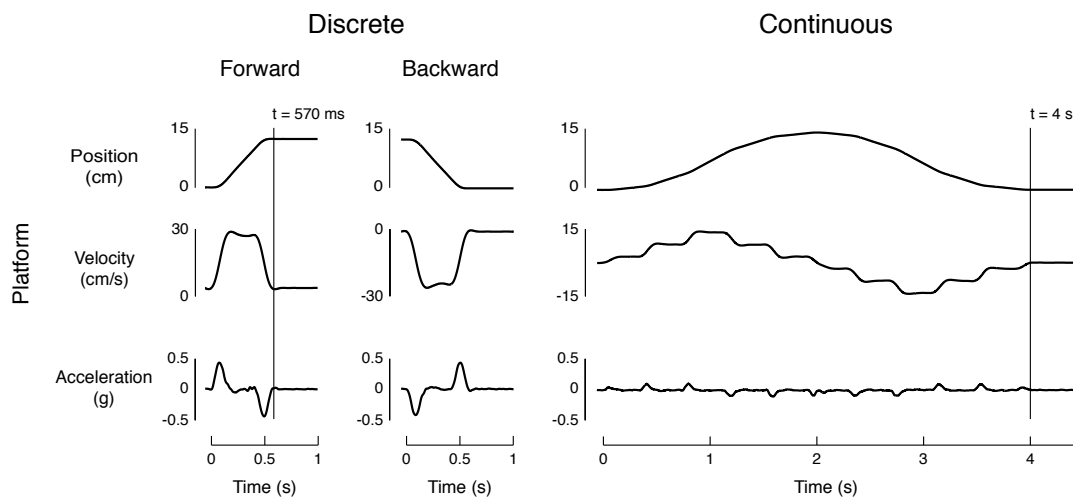
Figure 3.1. Perturbation characteristics. Discrete ramp-and-hold perturbations (two left panels) exhibited one acceleration burst in the direction of motion, resulting in one magnitude of velocity. Continuous perturbations (right panel) featured multiple acceleration bursts of equal magnitude in forward and backward directions, resulting in stepped velocities in forward and backward directions. Note that the first and last acceleration bursts were at half the magnitude of the other acceleration bursts to ensure that the platform did not have zero velocity in the middle of the perturbation.

3.2.3 Data collection

EMG activity was recorded at 1080 Hz from tibialis anterior (TA) and medial

gastrocnemius (MGAS) of the right leg using a Konigsberg telemetry system (Pasadena,

CA). Kinematic and kinetic data were also collected in all trials to estimate kinematics of

joint angles and CoM. Kinematic data were collected at 120 Hz using an 8 camera Vicon

motion capture system (Centennial, CO) and a custom 25-marker set that included head-

arms-trunk (HAT), thigh, shank, and foot segments. Kinetic data were collected at 1080

Hz from force plates under the feet (AMTI, Watertown, MA).

3.2.4 Data processing

Raw EMG data were processed using custom MATLAB routines. Data were high

pass filtered at 35 Hz, de-meaned, rectified, and then low pass filtered at 40 Hz as

previously reported (Torres-Oviedo and Ting 2007). CoM displacement and velocity

were calculated from kinematic data as a weighted sum of segmental masses (Winter

2005); CoM acceleration was calculated with respect to the feet from ground reaction

forces ($\mathbf{F}=m\mathbf{a}$) as previously reported (Welch and Ting 2009; 2008). Sagittal-plane joint

angles q_n for the ankle, knee, and hip were calculated from the dot product of vectors

from the joint center to adjacent body segments. Joint angles were then third-order

Butterworth low pass filtered at 5 Hz. Resting joint angles $q_{n\text{-rest}}$ were calculated as the

average angle from 50-500 ms preceding perturbations. Angular displacements θ_n were

defined as (q_n - $q_{n\text{-rest}}$). Angular velocities $\dot{\theta}_n$ and angular accelerations $\ddot{\theta}_n$ were

calculated as the first and second order derivatives of angular displacement, respectively.

3.2.5   Feedback model

To test our hypothesis that the nervous system uses delayed feedback of CoM

kinematics to modulate EMG at long-latencies, we reconstructed TA and MGAS activity

in discrete and continuous perturbations by using "jigsaw" models based on delayed

feedback of either CoM kinematics (Welch and Ting 2009) or joint kinematics (Figure

3.2A). Our model is based on the assumption that kinematic signals are linearly

combined to activate muscles (Figure 3.2B). Using sagittal displacement (**d**), velocity (**v**),

and acceleration (**a**), we reconstructed temporal patterns of TA and MGAS activity

(EMG$_n$) by assigning feedback gains (k_d, k_v, k_a) at a common time delay (λ), representing

delays in neural transmission and processing followed by half-wave rectifying

reconstructed muscle activity according to the equation

$$\mathrm{EMG}_n(t) = \lfloor k_d\mathbf{d}(t - \lambda) + k_v\mathbf{v}(t - \lambda) + k_a\mathbf{a}(t - \lambda)\rfloor$$

where k_d, k_v, and k_a designate feedback gains on CoM displacement, velocity, and

acceleration respectively, λ designates a time delay representing delays in neural

transmission and processing, and floor brackets $\lfloor\ \rfloor$ designate half-wave rectification of

reconstructed muscle activity defined as

$$\lfloor g \rfloor = \begin{cases} g, & g > 0, \\ 0, & g \leq 0. \end{cases}$$

where g represents the quantity within the brackets.

For each subject, EMG activity, CoM kinematics, and joint kinematics were averaged across trials and resampled at 1000 Hz. All analyses were performed on muscle activity beginning 50 ms before perturbation onset until 500 ms after perturbation offset. This corresponded to a 1.07 s time interval for discrete perturbations, and a 4.55 s time interval for continuous perturbations. For each muscle, we identified the three feedback gains (k_i) and common time delay (λ) that best reconstructed EMG activity according to the cost function

$$\min\left\{\mu_s \int_0^{t_{end}} e_m^2 dt + \mu_k \max\left(\left|e_m\right|\right)\right\}$$

The first term penalized the squared error (e_m) between averaged and simulated muscle activity with weight μ_s. The second term penalized the maximum error between simulated and recorded muscle activity at any point in time with weight μ_k. The ratio of $\mu_s{:}\mu_k$ was 10:1.

TA and MGAS activity were independently reconstructed using delayed feedback of CoM kinematics, yielding an independent set of feedback gains and time delay for each muscle in each perturbation type. Because TA and MGAS were only active in forward and backward discrete perturbations corresponding to posterior and anterior CoM acceleration respectively, TA was analyzed in forward discrete perturbations, and MGAS was analyzed in backward discrete perturbations. Both muscles were analyzed in continuous perturbations because the platform moved in both forward and backward directions. For all reconstructions, the feedback gains k_i were constrained to be between -5 and 5; this range was about an order of magnitude larger than the range of typical

feedback gain values. Due to conduction and processing delays, long-latency EMG activity in the lower limb occurs at 70-120 ms following perturbation onset (Horak and Macpherson 1996; Nashner 1976); the time delay λ was thus restricted to be between 60-130 ms, and the initial delay λ_0 was 100 ms.

We then evaluated whether TA and MGAS activity could be reconstructed using delayed feedback of joint angle kinematics to test the hypothesis that individual muscle activity is modulated by a variety of autogenic and heterogenic spinal reflexes (Nichols 1989; 1999). We reconstructed EMG activity of TA and MGAS independently from feedback of individual joint angles of the lower limb (ankle, knee, hip) as well as from combinations of joints (ankle/knee, knee/hip, ankle/hip). Thus, for the joint angle combinations, six input signals (three kinematic inputs per joint) were used, requiring six feedback gains to be identified (cf. Figure 3.2B). Because our model was unable to converge with more than six inputs, the combination of ankle/knee/hip kinematics was not evaluated. Feedback gains were restricted to values between -5 and 5.

For EMG reconstructions based on joint angles, we initially restricted the time delay λ to be between 30-120 ms with an initial delay λ_0 of 70 ms. This range encompassed previously recorded short latency muscle responses following translational support-surface perturbations via monosynaptic connections (40-65 ms) (Diener and Dichgans 1988; Diener et al. 1984; Nardone et al. 1990; Sinkjaer et al. 1996) as well as long latency responses (Horak et al. 1989; Horak and Macpherson 1996; Nashner 1976).

Finally, we reconstructed EMG from joint kinematic signals at negative latencies ($-100 \leq \lambda \leq -20$ ms) with an initial delay λ_0 of -60 ms to test whether torques generated

by EMGs were driving changes in joint kinematics at a electromechanical delay (Jacobs and Macpherson 1996; Macpherson et al. 1989).
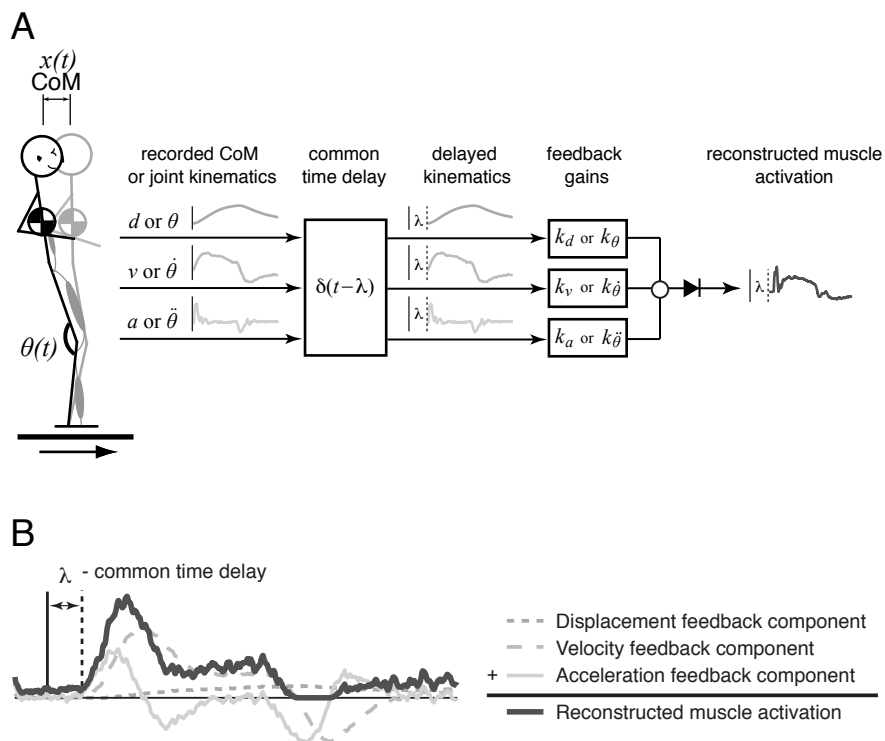
Figure 3.2. Feedback model of EMG activity. A, model schematic. Recorded sagittal CoM or single joint angle (ankle, knee, hip) kinematics were used as inputs to reconstruct muscle activity throughout discrete and continuous perturbations. In addition, TA and MGAS were reconstructed using combinations of joint kinematics (ankle/knee, knee/hip, ankle/hip). For joint combinations, the model was reformulated to have three input signals per joint (resulting in six input signals total). **B,** model assumptions. We assumed that each kinematic component could be multiplied by a feedback gain at a common time delay and linearly added to reconstruct muscle activity.

3.2.6 Statistical analyses

In all cases, we quantified the similarity between actual and reconstructed muscle patterns using r^2 (squared centered Pearson's correlation coefficient) and variability accounted for (VAF), defined as 100 × the square of Pearson's uncentered correlation coefficient (Zar 1999). Both r^2 and VAF comparisons were necessary to evaluate goodness-of-fit (Chvatal et al. 2011; Welch and Ting 2009). r^2 is high when the contours of EMG traces are well matched, but is less sensitive to magnitude. Conversely, VAF is high when the magnitudes of EMG traces are well matched, but is less sensitive to the contour of traces. Muscle traces were considered well-reconstructed when $r^2 \geq 0.5$ or VAF $\geq 75\%$. To evaluate the validity of muscle reconstructions against the threshold values for well-reconstructed muscle traces, one-tailed Student's t-tests were performed for the mean of muscle reconstructions against threshold with Bonferroni correction for multiple comparisons ($\alpha = 0.0125$).

We also compared the differences in magnitude and variance of velocity and acceleration feedback gains in discrete versus continuous perturbations. Based on previous modeling studies examining feedback gain variations across perturbation amplitudes (Bingham et al. 2011), we expected the feedback gains to be larger in magnitude and have more variance in continuous compared, which has small accelerations relative to discrete perturbations. We performed one-tailed paired t-tests on the mean magnitude of velocity and acceleration feedback gains with Bonferroni correction for multiple comparisons ($\alpha = 0.025$). We also used a one-tailed F-test of equality of variance to compare the variance of velocity and acceleration feedback gains with Bonferroni correction for multiple comparisons ($\alpha = 0.025$) (Zar 1999).

Previous studies have shown that EMG activity precedes joint angle displacement ; we therefore evaluated the temporal relationship between joint angle kinematics and muscle activity. Because changes in angular displacement are preceded by changes in angular acceleration, we compared the timing of peak EMG activity with the timing of peak ankle angular acceleration for TA and peak ankle and knee angular acceleration for MGAS. EMG data were low pass filtered at 5 Hz and peaks of activity were determined from custom MATLAB routines. Two-tailed Student's t-tests were performed for the difference in peak timing against a mean of zero.

Using r^2 and VAF as metrics, we then compared the degree to which the different kinematic inputs (CoM, individual joint angles, integrated combinations of joint angles) could reconstruct muscle activity in discrete and continuous perturbations. We performed a three-way ANOVA (subject × kinematic input × perturbation type) on r^2 and VAF for both TA and MGAS reconstructions (Zar 1999). We then verified the level of significance between groups using Tukey-Kramer post-hoc tests ($\alpha = 0.01$).

3.3   RESULTS

3.3.1   Summary

EMG responses in TA and MG during discrete and continuous perturbations were well-reconstructed by a delayed feedback model based on CoM kinematics. The delays identified by the model ranged from 80-100 ms, consistent with previously observed delays in postural responses. Mean feedback gain values were lower and less variable in the larger discrete perturbations compared to smaller continuous perturbations both across and within subjects. When EMGs responses were reconstructed using joint

kinematic feedback, delays were unphysiologically short (median $\lambda = 30$ ms), but optimization results were unreliable, as the chosen delays were frequently (364/552 trials – 66%) pinned to the lowest allowable values. Using single-joint kinematic delayed feedback, reconstruction values were significantly lower than using delayed CoM feedback. Using combinations of joint kinematic feedback improved EMG reconstructions, but were almost always significantly lower than using delayed CoM feedback. We then reproduced EMGs with negative delays, testing the hypothesis that the EMG signals precede and drive joint angle changes. EMG was found to precede joint angle changes by 70 ± 22 ms, consistent with electromechanical delays previously reported in the literature (Jacobs and Macpherson 1996; Macpherson et al. 1989). EMG reconstructions based on single- and multiple-joint kinematics improved with negative compared to positive delays, but in most cases were still significantly lower than using delayed CoM kinematics.

3.3.2   Long-latency delayed feedback of CoM reconstructs EMG responses in discrete and continuous perturbations

Whereas changes in CoM position, velocity, and acceleration were all in the same direction during the acceleration burst of discrete perturbations (Figure 3.3A, two left panels), CoM kinematics at the time of each acceleration pulse in continuous perturbations varied in magnitude and direction (Figure 3.3A, right panel). Therefore the CoM kinematics were more varied in continuous versus discrete perturbations, serving as a good test for the robustness of our feedback model. Consistent with the lower magnitudes of CoM velocity and acceleration in continuous perturbations, subjects anecdotally reported that these were "gentler" perturbations.

Throughout both discrete and continuous perturbations, muscle activity both lagged behind (Figure 3B, vertical lines) and resembled CoM kinematic traces (Figure 3B), suggesting that modulation of long-latency EMG is a continuous process as opposed to a discrete event. TA was active in forward perturbations and had a burst followed by a plateau of activity that resembled the superposition of posterior CoM acceleration and velocity. In continuous perturbations, bursts of TA activity were found at the beginning and end of the perturbation that resembled posterior CoM acceleration. MGAS was active in backward perturbations, and more closely resembled anterior CoM velocity traces in both discrete and continuous perturbations. In both discrete and continuous perturbations, delays of 80-100 ms were identified, consistent with previously reported delays in long-latency postural responses (Horak and Macpherson 1996; Nashner 1976).

Averaged TA and MGAS activity were well-reconstructed across both discrete and continuous perturbations ($r^2 \geq 0.5$ or VAF $\geq 75\%$) using long-latency delayed feedback of CoM kinematics with a fixed set of CoM feedback gains (k_d, k_v, k_a) for each trial (Figure 3.3B). TA was dominated by posterior CoM velocity and acceleration feedback, while MGAS was dominated by anterior CoM velocity feedback. Mean TA and MGAS reconstructions met our criterion for being well-reconstructed, and had either r^2 or VAF values that were significantly above threshold levels ($r^2 \geq 0.5$ or VAF $\geq 75\%$) in discrete and continuous perturbations across all subjects (Table 1, bold values). This criterion was also met for reconstructions from the majority of individual subjects (Table 1).
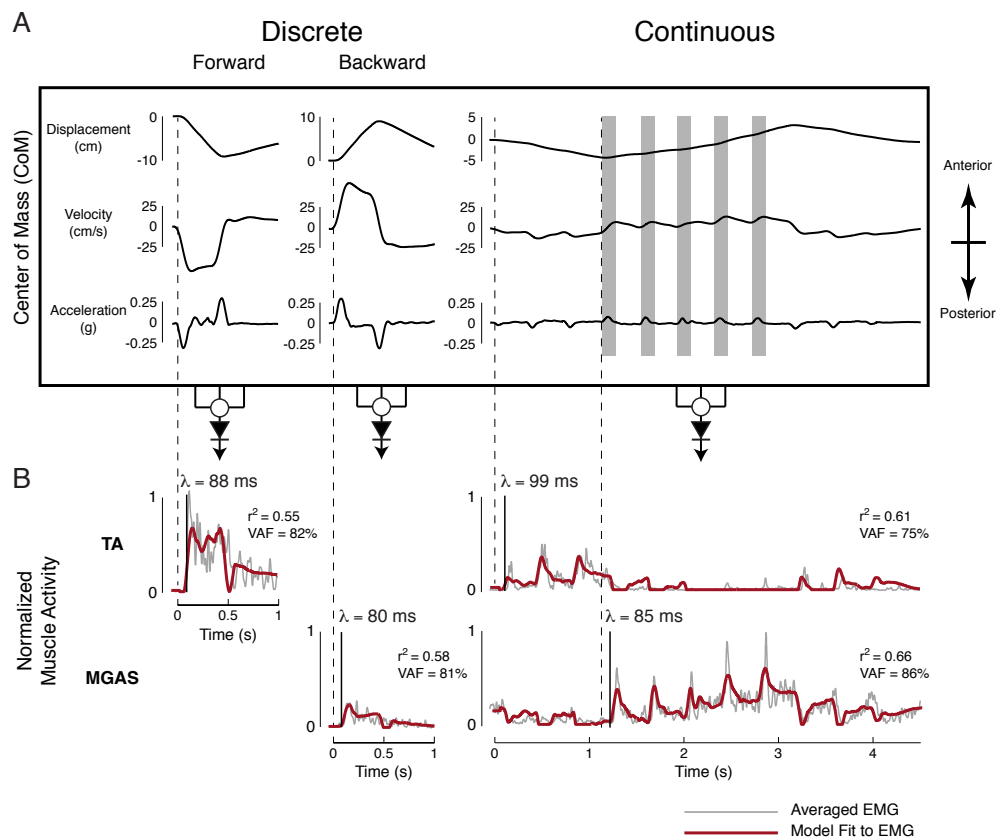
Figure 3.3. Postural responses to discrete and continuous support-surface translations. A, Average CoM kinematics for a representative subject. Discrete perturbations (two left panels) had one CoM position and velocity state for platform acceleration. TA was activated in forward perturbations and MGAS was activated in backward perturbations. For continuous perturbations (right panel), identical acceleration bursts (grey shaded boxes) were associated with CoM displacements that decreased in magnitude and CoM velocities that increased in magnitude. Positive values of CoM kinematics indicate anterior motion, and negative values indicate posterior motion. **B,** delayed CoM feedback model reconstruction of muscle activity. Both TA and MGAS were active in continuous perturbations with a delay of 80-100 ms between perturbation onset (vertical dashed lines) and EMG activity (vertical solid lines). Averaged TA and MGAS activity (grey traces) were well-reconstructed from delayed feedback of CoM (red traces) in both discrete and continuous perturbations. Muscle traces were considered well-reconstructed when $r^2 \geq 0.5$ or VAF $\geq 75\%$.

In both discrete and continuous perturbations, identified delays λ in all subjects were consistent with the magnitude of long-latency delays for postural responses in the lower limb (Horak and Macpherson 1996; Horak, Diener and Nashner 1989; Welch and Ting 2009). Moreover, delays were highly consistent for both TA and MGAS across subjects (TA – discrete: mean $\lambda \pm$ SD: 88 ± 7 ms; continuous: mean $\lambda \pm$ SD: 92 ± 14 ms; MGAS – discrete: mean $\lambda \pm$ SD: 88 ± 8 ms; continuous: mean $\lambda \pm$ SD: 86 ± 7 ms). Delays λ ranged from 80-99 ms for the representative subject shown (Figure 3.3B).

Differences in scaling of TA and MGAS activity with respect to CoM motion were observed in discrete and continuous perturbations, consistent with model predictions that the mean magnitude and range of feedback gains must decrease in larger perturbation amplitudes. CoM kinematic variables were larger in discrete compared to continuous perturbations (Figure 3.3A). However the relative change in the magnitude of TA and MGAS activity could not be explained by simply applying the same feedback gains found in the discrete case. Although TA activity was smaller in continuous perturbations, it decreased less than would be predicted by the decrease of CoM kinematics alone. Instead, higher feedback gains were required to predict TA activity. MGAS activity was actually larger in continuous versus discrete perturbations, also resulting in higher feedback gains for continuous perturbations. Both across and within all subjects, mean magnitudes of k_v and k_a were larger for both TA and MGAS in continuous versus discrete perturbations (Figure 3.4). Moreover, the range, or variance of k_v and k_a was less constrained in continuous perturbations both across subjects (Figure 4A) and within subjects (Figure 3.4B), reflecting trial by trial variability in feedback gains. No obvious trend was noted for CoM displacement gains across perturbations. The

feedback model was very sensitive to changes in gains, suggesting that these variations

were not due to incomplete convergence of parameters. These differences in mean and

variance of feedback gains are consistent with modeling a reduction in feasible gains with

perturbations of increasing amplitude (Bingham et al. 2011).

Table 3.1. Goodness-of-fit for center of mass (CoM) feedback model muscle reconstructions.

	tibialis anterior (TA)		medial gastrocnemius (MGAS)	
	Discrete	Continuous	Discrete	Continuous
r^2	**0.68±0.09‡**	**0.60±0.16†**	0.47±0.14	**0.65±0.13‡**
VAF	**87±5%‡**	72±10%	**82±6%‡**	**86±6%‡**
N	23/23	17/23	21/23	23/23

Bold values indicate well-reconstructed muscles

N: Number of individual subjects meeting criterion for well-reconstructed muscles

†: mean values significantly above well-reconstructed threshold at p < 0.0125 for n = 4 comparisons

‡: mean values significantly above well-reconstructed threshold at p < 10^{-4}
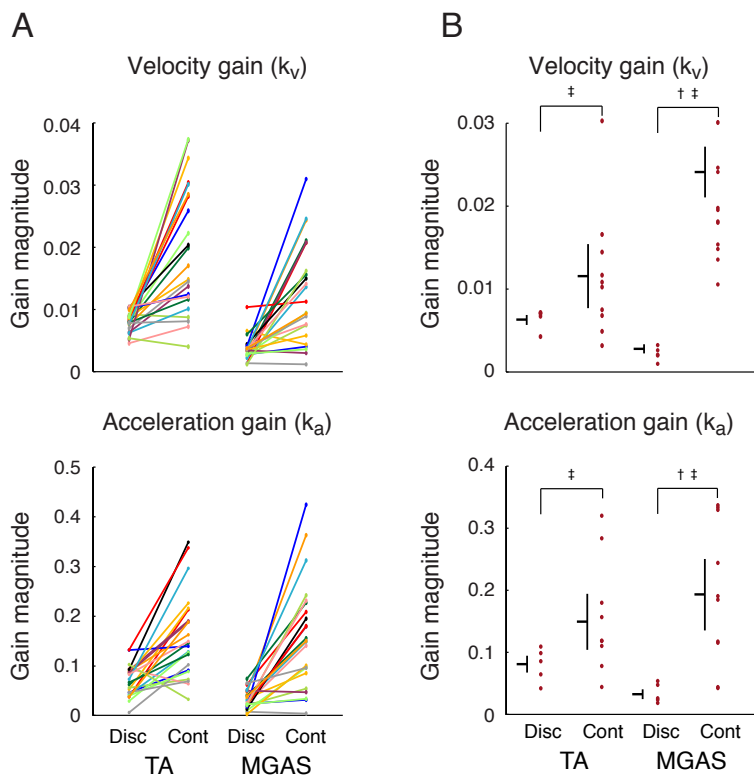
Figure 3.4. Delayed CoM feedback model gains for muscle reconstructions. A, feedback gains across subjects. Over all subjects, velocity (k_v) and acceleration (k_a) gains were increased with larger intersubject variability in continuous versus discrete perturbations. For both TA (left column) and MGAS (right column), each pair of connected dots represents the magnitude of feedback gains that best reconstructed averaged muscle activity for one subject in discrete and continuous perturbations (n = 23). **B,** feedback gains for a representative subject. Each dot represents the magnitude of feedback gains k_v and k_a for one trial (five discrete and ten continuous trials total). Average gains k_v and k_a (horizontal lines) were larger in continuous perturbations and had more variability (vertical lines) when compared to discrete perturbations. †: p < 0.025 for mean comparisons using Student's t-test; ‡: p < 0.025 for variance comparisons using F-test of equality of variance. Disc – discrete perturbations; Cont – continuous perturbations..

3.3.3   CoM kinematic changes precede EMG; EMG precedes joint kinematic changes

Whereas CoM kinematics were highly consistent across trials and had peak acceleration that preceded EMG activity, joint kinematics were more variable and had peak accelerations that were coincident with or followed EMG activity (Figure 3.5A – black vertical lines). However, the largest peaks in joint angle kinematics occurring after EMG onset actually corresponded to muscle shortening as opposed to stretch, suggesting that the evoked EMG activity was not due to a short-latency stretch response (typically at 40-65 ms in standing human). Instead, the later muscle shortening accelerations are consistent with the long-latency EMG signals evoked by the perturbation driving subsequent joint angle changes.

A majority of EMG reconstructions using joint kinematics yielded non-physiological delays. The time delay of our model λ was allowed be between 30-120 ms for reconstructions, a range that included both short- (40-65 ms) and long- latency (80-100 ms) responses for the lower limb (Carpenter et al. 1999; Nardone et al. 1990; Nashner 1976). However, the identified delays λ for EMG reconstructions using joint feedback were selected at the lower bound of delays (30 ms) in 66% (364/552) of reconstructions (cf. Figure 3.5B). Thus, the feedback model could not converge using short-latency delays for joint kinematic signals in a majority of cases. Moreover, the identified 30 ms delay was shorter than any physiological delays previously reported for short-latency responses to translational perturbations in humans (Horak and Macpherson 1996; Nashner 1976).

We therefore also performed EMG reconstructions using negative delays on joint kinematics; the negative delays modestly improved results, but allowed the optimizations to converge, further suggesting that changes in muscle activity cause changes in joint kinematics. When using positive delays for joint kinematic reconstructions, peaks were delayed compared to averaged EMG data and CoM kinematic reconstructions for discrete perturbations (Figure 3.5B). However, when muscle activity was reconstructed using negative delays, reconstruction peaks more closely matched peaks in EMG activity. The time delays used for model reconstructions (-70 ± 22 ms) were consistent with electromechanical delays (Jacobs and Macpherson 1996; Macpherson et al. 1989).
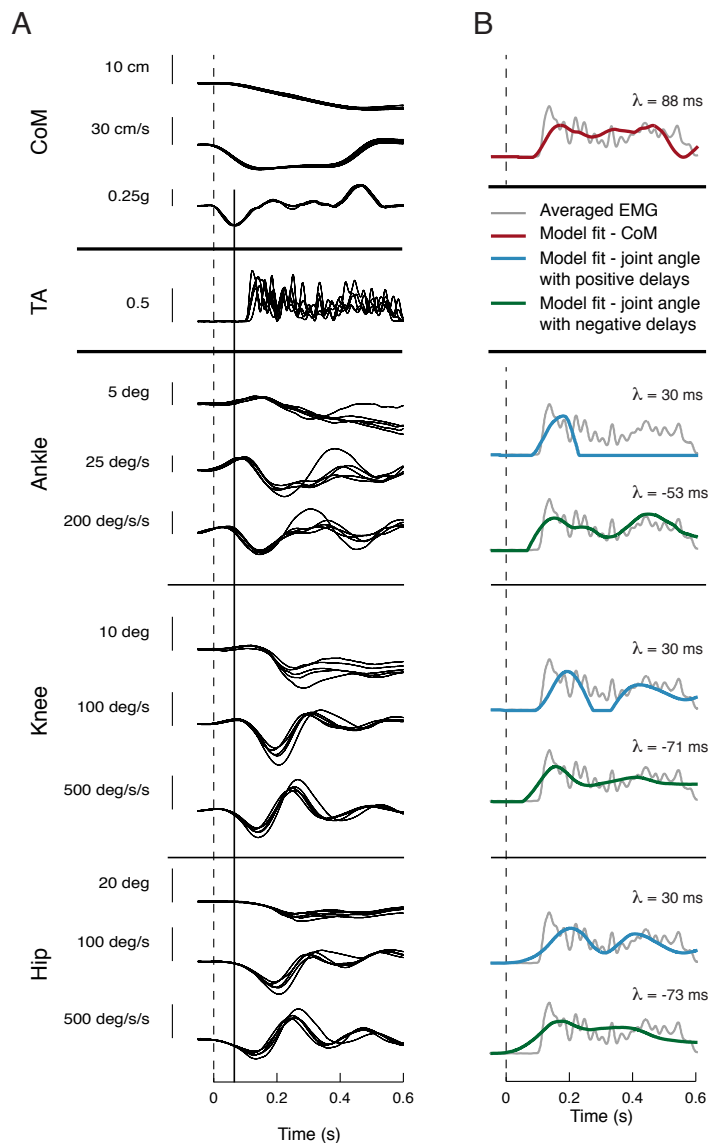
Figure 3.5. Temporal sequence of EMG, CoM kinematics, and joint kinematics. A, CoM versus joint kinematics for backward discrete perturbations. Joint kinematics were more variable across trials compared to CoM kinematics. Overlaid traces represent repeated trials. Peak CoM acceleration (black vertical line) precedes TA activity. In contrast, large peaks in joint angle kinematics occurred after EMG onset and corresponded to muscle contraction. Positive values indicate extension; negative values indicate flexion. Dashed vertical lines correspond to platform onset. **B,** comparison of reconstructions using CoM versus joint kinematic feedback. Reconstruction peaks using joint angle kinematics at positive delays (blue traces) occur after peaks in TA and CoM kinematic reconstructions (red traces). Reconstruction peaks better match TA when using negative delays (blue traces), consistent with electromechanical delays.

3.3.4   Delayed CoM kinematics reconstruct muscle activity better than joint kinematics

Joint kinematic feedback with a positive delay was unable to reproduce EMG as well as CoM kinematic feedback. In a representative subject, best-fit TA and MGAS reconstructions are shown using joint versus CoM kinematic feedback at positive delays (Figures 3.6 and 3.7, blue versus red traces). As in Figure 3.5, best-fit delays identified for joint kinematic feedback were shorter than physiological delays and likely unreliable. Delayed feedback of CoM kinematics produced higher goodness-of-fit values than individual joint feedback in both discrete and continuous perturbations (Figures 3.6A and 3.7A). Moreover, even when using the best possible fits, the joint that the muscle crossed did not reliably reconstruct muscle activity; although TA only crosses the ankle joint, TA reconstructions were better using knee kinematics than ankle kinematics for both discrete and continuous perturbations. When integrated combinations of joint kinematics were used, reconstructions improved (Figures 3.6B and 3.7B – blue traces). Nevertheless, on average, integrated joint feedback was still not as good at delayed CoM feedback (Figures 3.6B and 3.7B – red versus blue traces).

Joint kinematic feedback with a negative delay slightly improved EMG reconstructions compared to positive delays, but still did not reproduce EMG as well as CoM feedback. With negative delays, joint kinematics were used to reconstruct antecedent EMG activity, testing the hypothesis that changes in EMG activity produces changes in joint angles. On average, EMG reconstructions were modestly improved using negative delays on joint kinematics (Figures 3.6 and 3.7, green versus blue traces); moreover, the identified negative delays converged within the bounds of the model and

were more reliable than positive delays. However, goodness of fit was still lower than

EMG reconstructions using feedback of CoM kinematics (Figures 3.6 and 3.7, green

versus red traces). Using integrated combinations of joint kinematics improved

reconstructions, similar to reconstructions using joint kinematic feedback at positive

delays. This result reflects the fact that torques produced from EMG at a single joint can

also accelerate many joints in a multilink system due to dynamic coupling (Zajac and

Gordon 1989).

Muscle reconstructions using delayed feedback of CoM were significantly more

similar to averaged EMG data than reconstructions using joint kinematic feedback at both

positive and negative delays (Figure 3.8). There was a significant effect of kinematic

input on EMG reconstructions for TA and MGAS (TA – r^2: F[6,321] = 46.36, p < 10^{-16};

VAF: F[6,321] = 34.8, p < 10^{-16}; MGAS – – r^2: F[6,321] = 36.51, p < 10^{-16}; VAF:

F[6,321] = 18.32, p < 10^{-16}). Across all subjects, TA and MGAS reconstructions using

delayed feedback of CoM kinematics (Figure 3.8 – red bars) had significantly higher

values of r^2 and VAF than reconstructions using individual joint angle kinematics at

positive delays (Figure 3.8 – blue bars) (p < 10^{-4} for all r^2/VAF comparisons using

Tukey-Kramer post-hoc analysis). Similarly, muscle reconstructions using delayed

feedback of CoM kinematics were significantly higher than combinations of knee/hip or

ankle/hip kinematics using positive delays (p < 0.01 for all r^2/VAF comparisons using

Tukey-Kramer post-hoc analysis). Goodness-of-fit values for reconstructions using

negative delays were higher on average compared to positive delays (Figure 3.8 – green

versus blue bars). As a result, fewer comparisons between CoM and joint angle

reconstructions were significant at the α = 0.0125 level. Nevertheless, reconstructions

using CoM kinematics had higher mean goodness-of-fit values in all but two
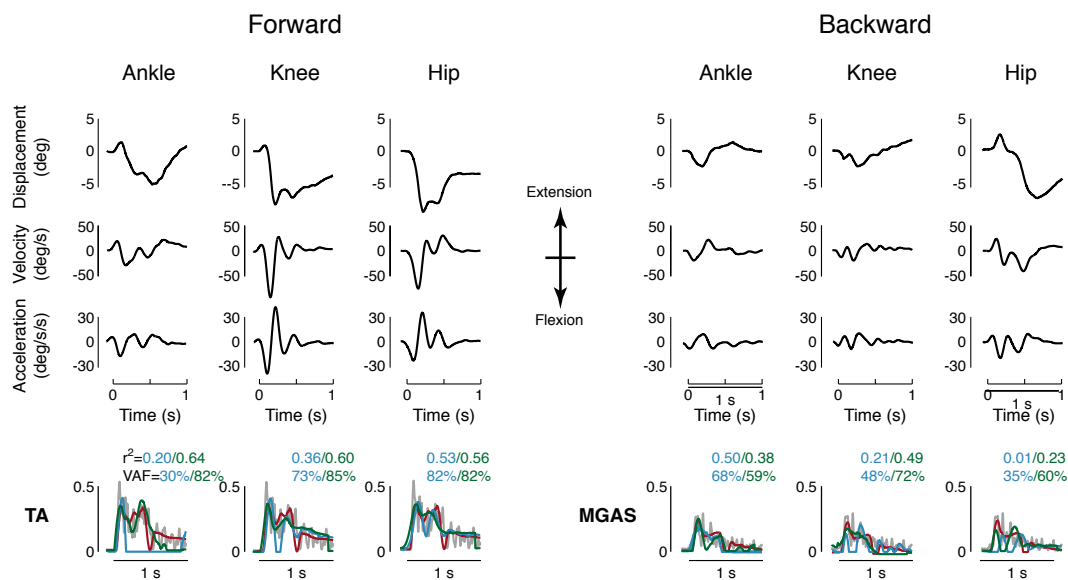
comparisons.
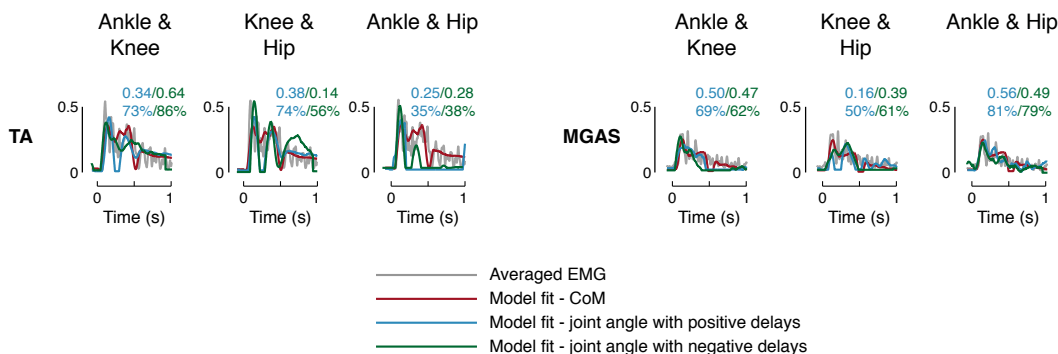
Figure 3.6. Feedback model reconstruction of muscle activity in discrete perturbations using CoM versus joint angle kinematics. Average muscle activity and joint angle kinematics for ankle, knee, and hip are shown for a subject representative of the mean of our results. Positive values indicate extension; negative values indicate flexion. **A,** individual joint reconstructions. **B,** joint combination reconstructions. Joint kinematic reconstructions were improved on average using negative delays (green traces) compared to positive delays (blue traces). TA reconstructions using delayed feedback of knee angle kinematics were most similar to CoM reconstructions. MGAS reconstructions using ankle angle kinematics were most similar to CoM reconstructions. Reconstructions were improved when using integrated combinations of joint angles, particularly ankle/knee. Nevertheless, muscle reconstructions using delayed feedback of CoM kinematics (red traces) better matched EMG than reconstructions using joint angles.
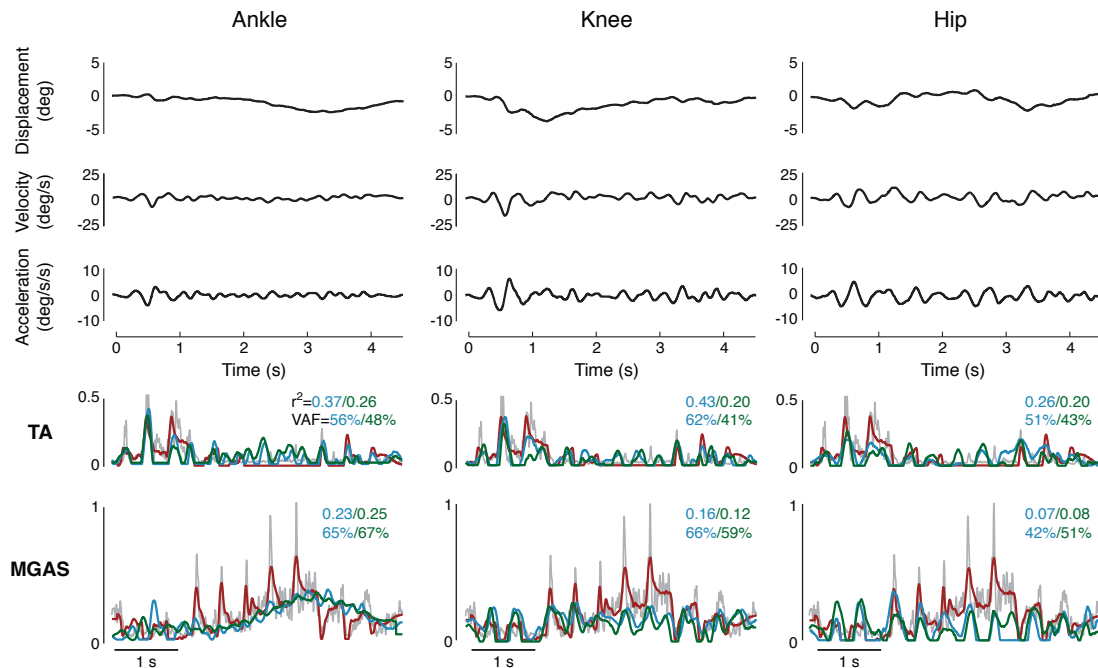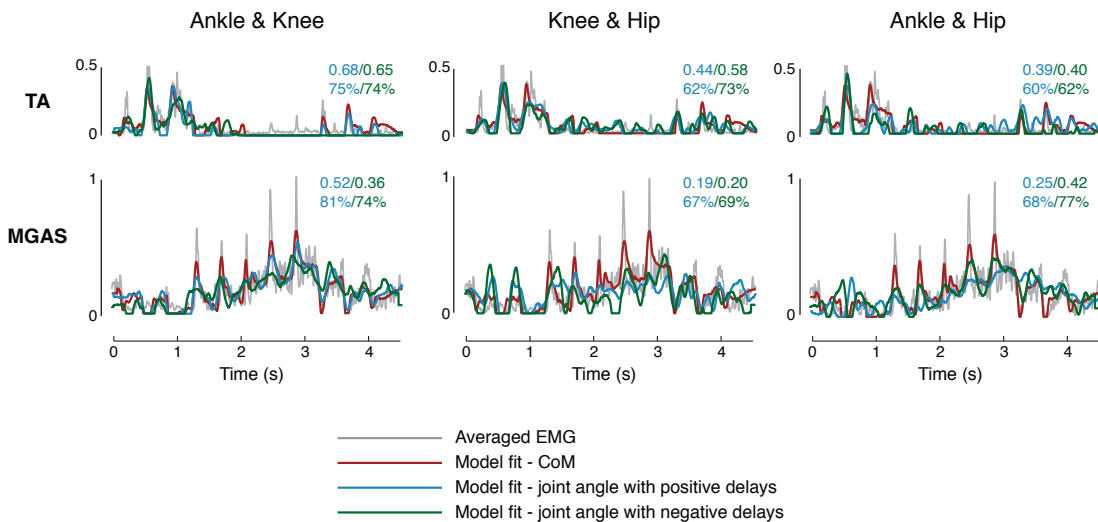
Figure 3.7. Feedback model reconstruction of muscle activity in continuous perturbations using CoM versus joint angle kinematics. Muscle reconstructions are shown for the same subject as in Figure 3.6. **A,** individual joint reconstructions. **B,** joint combination reconstructions. Muscle reconstructions using delayed feedback of CoM kinematics (red traces) had higher goodness-of-fit values than reconstructions using joint angles at either positive (blue traces) or negative (green traces) delays.
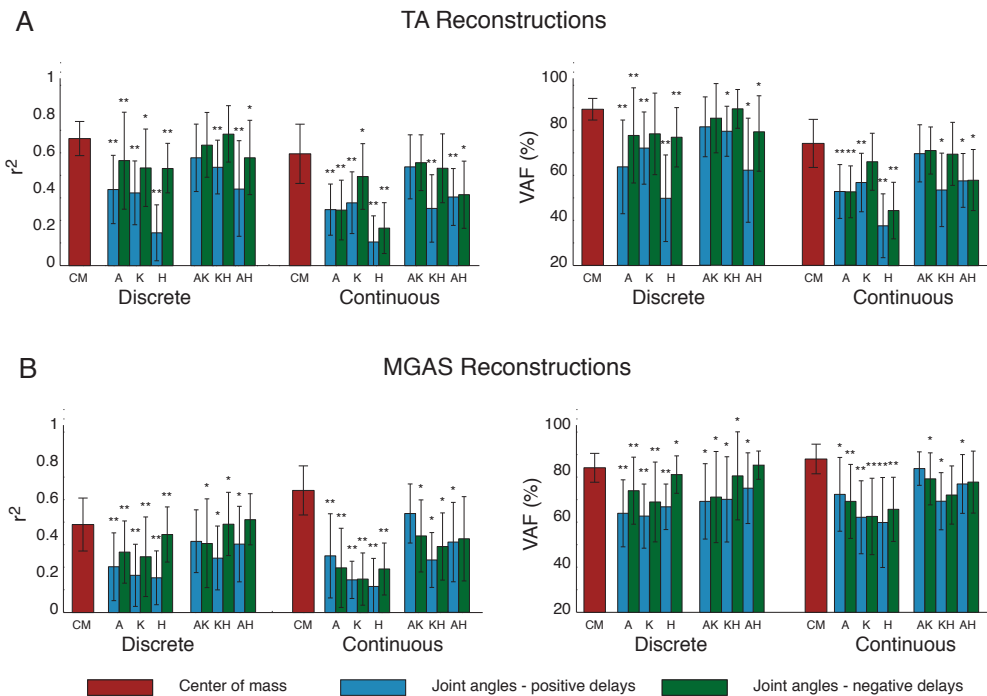
Figure 3.8 Goodness-of-fit comparisons for muscle reconstructions using delayed feedback of CoM versus individual and integrated combinations of joint kinematics at positive and negative delays. **A,** TA reconstructions; **B,** MGAS reconstructions. Muscle reconstruction measures (r^2 and VAF) were significantly higher using delayed feedback of CoM kinematics (red bars) versus individual or integrated joint kinematic feedback (knee/hip, ankle/hip) at positive delays (blue bars). Reconstructions improved on average when using joint kinematic feedback at negative delays (green bars). *: $p < 0.01$ for mean comparisons; **: $p < 10^{-4}$ for mean comparisons using Tukey-Kramer post-hoc tests. A – ankle; K – knee; H – hip; AK – ankle/knee; KH – knee/hip; AH – ankle/hip.

3.4   DISCUSSION

3.4.1   Summary

In this study, we compared whether task- versus joint-level control could sufficiently explain reactive long-latency muscle activity in a human balance task. We found that task-level feedback of CoM kinematics could explain muscle activity better than local-level feedback of joint kinematics. Changes in EMG often preceded changes in joint kinematics; thus, positive delays identified by the model were shorter than those previously reported in the literature, and EMG reconstructions using joint kinematics were slightly better when using negative compared to positive delays. Moreover, joint kinematic reconstructions were improved when using joint combinations. These data suggest that the nervous system continuously uses task-level feedback of CoM at long latencies to activate muscles during balance control, and that changes in EMG produce coordinated changes in joint torques. Further, the data suggest that task-level feedback of CoM is robust in a variety of perturbation types with varying complexity.

3.4.2   Task-level feedback in balance control

We propose that delayed feedback of task-level variables represents a common mechanism of motor control in a wide range of motor tasks. A variety of feedback models based on CoM motion have been shown to reproduce joint torques in postural sway and standing balance (Collins and De Luca 1994; Kuo 1995; Peterka 2000; 2002; van der Kooij and de Vlugt 2007). However, joint torques do not accurately represent neural outputs because many muscle activation patterns can give rise to the same joint torque (Gottlieb et al. 1995). As opposed to joint torque, muscle activity provides a more

accurate estimation of neural outputs and neural structure, as motoneurons synapse directly onto motor units at the neuromuscular junction, neural summation does not occur at the level of motor units, and motor units exhibit all-or-none responses to motoneuron firing (Latash 2008). In reactive arm movements, long-latency EMG activity of elbow and shoulder muscles has been shown to be modulated in response to whole limb position (Kurtzer et al. 2008). However, these studies have correlated EMG to limb kinematics over large time bins that do not capture the fine temporal features of EMG. Here we have explicitly shown that CoM feedback can directly modulate EMG throughout the entire time course of postural responses to perturbations. Moreover, we reproduced the entire time course of a mono- and bi-articular antagonistic muscle pair, suggesting that a variety of divergent local motor outputs can be reconstructed by task-level feedback. Thus, our results suggest that task-level feedback of CoM is used to coordinate motoneuronal outputs during balance tasks.

The data further suggest that local-level feedback of joint angles is insufficient to modulate neural outputs to muscles. Task-level feedback of CoM kinematics produced more realistic muscle reconstructions with significantly better goodness-of-fit values than joint kinematic feedback. Similarly, local changes in joint angle were also insufficient to explain long-latency muscle activity in arm movements (Kurtzer et al. 2008). Our results were not surprising because individual muscles do not produce consistent functional outputs for maintaining balance (Nashner 1977). Rather, the functions of individual muscles may vary depending on the state of other muscles (van Antwerp et al. 2007). By contrast, task-level control of maintaining the body CoM over the base of support is sufficient to maintain upright balance (Massion 1994).

Our data support a causal relationship of motor outputs where changes in CoM kinematics modulate long-latency EMG, which further produces coordinated changes in joint kinematics. Using our model, we were unable to identify physiologically plausible EMG latencies following joint kinematics. Instead, EMG activity preceded periods of muscle shortening as opposed to stretch. Thus, we were able reconstruct antecedent EMG activity from joint kinematics at negative latencies; these latencies (-70 ± 22 ms) were consistent with electromechanical delays (Jacobs and Macpherson 1996; Macpherson et al. 1989). Furthermore, reconstructions were modestly improved with closer peak timings using joint kinematics at negative compared to positive delays. We also noted that integrated feedback of multiple joints improved muscle reconstructions, particularly at negative latencies. Such coordination of joint segments can result from dynamic coupling, where the activation of a single muscle accelerates multiple joint segments (Zajac and Gordon 1989). Similarly, joint torques are better reconstructed in postural responses using feedback of multiple joints (Park et al. 2004) as opposed to individual joint feedback.

Differences in task-level versus local-level modulation of EMG may be partially explained by inherent limitations in data processing and the feedback model. Whereas CoM acceleration is calculated at high frequency (1080 Hz) from ground reaction forces, joint angular accelerations must be calculated from reflective markers at lower frequency (120 Hz). Thus, the poorer reconstructions from joint kinematics may simply exist because lower frequency joint kinematic data cannot reproduce higher frequency EMG signals. Moreover, the feedback model could not converge when more than two joints were used as kinematic inputs. Reconstructions improved when using combinations of

joint kinematics (Figure 3.8), and task-level CoM displacement and velocity is calculated from the integration of many local-level joint centers. Thus, it is possible that the nervous system may use integrated feedback of multiple local-level variables to modulate EMG. As a result, it remains to be seen whether task-level feedback is due to the explicit calculation of CoM or may be distributed throughout multiple local spinal cord and/or brainstem circuits.

It is feasible that the nervous system uses task-level control of motor outputs because task-level variables can be encoded throughout the neural axis. For balance control, it is necessary to estimate CoM; In order to do so, proprioceptive information across body segments must be integrated with vestibular and/or visual information (Peterka 2002), possibly in higher centers. Indeed, in postural control studies, reticular formation neurons respond to task-level changes in limb orientation (Deliagina et al. 2008) or equilibrium (Stapley and Drew 2009). In voluntary reaching tasks, task-level variables including movement direction, velocity, and endpoint force are represented in pyramidal neurons of motor cortex (Georgopoulos et al. 1982). Primary motor cortex neurons have also been shown to fire in response to other task-variables including hand location (Sergio and Kalaska 1997) and arm orientation (Scott and Kalaska 1997). Information about orientation and limb length can be assembled from afferent signals originating in the dorsal root ganglia (Weber et al. 2007); moreover the dorsal spinocerebellar tract may encode information about limb length, orientation (Poppele et al. 2002), and inter-limb coordination (Poppele et al. 2003). Individual representations of task-variables may be further assembled in higher centers to form control schemes that

meet the specific demands of a task, as well as to adapt to new scenarios (Hwang et al. 2003).

3.4.3 Robustness of task-level feedback

Here we have shown that long-latency EMG is due to continuous feedback based on task-level performance as opposed to a discrete event that triggers a preprogrammed response. In contrast to discrete sagittal perturbations that elicit stereotyped EMG activity and CoM kinematics (Horak and Macpherson 1996; Welch and Ting 2008), continuous perturbations yielded robust and varied combinations of CoM kinematics that to the best of our knowledge have not been previously tested. Our model was still able to reconstruct EMG in long (~4 s) continuous perturbations using long-latency feedback of CoM at a constant delay. While we have shown that long-latency EMG activity can be attributed to delayed feedback of CoM in an antagonistic muscle pair, the same control scheme can be used to predict muscle activity in muscles of the leg and trunk (Welch and Ting 2009; 2008). Thus individual muscles throughout the body can be activated via task-level control. This may be accomplished from the convergence of a number of nested pathways, including autogenic and heterogenic circuits (Nichols 1989), cortical and subcortical feedback loops (Jacobs and Horak 2007), and descending corticospinal tracts.

Our results support the idea that the nervous system uses the same feedback control scheme in standing balance tasks, regardless of feedforward influences on muscle activity. In arm perturbations, long-latency EMG can be explained by the superposition of reactive and voluntary neural commands (Pruszynski et al. 2011), both of which are part of the same task-dependent control process (Scott 2004). Here, we demonstrated that delayed feedback of CoM could explain muscle activity during postural responses to both

discrete and continuous perturbations. Moreover, continuous perturbations were

sufficiently long enough (~4 s) to incorporate the effects of feedforward descending and

cognitive influences (Jacobs and Horak 2007). We thus considered it likely that subjects

could use feedforward commands to predict EMG responses throughout continuous

perturbations. While it has been shown that subjects can rapidly adapt postural strategies

during perturbations (Keshner et al. 1987; Nashner 1976), we have shown that the

majority of temporal features of EMG throughout postural responses of long timescales

can be explained solely by feedback mechanisms. Thus, our data suggest that

feedforward processes may only provide a minor contribution during balance control.

     To use the same feedback control scheme over a variety of perturbation types, the

exact sensorimotor transformations may be flexibly chosen among a feasible set that is

dependent on perturbation characteristics. Our results suggest that the range of feedback

gains that an individual can use decreases as perturbation magnitude increases. Because

discrete perturbations were of larger amplitude and resulted in larger magnitudes of CoM

kinematics than continuous perturbations, the smaller set of gains used in discrete

perturbations may reflect a smaller set of feasible transformations that can be used to

generate appropriate muscle activity. Both muscle and torque feedback gains have been

known to scale with perturbation magnitude (Park et al. 2004; Welch and Ting 2009).

Further, it has been recently shown that when perturbation magnitudes increase, feedback

gains decrease in magnitude and range of gains decrease to maintain stability in postural

control (Bingham et al. 2011). As opposed to independently selecting gains for

perturbations, gains may be automatically adjusted based on available feedback, a

process known as gain scheduling (Kuo 1995). The decrease in range of gains seen in

larger perturbations may correspond to a decrease in postural strategies: for example,

although humans can exhibit a wide variety of postural strategies for balance (Creath et

al. 2005; Runge et al. 1999), different perturbation amplitudes can favor the selection of a

particular postural strategy via gain scheduling due to the inherent biomechanical

constraints of the body (Kuo and Zajac 1993; Pai and Patton 1997).

CHAPTER 4: A HIERARCHICAL MODEL FOR HUMAN STANDING BALANCE THROUGHOUT MULTIDIRECTIONAL POSTURAL PERTURBATIONS THAT CHANGE DIRECTION

4.1 INTRODUCTION

It has long been hypothesized that the nervous system is hierarchically organized to produce a wide variety of motor outputs based on task-level constraints (Brown 1914; Jackson 1889; Kurtzer et al. 2008; Loeb et al. 1999; Marsden et al. 1981; McCrea and Rybak 2008; Ting 2007). Due to muscular redundancy however, it remains unknown how the nervous system maps task-level goals to high-dimensional motor outputs (Bernstein 1967). Moreover, it is unclear how the nervous system may map high-dimensional sensory inputs from muscle, joint, and cutaneous receptors to task-level variables, or how such sensory inputs are transformed to motor outputs.

Spatially-fixed (SF) muscle synergies have been proposed as a general neural mechanism whereby task-level goals can be mapped to execution-level motor commands (Kargo et al. 2010; Safavynia and Ting 2012; Torres-Oviedo and Ting 2007; 2010). Defined as groups of muscles with fixed ratios of co-activation, SF muscle synergies have been hypothesized to be recruited by variable temporal neural commands. SF muscle synergies have been identified during a variety of motor tasks in a variety of species (Clark et al. 2010; Hart and Giszter 2004; Overduin et al. 2008; Saltiel et al.

2001; Ting and Macpherson 2005; Torres-Oviedo et al. 2006; Torres-Oviedo and Ting 2007; Tresch et al. 1999) and are robustly shared across tasks with different dynamics (Cheung et al. 2005; Chvatal et al. 2011; d'Avella and Bizzi 2005; Kargo et al. 2010). Moreover, the structure of SF muscle synergies is preserved following the removal of sensory feedback (Cheung et al. 2005; Kargo et al. 2010) and descending influences from supraspinal centers (Roh et al. 2011), suggesting that muscle synergies represent an inherent structure in the nervous system. Although much work has focused on identifying the similarity in SF muscle synergy structure across tasks, hierarchical control of SF muscle synergies has largely remained unstudied, and mainly limited to simulations of movement (Berniker et al. 2009; Neptune et al. 2009).

We have recently demonstrated hierarchical control of SF muscle synergies in a postural task (Safavynia and Ting 2012). In order to maintain balance, it is necessary to maintain the body center of mass (CoM) over the base of support (BoS) (Horak and Macpherson 1996; Massion 1994). Using a "jigsaw" model based on delayed feedback of CoM kinematics, we demonstrated that SF muscle synergy recruitment could be described throughout discrete support-surface perturbations (Safavynia and Ting 2012). In the jigsaw model, the recruitment of each SF muscle synergy was reconstructed by assigning a three feedback gains (one for each component of CoM motion – displacement, velocity, acceleration) at a common time delay that resulted in the best correlations between input and output signals. Similarly, the temporal recruitments of SF muscle synergies have been shown to be modulated in response to task-level variables such as movement speed (Clark et al. 2010; d'Avella et al. 2008)}, mechanical constraints (Hug et al. 2011), and limb configuration (Cheung et al. 2009; Muceli et al. 2010; Ting

and Macpherson 2005; Torres-Oviedo et al. 2006; Torres-Oviedo and Ting 2010). These findings suggest that the nervous system uses task-level goals to recruit SF muscle synergies throughout and across tasks, consistent with a hierarchical neural control scheme. However, the jigsaw model was only applied to sagittal perturbations where the body started at rest, and different feedback gains were required for each perturbation direction. Thus, it remains unknown whether varying patterns of SF muscle synergy recruitment across perturbation directions can be explained under a common feedback control scheme. Moreover, it remains unknown whether our previous findings generalize to more dynamic conditions in which CoM kinematics are more varied.

We hypothesize that SF muscle synergies are consistently and continuously modulated by task-level goals to robustly produce complex motor outputs over a variety of sensorimotor states. In voluntary reaching tasks, it has been demonstrated that muscle synergies are consistent across reaching directions (d'Avella et al. 2008; d'Avella et al. 2006) and differentially modulated during movements with changing target directions (d'Avella et al. 2011). In postural control, SF muscle synergies have been associated with moving the CoM in unique directions (Chvatal et al. 2011; McKay and Ting 2008; Ting and Macpherson 2005; Torres-Oviedo et al. 2006). It is thus likely that SF muscle synergies would be consistently recruited to a particular direction of CoM motion. Moreover, the entire timecourse of postural muscle activity can be described by task-level CoM feedback throughout long, continuous sagittal perturbations that feature changing direction of CoM (Safavynia and Ting in prep). Because SF muscle synergies represent of muscle activity, it is also likely that they would be continuously recruited by task-level feedback over dynamic perturbations.

To test whether task-level feedback of SF muscle synergies is robust across sensorimotor states, we introduced novel, biphasic perturbations that changed direction. We first perturbed the body in forward or backward directions from rest; once the body was moving in the sagittal direction, we perturbed it again in one of 12 directions to achieve a variety of dynamic body configurations (Figure 4.1). We predicted that the same SF muscle synergies would be consistently recruited to a particular direction of CoM motion throughout postural responses to both discrete and biphasic multidirectional perturbations. Using the jigsaw model, we first identified whether SF muscle synergy recruitment patterns could be well-reconstructed across discrete and biphasic perturbations from CoM kinematics along the direction of maximal SF muscle synergy recruitment. We then predicted SF muscle synergy recruitment patterns across directions in discrete and biphasic perturbations.

4.2   METHODS

4.2.1   Summary

In order to evaluate the robustness of delayed CoM feedback on SF muscle synergy recruitment across sensorimotor states, we developed biphasic perturbations that perturbed the body in multiple directions while it was already moving. We recorded human postural responses to discrete and biphasic perturbations and extracted SF muscle synergies from all perturbation types. After the structure of SF muscle synergies was found to be similar across conditions, we reconstructed EMG activity during discrete and biphasic perturbations using SF muscle synergies extracted from discrete perturbations. We then applied a delayed-feedback model based on CoM kinematics to SF muscle synergy recruitment patterns across all perturbation types in the direction of maximal SF

muscle synergy recruitment tuning. Lastly, SF muscle synergy recruitment patterns were predicted across all directions and perturbation types using feedback gains identified from the maximal tuning direction.

4.2.2   *Experimental design*

We designed discrete and biphasic perturbations of the support surface in the horizontal plane to test the robustness of task-level feedback on SF muscle synergy recruitment throughout static and dynamic states (Figure 4.1). Discrete ramp-and-hold translations were administered in 12 equally spaced directions in the horizontal plane; the direction of movement was specified in which 0° indicated rightward platform movement and the angle of perturbation increased in a counterclockwise manner. Biphasic perturbations were also administered in the same directions as discrete perturbations, but were preceded by either a forward or a backward premovement (Figure 4.1A). Discrete perturbations lasted 570 ms and were 12 cm in displacement, 30 cm/s in peak velocity, and 0.5g in peak acceleration; data for a rightward perturbation are shown (Figure 4.1B – left panel). Biphasic perturbations lasted 760 ms and began with either a forward (Biphasic-F) or backward (Biphasic-B) premovement with an acceleration pulse of 0.25g, resulting in a velocity of 15 cm/s (Figure 4.1B – two right panels). A second acceleration was applied in multiple directions to yield a final direction of movement that matched discrete perturbations. The second acceleration was applied at 400 ms following perturbation onset; this corresponded to the time that the platform moved half of the total displacement of discrete perturbations (6 cm). The resulting biphasic perturbation featured the same maximum displacement (12 cm) and peak velocity (30 cm/s) as discrete perturbations. All perturbations were administered using a custom 2-axis
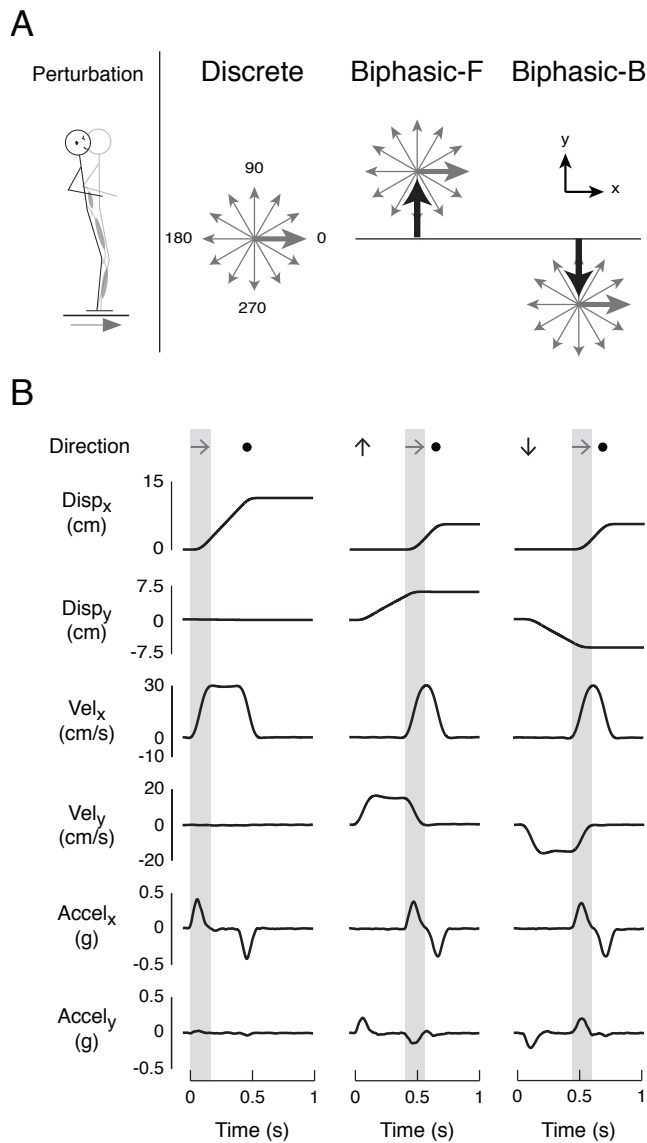
Figure 4.1. Experimental design. A, administered perturbations. Discrete ramp-and-hold perturbations were administered in 12 equally spaced directions in the horizontal plane. Biphasic perturbations featured either a forward or backward premovement before moving in one of the 12 directions administered in discrete perturbations. **B,** perturbation characteristics for rightward perturbations. Black arrows indicate the time of premovement, grey arrows indicate rightward movement, and black circles indicate platform deceleration. Shaded boxes indicate periods of rightward acceleration. Disp – displacement; Vel – velocity; Accel – acceleration.

perturbation platform commanded with a Baldor NextMove ESB controller (Fort Smith, AR) through a custom MATLAB interface.

4.2.3   Data collection

12 healthy subjects (6 male, 6 female; mean age ± SD: 23 ± 4 years) participated in an experimental protocol approved by the Institutional Review Boards of Emory University and the Georgia Institute of Technology. In order to minimize adaptation while maximizing variability, we randomly presented five repetitions of discrete perturbations over 12 directions for a total of 60 trials as in previous studies (Safavynia and Ting 2012; Torres-Oviedo and Ting 2007). Following the discrete perturbations, 120 biphasic perturbations were randomly presented (5 repetitions × 12 directions × 2 premovement directions). In order to eliminate confounding effects of fatigue, subjects were given a mandatory rest period of 5 minutes after every set of 60 trials.

EMG activity was recorded from 16 muscles over the right leg and trunk. The muscles recorded include: rectus abdominis (REAB), tensor fascia lata (TFL), tibialis anterior (TA), semitendinosus (SEMT), biceps femoris, long head (BFLH), rectus femoris (RFEM), peroneus longus (PERO), medial gastrocnemius (MGAS), lateral gastrocnemius (LGAS), erector spinae (ERSP), external oblique (EXOB), gluteus medius (GMED), vastus lateralis (VLAT), vastus medialis (VMED), soleus (SOL), and adductor magnus (ADMG). In three subjects, SEMT activity was missing due to faulty leads. Raw EMG data were collected at 1080 Hz and then processed according to custom MATLAB routines. Data were high pass filtered at 35 Hz, de-meaned, rectified, and then low pass filtered at 40 Hz.

Kinematic and kinetic data were collected for an estimation of CoM. Kinematic data were collected at 120 Hz using an 8 camera Vicon motion capture system (Centennial, CO) and a custom 25-marker set that included head-arms-trunk (HAT), thigh, shank, and foot segments. Kinetic data were collected at 1080 Hz from force plates under the feet (AMTI, Watertown, MA). CoM displacement and velocity were calculated from kinematic data as a weighted sum of segmental masses (Winter 2005); CoM acceleration was calculated from ground reaction forces (**F**=m**a**).

4.2.4   *Data processing*

To test the robustness of delayed CoM feedback modulating SF muscle synergy recruitment in static and dynamic states, it was first necessary to evaluate the similarity of SF muscle synergy structure across discrete and biphasic perturbations. For each trial EMG data were parsed into 10 ms bins and mean activity in each bin was calculated. Each muscle was then normalized to maximum EMG activity across all trials and perturbation types for visualization purposes. Three data matrices were assembled (one for each perturbation type – discrete, forward biphasic, backward biphasic) that consisted of normalized, binned EMG activity during the epoch that corresponded to multidirectional platform acceleration (Figure 4.1B – grey shaded boxes). For discrete perturbations, this epoch began at the start of the perturbation and lasted 170 ms. Because the platform was already moving in biphasic perturbations, this epoch began 400 ms after perturbation onset and was slightly shorter (160 ms). EMG epochs were chosen at a delay of 100 ms with respect to platform motion because postural muscle activity begins ~100 ms following a perturbation (Horak and Macpherson 1996). Thus, EMG epochs were

chosen at 100-270 ms following discrete perturbation onset, and 500-770 ms following biphasic perturbation onset.

4.2.5   Muscle synergy extraction

We used non-negative matrix factorization (NNMF) to extract SF muscle synergies from EMG activity in discrete and biphasic perturbations (Lee and Seung 1999; Ting and Chvatal 2011). The NNMF algorithm is a linear decomposition technique that decomposes an original EMG matrix $\mathbf{E}$ into spatial muscle weightings $\mathbf{W}$ and temporal recruitment patterns $\mathbf{C}$. For spatially fixed muscle synergies, the muscular composition $\mathbf{W}$ does not change, although the recruitment coeffiecients $\mathbf{C}$ can vary at each time point for each trial. The NNMF algorithm chooses non-negative matrices $\mathbf{W}$ and $\mathbf{C}$ at random initially and modifies their composition to minimize the sum of squared errors between the actual ($\mathbf{E}$) and reconstructed ($\mathbf{E}^{*}$) EMG matrices as shown below:

$$\mathbf{E} = \mathbf{WC} + \text{ error}$$

$$\text{error} = \sum_{i}\sum_{j}(\mathbf{E}_{ij} - \mathbf{E}_{ij}^{*})^{2}$$

For a pre-specified number of SF muscle synergies N_{syn}, the activity of a muscle $\mathbf{M}_i$ is reconstructed by linearly combining muscle weightings $\mathbf{W}_i$ with temporal recruitment patterns $\mathbf{C}$ according to the equation

$$\mathbf{M}_i = \sum_{j=1}^{N_{syn}} w_{i,j}\mathbf{C}_j$$

We extracted SF muscle synergies as in previous studies (Chvatal et al. 2011; Safavynia and Ting 2012). Briefly, we constructed our three data matrices to have the dimensions $m \times s$, where m is the number of muscles and s is the number of samples (bins $\times$ directions $\times$ repetitions). We then scaled the rows of the data matrices to have unit variance, weighting the variance of each muscle equally. Because there were large differences in magnitudes of EMG activity across discrete and biphasic perturbations, we scaled each data matrix to its own unit variance. We then ran the NNMF algorithm; after the algorithm was complete, the scaling was removed from the data matrix, and each SF muscle synergy was normalized to its maximum muscle composition, resulting in muscle compositions between 0 and 1.

4.2.6   Muscle synergy analysis

We used a combination of global and local criteria to determine the fewest number of SF muscle synergies (N_{syn}) to faithfully reconstruct the EMG data matrices as in previous studies(Chvatal et al. 2011; Safavynia and Ting 2012; Torres-Oviedo and Ting 2007; 2010). We extracted 1-16 SF muscle synergies and evaluated goodness-of-fit between actual and reconstructed EMG using variability accounted for (VAF), defined as $100 \times$ the square of Pearson's uncentered correlation coefficient (Zar 1999). We included SF muscle synergies until our previous criteria were met (Safavynia and Ting 2012), which included increasing the number of SF muscle synergies as long as total VAF and VAF across muscles improved. We validated N_{syn} using factor analysis (Tresch et al. 2006). We then verified N_{syn} against a shuffled matrix of the same data using bootstrapping (Cheung et al. 2009) and ensured that the VAF confidence intervals (CIs)

of SF muscle synergies extracted from actual versus shuffled data were non-overlapping. VAF of muscle synergies extracted from actual data were 7.3 ± 3.3 CIs higher than VAF of muscle synergies extracted from shuffled data (Figure A1). For each perturbation type, muscle synergies extracted from actual data were able to explain EMG variability of postural responses (Table 4.1).

We also determined the structural consistency of SF muscle synergies across perturbation types as in previous studies (Chvatal et al. 2011; Safavynia and Ting 2012). We calculated Pearson's correlation coefficients (r) between pairs of SF muscle synergies: for subjects that had 16 muscle recordings, we considered a pair of SF muscle synergies to have consistent structure if $r > 0.623$, which corresponds to the critical value of r^2 for 16 elements at $p = 0.01$ ($r^2 = 0.388$) (Figure A2); for the three subjects that had 15 muscle recordings, SF muscle synergies with $r > 0.641$ were considered consistent ($r^2 = 0.411$; $p = 0.01$). Critical values of r were validated against a distribution of chance r values (Berniker et al. 2009). Because SF muscle synergy structure was consistent across perturbation types for all subjects (Figure A2), SF muscle synergies extracted from discrete perturbations were used to reconstruct EMG activity throughout all perturbation types and directions, yielding observed temporal recruitment patterns. Over all perturbation types, EMG variability reconstructed from discrete SF muscle synergies was similar to EMG variability reconstructed from each condition individually (Table 4.1).

4.2.7   Feedback model

To test the hypothesis that SF muscle synergies are robustly recruited by delayed task-level feedback in static and dynamic states, we reconstructed SF muscle synergy recruitment patterns using a "jigsaw" model based on delayed feedback of CoM

Table 4.1. Variability accounted for (VAF) of SF muscle synergy reconstructions.

VAF	Discrete		Biphasic-F		Biphasic-B	
	Total	Muscle	Total	Muscle	Total	Muscle
Recon-condition	$87 \pm 3\%$	$83 \pm 6\%$	$89 \pm 3\%$	$85 \pm 12\%$	$89 \pm 3\%$	$82 \pm 14\%$
Recon-discrete	$87 \pm 3\%$	$83 \pm 6\%$	$85 \pm 6\%$	$83 \pm 5\%$	$82 \pm 4\%$	$81 \pm 6\%$

Values indicate mean and standard deviation of VAF

Recon-condition: reconstructions of EMG using SF muscle synergies extracted from each condition individually

Recon-discrete: reconstructions of EMG using SF muscle synergies extracted from discrete perturbations

kinematics as in our previous study (Safavynia and Ting 2012) (Figure 4.2). The model

assumes that CoM kinematic signals are linearly combined to recruit SF muscle synergies

in a feedback manner. Using CoM horizontal displacement (**d**), velocity (**v**), and

acceleration (**a**), we reconstructed recruitment patterns C for each SF muscle synergy W_i

(C_{W_i}) by assigning feedback gains (k_d, k_v, k_a) at a common time delay (λ), representing

neural transmission and processing time, and then half-wave rectifying the muscle

synergy recruitment pattern found using the equation below:

$$\mathbf{C}_{W_i} = k_d\mathbf{d}(t - \lambda) + k_v\mathbf{v}(t - \lambda) + k_a\mathbf{a}(t - \lambda)$$

Because the frequency content of reconstructed EMG was lower than that of processed

EMG, observed SF muscle synergy recruitment patterns were low pass filtered at 20 Hz

to match the frequency content of input and output signals (Figure A3). The SF muscle

synergy recruitment patterns were then averaged across repeated trials for each direction

in the same perturbation type and re-sampled at 1000 Hz. Each component of CoM

motion was averaged, interpolated and re-sampled at 1000 Hz to match sampling rates of

inputs and outputs to the model. All analyses were performed on SF muscle synergy

recruitment patterns from 50 ms before perturbation onset to 500 ms after perturbation

offset. This corresponded to a 1.07 s time interval for discrete perturbations, and a 1.26 s

time interval for biphasic perturbations. The initial feedback gains k_i were constrained to

be between 0 and 5; this range was about an order of magnitude larger than the range of

typical feedback gain values. The time delay λ was restricted to be between 90-140 ms, a

range encompassing physiological delays of muscle activity to postural responses (Horak

and Macpherson 1996). The model identified the three feedback gains (k_i) and a common

time delay (λ) that best reproduced the averaged SF muscle synergy recruitment pattern

according to the cost function

$$\min\left\{\mu_s \int_0^{t_{end}} e_m^2 dt + \mu_k \max\left(\left|e_m\right|\right)\right\}$$

The first term penalized the squared error (e_m) between recorded and simulated muscle

synergy recruitment patterns throughout the perturbation with weight μ_s. The second

term penalized maximum error between simulated and recorded data at any point in time

with weight μ_k. The ratio of $\mu_s{:}\mu_k$ was 10:1.

We reconstructed SF muscle synergy recruitment patterns using delayed

feedback of CoM over all perturbation types and directions. First, we identified the

maximum CoM acceleration tuning direction of each muscle synergy; we then projected

CoM kinematic vectors along the direction of maximum CoM acceleration. Because

CoM acceleration direction was always oriented opposite platform acceleration direction,

averaged SF muscle synergy recruitment patterns for each perturbation type were fit from

trials directed opposite the direction of maximum CoM acceleration. We quantified the

similarity between actual and reconstructed SF muscle synergy recruitment patterns using

both r^2 and VAF, as r^2 is more sensitive to the contour of traces and VAF is more

sensitive to the magnitude of traces. SF muscle synergy recruitment patterns were

considered well-reconstructed when $r^2 \geq 0.5$ or VAF $\geq 75\%$ (Safavynia and Ting 2012).

Once feedback gains were identified from feedback model reconstructions of SF muscle

synergies in their maximal tuning direction for each perturbation type, recruitment
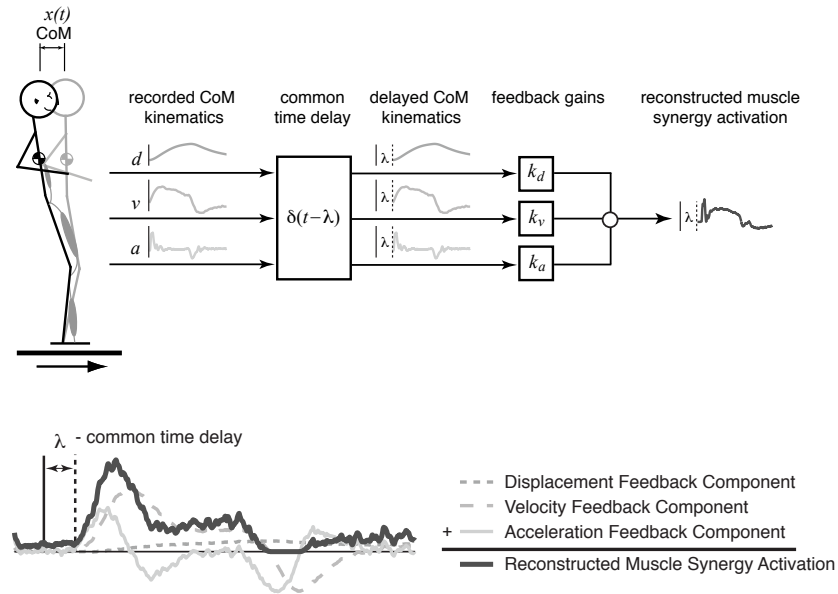
Figure 4.2. Delayed feedback model. Recorded CoM kinematics were used to reconstruct muscle synergy recruitment patterns throughout multidirectional discrete and biphasic perturbations. Each component of CoM motion is multiplied by a feedback gain at a common time delay and linearly added to produce a reconstructed muscle synergy recruitment pattern.

patterns of well-reconstructed SF muscle synergies were predicted over all directions using the same feedback gains.

4.3 RESULTS

4.3.1 Summary

For each subject, a consistent set of SF muscle synergies was identified across discrete and biphasic perturbations. SF muscle synergies were found to have consistent directional tuning with respect to CoM acceleration in both discrete and biphasic perturbations. Along their maximal tuning direction, the temporal patterns of recruitment of a majority of SF muscle synergies were well-reconstructed throughout postural responses by delayed feedback of CoM kinematics. For each perturbation type (discrete, forward biphasic, backward biphasic), SF muscle synergy recruitment patterns were well-predicted across directions using a fixed set of feedback gains. Thus, the recruitment of SF muscle synergies can be described in a variety of dynamic states using a common feedback rule.

4.3.2 Postural responses throughout perturbations

CoM kinematics and EMG activity differed during postural responses to discrete versus biphasic perturbations (Figure 4.3). In response to a discrete rightward perturbation, the body initially accelerated leftward (grey shaded boxes). CoM kinematic vectors (**d**, **v**, **a**) were oriented in similar directions, opposite the direction of platform movement. By contrast, CoM kinematics were decoupled in magnitude and direction
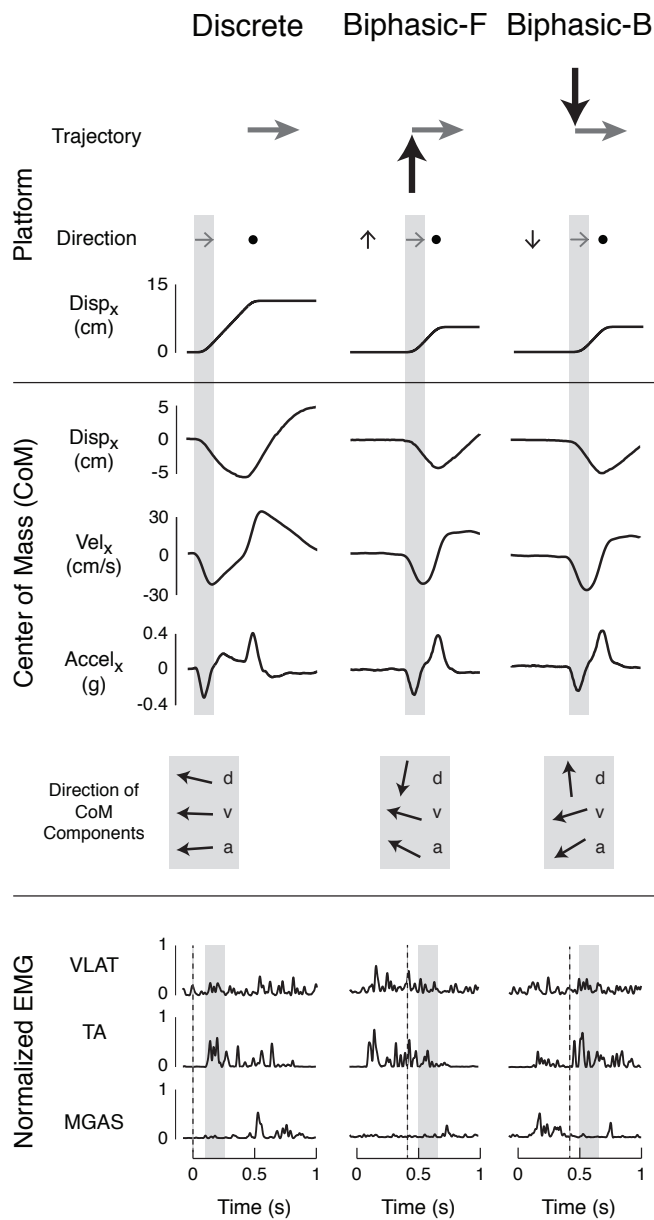
Figure 4.3. Representative postural responses to rightward perturbations. Subjects exhibited CoM motion in the frontal plane over all perturbation types. However, the direction of CoM components relative to the feet during rightward platform acceleration varied across perturbation types and were more dissociated from each other. Direction of CoM components were averaged across shaded region. Muscular responses lagged behind CoM acceleration onset by ~100 ms (compare grey shaded boxes to black dotted lines) and varied across perturbation types. Disp – displacement; Vel – velocity; Accel – acceleration.

during postural responses to biphasic perturbations. During the period of rightward

platform acceleration (Figure 4.3 – grey shaded boxes), frontal CoM velocity was larger

when preceded by a backward premovement (Biphasic-B) versus a forward premovement

(Biphasic-F). Conversely, frontal CoM acceleration was larger in forward biphasic

perturbations compared to backward biphasic perturbations. For forward biphasic

perturbations, CoM velocity and acceleration were oriented more leftward and forward

during rightward accelerations. CoM displacement was always directed backward during

the second platform acceleration, regardless of the direction of platform movement.

Conversely, CoM velocity and acceleration were oriented leftward and backward during

rightward platform acceleration in backward biphasic perturbations, with CoM

displacement always directed forward. EMG activity varied across perturbation type as

well: although TA was active during rightward perturbations, it was less active when

preceded by a forward premovement. MGAS was not active during rightward

perturbations, but active during the premovement of backward biphasic perturbations.

This variability in responses was seen across all perturbation directions and types.

4.3.3   *Consistency of SF muscle synergy tuning*

For all subjects, SF muscle synergies were maximally tuned to similar directions

of platform movement across perturbation types, but featured different tuning breadths

and magnitudes. For example, subject 6 had 6 SF muscle synergies maximally tuned to

four unique perturbation directions: in discrete perturbations, SF muscle synergy W1 was

tuned to 210° perturbations, W2 was tuned to 120° perturbations, W3 was tuned to 90°,

W4 was tuned to 300°, W5 was tuned to 120°, and W6 was tuned to 90° (Figure 4.4). W5

and W6 had more noisy tuning curves and were tuned in the same directions as W2 and W3, respectively. W5 and W6 had large contributions of hip muscles (W5: ERSP, GMED; W6, REAB). Note that some SF muscle synergies (i.e. W1, W3) had a single tuning direction, while other SF muscle synergies (i.e. W2 and W4) had a second tuning direction that was lower in magnitude. Across all subjects; 63 of 71 (89%) SF muscle synergies had peak tuning within 30° across perturbation types. However, the magnitude and breadth of tuning varied across perturbation types. In subject 6, W1-W4 had recruitment coefficients that were larger in magnitude in discrete versus biphasic perturbations. W3 was more broadly tuned in discrete perturbations; conversely, W1 was more broadly tuned in forward biphasic perturbations.

Differences in breadth of tuning of SF muscle synergies across discrete and biphasic perturbations were resolved when SF muscle synergy recruitment was evaluated with respect to CoM acceleration direction (Figure 4.5). For example, muscle synergy W1 in subject 8 was composed mainly of calf muscles and was recruited over backward-leftward perturbation directions. While peak tuning differed by 30° between discrete (grey) and biphasic (colored) perturbations, W1 was more broadly tuned in forward biphasic perturbations and more narrowly tuned in backward biphasic perturbations (Figure 4.5 – second panel). However, when evaluating muscle synergy recruitment with respect to CoM acceleration direction, W1 tuning curves became more similar in breadth across perturbation types (Figure 4.5 – third panel). Moreover, peak tuning of W1 in backward biphasic perturbations shifted to align with peak tuning of W1 in discrete perturbations. Note that CoM acceleration direction was exactly opposite platform direction for discrete perturbations, but was clustered to forward directions in biphasic
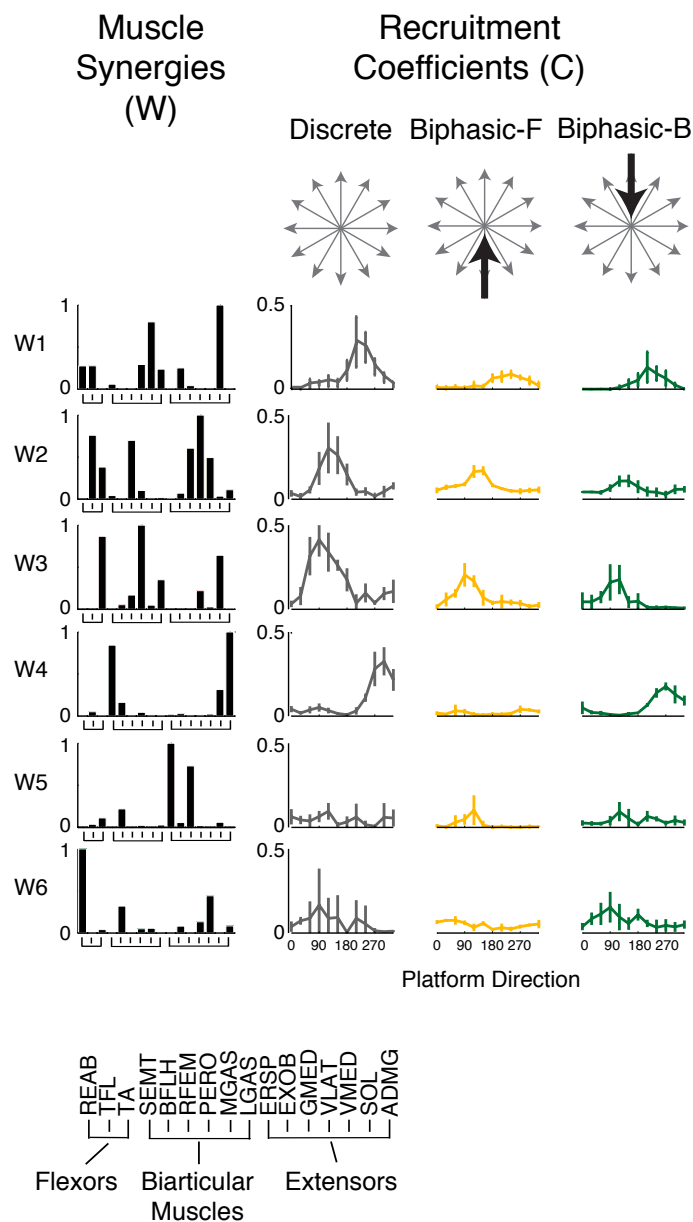
Figure 4.4. SF muscle synergy recruitment across perturbation types. SF muscle synergy recruitment tuning was evaluated throughout platform accelerations that corresponded to multidirectional movements with a delay of 100 ms (Figure 3 – shaded boxes for CoM and muscle activity). Curves indicate trial averages of muscle synergy recruitment patterns throughout the platform acceleration epoch; vertical lines indicate standard deviation of the mean. SF muscle synergies extracted from discrete perturbations are shown for a representative subject (subject 6). Although the magnitude of muscle synergy recruitment is modulated across perturbation types, the maximal tuning direction of muscle synergies is similar across perturbation types.
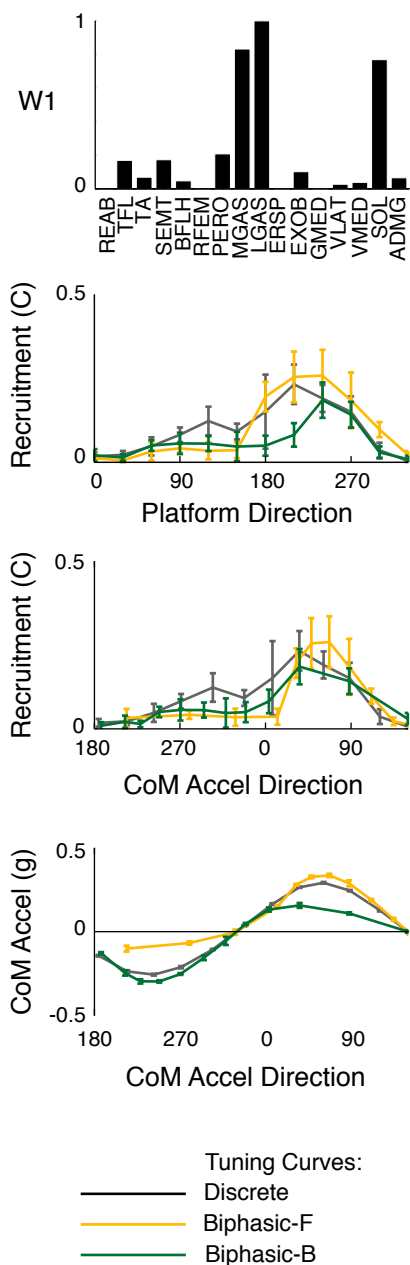
Figure 4.5. Tuning of SF muscle synergies to platform versus CoM acceleration direction. *Top panel*: SF muscle synergy W1 for subject 8. *Second panel*: SF muscle synergy tuning versus platform direction. Compared to discrete perturbations, SF muscle synergy tuning is broader in forward biphasic perturbations and narrower in backward biphasic perturbations. Curves indicate trial averages of SF muscle synergy recruitment patterns throughout the platform acceleration epoch; vertical lines indicate standard deviation of the mean. *Third panel*: SF muscle synergy tuning versus CoM acceleration direction. SF muscle synergy tuning is more consistently tuned across perturbation types to CoM acceleration direction versus platform direction. Note that CoM acceleration direction is opposite platform direction. *Bottom panel*: Projection of CoM acceleration vector along the direction of maximal CoM acceleration tuning (60°) across perturbation directions. CoM acceleration magnitude tuning curves resemble SF muscle synergy tuning curves as a function of CoM acceleration direction.

perturbations preceded by a forward premovement, and was clustered to backward directions in biphasic perturbations preceded by a backward premovement.

Differences in magnitude of SF muscle synergies across discrete and biphasic perturbations reflected observed differences in CoM acceleration magnitude across perturbation directions. For a representative subject (subject 8), W1 was maximally tuned to a CoM acceleration direction of ~60° across perturbation types (Figure 4.5 – third panel). However, the magnitude of forward biphasic perturbations was larger than that of discrete perturbations, and the magnitude of backward biphasic perturbations was smaller than that of discrete perturbations. Because SF muscle synergies were maximally recruited to ~60° CoM acceleration directions, we considered it likely that differences in the projection of CoM acceleration in the 60° direction across perturbation directions and types were responsible for modulating SF muscle synergy recruitment. For all perturbation types, the projection of CoM acceleration magnitude across directions matched that of SF muscle synergy recruitment with respect to CoM acceleration direction (Figure 4.5 – bottom panel). Moreover, for forward CoM acceleration directions, CoM acceleration magnitude was highest in forward biphasic perturbations and lowest in backward biphasic perturbations, similar to differences in SF muscle synergy recruitment magnitudes.

Similar SF muscle synergies were identified across subjects and had consistent tuning (Figure 4.6). 12 different SF muscle synergies were identified across all subjects; five of 12 SF muscle synergies were consistent in at least nine of 12 subjects. W1 was identified in all 12 subjects (Figure 4.6A); W1 was composed mainly of calf muscles (MGAS, LGAS, SOL) and had single tuning in response to forward-rightward CoM

acceleration directions (Figure 6B). W2 was identified in 11 subjects and composed

mainly of quadriceps muscles (RFEM, VLAT, VMED) (Figure 4.6C). In eight of 11

subjects, W2 had double tuning: W2 was largely recruited in response to backward CoM

acceleration directions and also recruited to a lesser extent in response to forward CoM

accleration directions (Figure 4.6D – black traces). In three of 11 subjects, W2 was only

tuned in response to backward CoM accleration directions (Figure 6D – grey traces).

4.3.4   *CoM feedback predicts SF muscle synergy recruitment in static and dynamic states*

Across subjects, a majority of SF muscle synergy recruitment patterns in their

maximal tuning direction were well-reconstructed using delayed CoM feedback

throughout discrete perturbations and biphasic perturbations that changed direction

(Figure 4.7). For example, SF muscle synergies from subject 6 (cf. Figure 4.4) were

tuned to unique CoM acceleration directions, opposite the direction of platform tuning

(Figure 4.7 – two left panels). Five of the six SF muscle synergies (W1-W4, W6) were

independently well-reconstructed by delayed CoM feedback across perturbation types.

W5 was not well-reconstructed by the feedback model across perturbation types and was

composed of muscles with actions at the hip and trunk (ERSP, GMED). Similarly, over

all subjects, 53 of 71 SF muscle synergies (75%) were well-reconstructed in their

maximal CoM acceleration tuning direction ($r^2 = 0.68 \pm 0.18$, median $r^2 = 0.71$;

VAF = 87 ± 6%, median VAF = 88%). Time delays were between 90-120 ms for all

reconstructions, consistent with postural delays described in the literature. Of the 53 well-

reconstructed SF muscle synergies, 36 (68%) were single-tuned, and the remaining 17

(32%) were double-tuned. For the 18 SF muscle synergies that were not well-
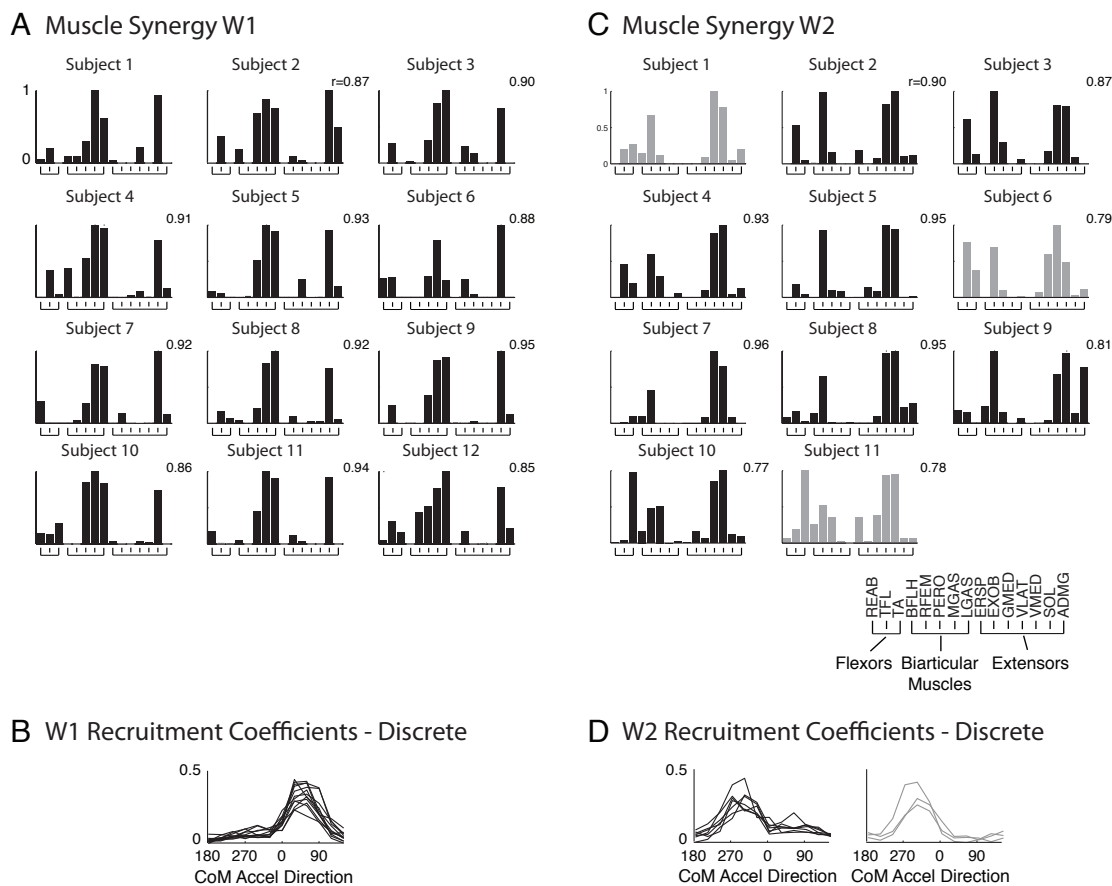
Figure 4.6. Consistency of SF muscle synergy structure and tuning across subjects. A, consistency of SF muscle synergy W1 structure. W1 was identified in all 12 subjects and had a high level of constistency (r = 0.90 ± 0.03). **B,** SF muscle synergy W1 tuning. W1 had unimodal tuning in all subjects in response to backward-leftward perturbations (forward-rightward CoM acceleration directions). **C,** consistency of SF muscle synergy W2 structure. W2 was identified in 11 of 12 subjects (r = 0.87 ± 0.08). **D,** SF muscle synergy W2 tuning. For eight of 11 subjects, W2 had bimodal tuning (black traces). Three of 11 subjects had unimodal tuning (grey traces). Grey SF muscle synergies in Figure 4.6C correspond to grey tuning curves in Figure 4.6D.
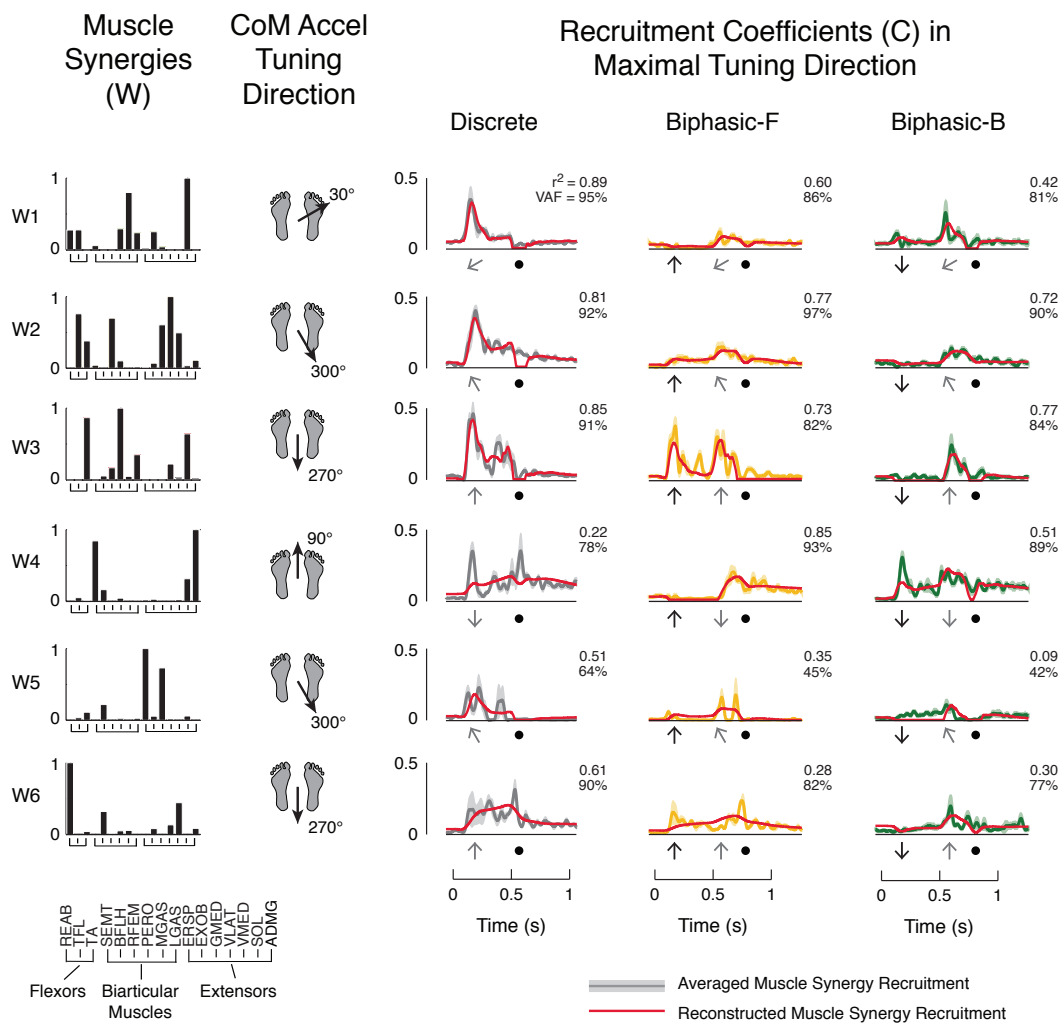
Figure 4.7. Feedback model reconstruction of SF muscle synergies in their maximal tuning direction. *Two left panels*: SF muscle synergy structure and maximal tuning direction with respect to CoM acceleration. Data are shown for the same subject as in Figure 4.4. *Right panel*: feedback model reconstructions of SF muscle synergy recruitment patterns in the direction of maximal tuning. Average SF muscle synergy recruitment patterns for W1-W4 were well-reconstructed by the feedback model across discrete and biphasic perturbations. Numbers indicate r^2 (top) and VAF (bottom) values for reconstructions. Grey, yellow, green lines: averaged muscle synergy recruitment patterns. Shaded regions indicate one standard deviation of the mean. Red lines: feedback model reconstructions.

reconstructed, 17 had major contributions of muscles that had actions at the hip and trunk (ERSP, EXOB, REAB, GMED).

Each well-reconstructed SF muscle synergy was recruited in response to the projection of CoM kinematics along its maximal CoM acceleration direction, despite changes in platform direction (Figure 4.7). For subject 6, W3 was tuned to 270° (backward CoM acceleration); as such, biphasic perturbations that featured two forward movements caused two bursts of recruitment equal in magnitude (Figure 4.7 – W3 yellow trace). Moreover, W3 was not recruited in backward biphasic perturbations until the platform moved forward, causing backward CoM motion (W3 green trace). Although W2 also had two bursts of recruitment in forward biphasic perturbations, the second burst was larger in magnitude than the first. Using the projection of CoM motion along the maximal tuning direction of W2 (300°), the feedback model could account for differences in magnitude observed when changing direction due to the second perturbation. Similarly, the feedback model accounted for two bursts of recruitment in W1 and W4 during backward biphasic perturbations and only one burst of recruitment during forward biphasic perturbations.

For each perturbation type, a fixed set of feedback gains (k_d, k_v, k_a) predicted the temporal patterns of recruitment of SF muscle synergies with single tuning across directions. SF muscle synergy recruitment patterns were predicted by multiplying the feedback gains identified by model fits to the projection of CoM motion along the maximal CoM tuning direction. For example, W1 in subject 1 was maximally tuned to 60° (Figure 4.8A); SF muscle synergy recruitment patterns were thus fit to 240° perturbations and predicted over remaining directions. As the perturbation direction

differed from 240°, SF muscle synergy recruitment was modulated in response to the

projection of CoM motion along the 60° direction. For example in discrete 180°

(leftward) perturbations, W1 was not recruited as much as in 240° perturbations (Figure

8B). Nevertheless, SF muscle synergy recruitment in leftward perturbations can be

predicted by applying the same feedback gains identified from 240° perturbations to

CoM motion evoked during leftward perturbations projected along the 60° direction,

Note that in discrete perturbations that are in the direction of CoM tuning (60°), W1 was

inhibited compared to background levels until the platform decelerated (Figure 4.8B);

during platform deceleration (black dots), CoM motion was again moving in the direction

of maximum tuning. Similarly for biphasic perturbations, recruitment of W1 following

the second perturbation was modulated in response to the projection of CoM motion

along the maximum tuning direction (Figure 4.8C and 4.8D). Moreover, the model

predicted inhibition of W1 compared to background during forward premovements and

the same level of W1 recruitment during backward premovements, consistent with actual

data.

The temporal patterns of recruitment of double tuned SF muscle synergies could

also be predicted across directions and perturbation types using two fixed sets of

feedback gains. Similar to seven other subjects, W2 in subject 2 and had a large CoM

acceleration tuning at 300°, and a smaller but distinct tuning at 90° (Figure 4.9A). Model

predictions of W2 recruitment based on CoM tuning of 300° (red traces) matched actual

recruitment patterns over forward perturbation directions but not in backward directions

(Figure 4.9B). Alternatively, W2 recruitment in backward directions was predicted using

a second set of feedback gains based on CoM tuning of 90° (blue traces). As revealed by

the feedback gains, W2 was more responsive to CoM acceleration and position in forward perturbation directions, but was more responsive to CoM velocity in backward directions.

Tuning curves of SF muscle synergies with both single and double tunings were predicted by delayed CoM feedback (Figure 4.10). Using feedback gains identified from model fits in the maximal tuning direction (cf. Figure 4.8), the tuning of SF muscle synergy W1 in subject 1 was predicted over directions (Figure 4.10 – top row). The tuning of SF muscle synergy W2 in subject 2 was predicted using two model fits (Figure 4.10 – bottom row), each with a unique set of feedback gains (cf. Figure 4.9). For W2, tuning peaks in forward and backward directions were separately predicted using the feedback model across perturbation types. For well-reconstructed muscle synergies, tuning curves were well-predicted using either one or two sets of feedback gains across all subjects and perturbation types. ($r^2 = 0.62 \pm 0.28$, median $r^2 = 0.73$; VAF $= 78 \pm 18\%$, median VAF $= 83\%$).
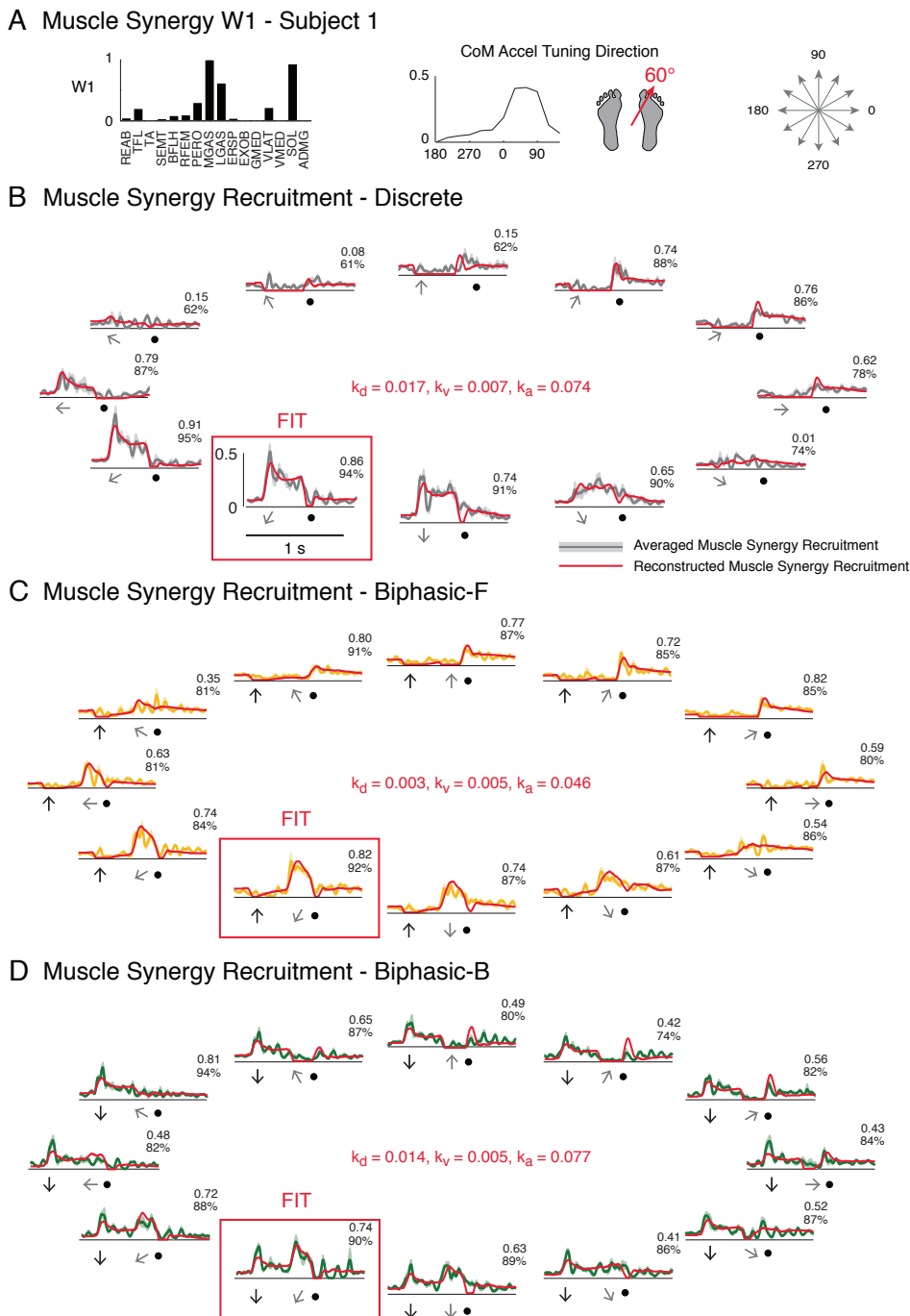
Figure 4.8. Predictions of single tuned SF muscle synergy recruitment patterns across directions based on feedback model fits of SF muscle synergy recruitments to their maximal tuning direction. A, SF muscle synergy structure and maximal CoM acceleration tuning direction. Data are shown for subject 1. **B,** feedback model fit and predictions of discrete perturbations. SF muscle synergy recruitment was reconstructed in the direction of maximal tuning. Feedback gains identified from maximal tuning directions (FIT) were applied to all other perturbation directions. Note that CoM acceleration direction is opposite platform direction. **C,** feedback model fit and predictions of forward biphasic perturbations. **D,** feedback model fit and predictions of backward biphasic perturbations. Numbers indicate r^2 (top) and VAF (bottom) values for predictions. Black arrows indicate the time and direction of premovement, grey arrows indicate time and direction of movement, and black circles indicate platform deceleration.
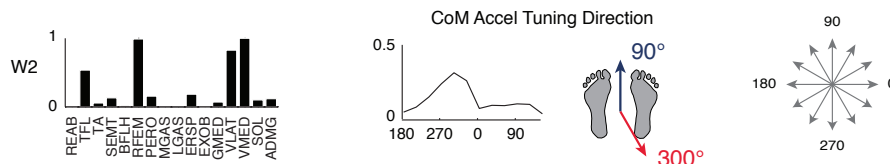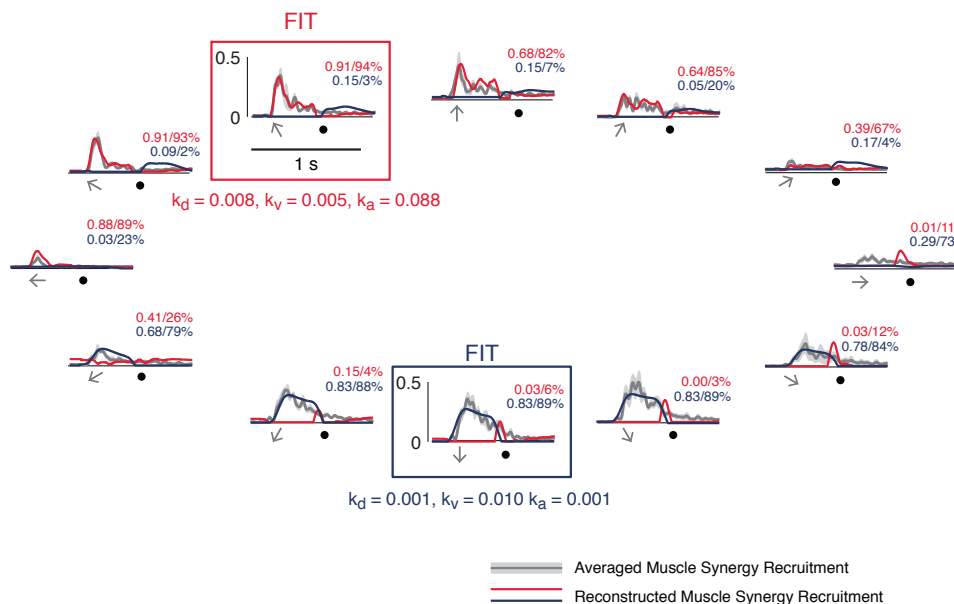
Figure 4.9. Predictions of double tuned SF muscle synergy recruitment patterns across directions based on feedback model fits of muscle synergy recruitment in two directions. A, SF muscle synergy structure and maximal CoM acceleration tuning directions. SF muscle synergy W2 in subject 2 had two maximal tuning directions. **B,** feedback model fit and predictions of discrete perturbations. SF muscle synergy recruitment was reconstructed in two directions. Feedback gains identified from maximal tuning directions (FIT) were applied to all other perturbation directions. Note that CoM acceleration direction is opposite platform direction. Numbers indicate r² (top) and VAF (bottom) values for predictions. Grey arrows indicate time and direction of movement, and black circles indicate platform deceleration.
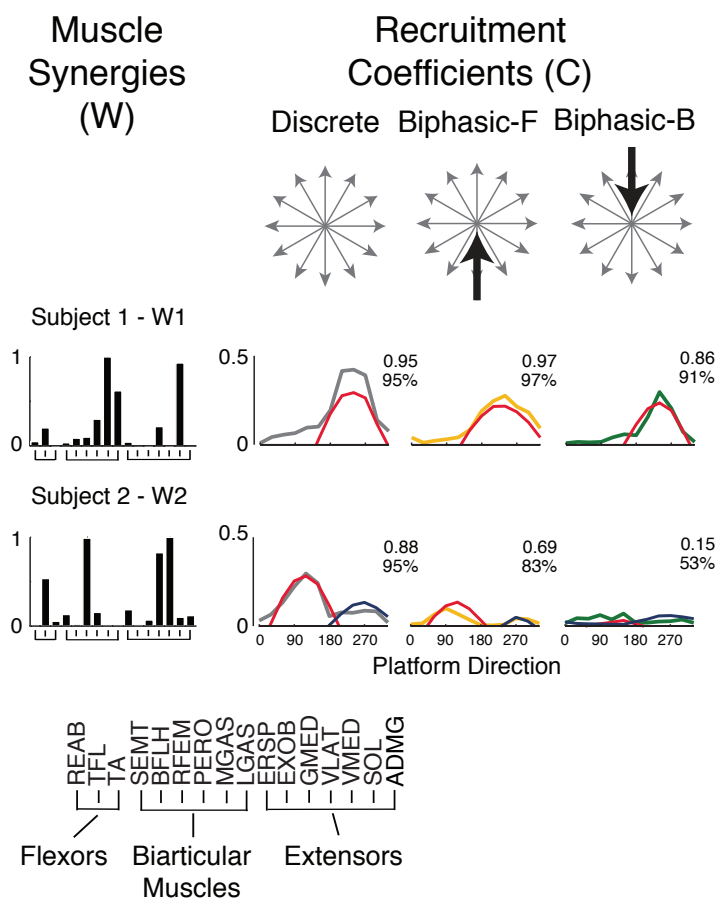
Figure 4.10. Tuning curve predictions for SF muscle synergy recruitment tuning patterns. Data are shown for SF muscle synergy W1 in subject 1 (Figure 4.8) and SF muscle synergy W2 in subject 2 (Figure 4.9). Numbers indicate r^2 (top) and VAF (bottom) values for predictions. SF muscle synergy tuning curves were well-reconstructed by delayed feedback of CoM in all subjects ($r^2 = 0.62 \pm 0.28$; median $r^2 = 0.73$; VAF = $78 \pm 18\%$; median VAF = 83%). Note that double-tuned muscle synergies required two separate fits in disparate directions.

4.4 DISCUSSION

4.4.1 Summary

Taken together, our results suggest that the nervous system uses task-level control of SF muscle synergies to consistently and flexibly produce motor outputs necessary for maintaining balance. We found that SF muscle synergies were modulated in response to task-level variables, namely the projection of CoM kinematics along a particular tuning direction. Moreover, the recruitment of SF muscle synergies was predicted in a variety of multidirectional perturbations based on the initial and perturbed state of the system. Our results suggest that there is a consistent spatial and temporal structure of motor outputs across static and dynamic perturbation states, and that the observed motor structure is independent of body states. Thus, the nervous system may use task-level control of SF muscle synergies as a general organization for motor outputs.

4.4.2 A hierarchical theory of postural control

Our results suggest that task-level control of SF muscle synergies may represent a common and robust mechanism for human balance control, consistent with a hierarchical neural organization. We have previously shown that delayed feedback of CoM could describe SF muscle synergy recruitment in discrete sagittal perturbations (Safavynia and Ting 2012). We extend this work to demonstrate that a small set of sensorimotor transformations based on task-level goals can modulate the temporal recruitment of SF muscle synergies across directions. Previous work in postural control has shown that SF muscle synergies are directionally tuned and produce consistent motor outputs that function to move the CoM in specific directions (Chvatal et al. 2011; Ting and Macpherson 2005; Torres-Oviedo et al. 2006; Torres-Oviedo and Ting 2007; 2010). In

concert with previous studies, we were able to predict both the temporal modulation and directional tuning of SF muscle synergies in response to the projection of CoM along a unique direction. By hierarchically controlling the directional actions of SF muscle synergies in response to task-level goals, the nervous system can flexibly restore the CoM over the base of support (BoS) over a wide range of perturbations. Thus, we have identified a common hierarchical mechanism where task-level variables can be consistently mapped to SF muscle synergies to produce a wide variety of motor outputs.

We propose that the nervous system uses continuous feedback to modulate motor outputs to maintain standing balance. In order to maintain standing balance, the nervous system must combine information about the current state of the body and the effect of the perturbation (Bingham et al. 2011; Mergner 2010; Pai and Patton 1997; Pai et al. 1998; Peterka 2002; van der Kooij and de Vlugt 2007). Using biphasic perturbations that changed directions, we demonstrated that task-level feedback continuously modulated SF muscle synergy recruitment to maintain balance based on the initial and perturbed state of the system. When preceded by a forward or backward movement, SF muscle synergies were recruited not only to the change in CoM kinematics, but rather to the absolute deviation of CoM kinematics in a particular direction, suggesting that the nervous system continuously corrects errors in balance control by integrating signals due to both prior motion and the current perturbation. Simulations of continuous feedback control have also been used to explain postural responses during quiet sway (Peterka 2000) and continuous oscillations with or without visual feedback (van der Kooij and de Vlugt 2007); it is thus possible that the same delayed-feedback mechanisms are employed continuously during both postural sway and postural responses to perturbations.

Here we extend our prediction of SF muscle synergy recruitment using purely feedback mechanisms to long timescales that can incorporate influences from descending voluntary commands (Burleigh et al. 1994; Jacobs and Horak 2007). Additionally, feedforward mechanisms have been known to influence postural responses (Collins and De Luca 1993; Keshner et al. 1987; Shumway-Cook and Woollacott 2000). Such feedforward mechanisms may be involved in the initial selection of a set of gains for a perturbation, as the identified feedback gains were different between discrete and biphasic perturbations.

Our model also predicts inhibition of muscle activation at the level of SF muscle synergy recruitment. Inhibition of tonic muscle activation has been observed in early epochs following postural responses in cat (Ting and Macpherson 2004) and can be evoked during postural responses in human (Horak et al. 2001); such inhibition could arise from a number of sources, including spinal reflexes (Eccles 1967) and descending commands (Lundberg 1979). While we chose to use non-negative matrix factorization (NNMF) to identify SF muscle synergies because muscles cannot be negatively activated (Ting and Chvatal 2011), compared to other component analyses, NNMF fails to account for inhibition of muscles (Torres-Oviedo and Ting 2007; Tresch et al. 2006). Thus, the utility of SF muscle synergies identified from NNMF has been largely limited to studying positive activations. Using the feedback model, we demonstrated that inhibition of SF muscle synergies is possible at the level of recruitment as opposed to the structure of the SF muscle synergy itself, consistent with hierarchical control (Figure 4.8). It is possible that the recruitment of a different SF muscle synergy tuned to a different direction of CoM motion may be responsible for such inhibition, as previous data has demonstrated

that the recruitment of SF muscle synergies associated with different motor strategies are negatively correlated (Torres-Oviedo and Ting 2007).

4.4.3   Flexibility in task-level mapping

Our findings suggest that the nervous system may flexibly alter sensorimotor transformations during dynamic balance control to account for intrinsic musculoskeletal properties. While we could predict SF muscle synergy recruitment in both discrete and biphasic perturbations, feedback gains were inconsistent across perturbation types, and the initial burst of SF muscle synergy recruitment was often under-predicted in biphasic perturbations (Figure 4.8). Taken together, these results suggest that the nervous system modulates the specific sensorimotor transformations in static and dynamic states. It is possible that such modulation is necessary to account for intrinsic properties of muscle spindles in static and dynamic states. Muscle spindles are more sensitive when muscles are stretched from rest as opposed to when they are dynamically moving (Haftel et al. 2004; Nichols and Cope 2004) due to history- and time-dependent cross-bridge linkages in muscle (Campbell and Moss 2002; 2000; Getz et al. 1998). While previous formulations of the jigsaw model limited CoM acceleration feedback to the initial postural response to account for muscle stiction (Welch and Ting 2009), our model predictions from biphasic perturbations suggest that the nervous system continuously responds to CoM acceleration but with different gains depending on body state. The changes in gains could thus result from direct modulation of the fusimotor system (Matthews 1981) to account for history dependent properties of muscle spindles. Alternatively, muscle activity could be modulated in dynamic states due to the

superposition of competing influences that act at long latencies, including descending commands (Jacobs and Horak 2007; Trivedi et al. 2010).

SF muscle synergies may be flexibly recruited by multiple sensorimotor transformations based on task-level motion of CoM. For example, SF muscle synergy W2 was composed mainly of quadriceps muscles and had bimodal tuning in a majority of subjects (Figure 4.6). In order to predict W2 tuning, W2 required two separate sensorimotor transformations based on CoM kinematics in forward and backward directions. While quadriceps SF muscle synergies have been previously shown to move the CoM backwards (Chvatal et al. 2011), the results relied on component analyses that could only identify one direction of CoM motion per SF muscle synergy. Simulations of human walking indicate that quadriceps SF muscle synergies are recruited in concert with other SF muscle synergies, but function to aid in body support as opposed to propulsion of body CoM (Neptune et al. 2009); thus in postural control, bimodal quadriceps SF muscle synergies may be recruited in concert with distinct unimodal SF muscle synergies to stabilize the limb during anteroposterior CoM motion. However, it is unclear whether the bimodal SF muscle synergies themselves would be concurrently recruited with unimodal SF muscle synergies, or whether they would be separately recruited by spatial summation of separate sensory signals.

In contrast to CoM feedback, SF muscle synergies with actions at the trunk may be recruited by other task-level variables such as orientation. The majority of poorly-reconstructed SF muscle synergies were comprised mainly of muscles with actions at the trunk. SF muscle synergies with trunk actions were recruited over a wide range of directions (e.g. W5 and W6 – Figure 4), inconsistent with the idea that CoM motion

along a particular direction modulates SF muscle synergy recruitment. Alternatively, trunk SF muscle synergies may by recruited to minimize deviations from vertical to maintain a vertical orientation. In postural control, orientation is likely to be a task-level goal in addition to CoM (Kluzik et al. 2005; Macpherson et al. 1997; Massion 1994). Moreover, due to the biomechanics of bipedal stance, muscles with hip actions may be more heavily influenced by sensory feedback and/or descending control. It is important to note that the structure of SF muscle synergies with trunk actions has been the least consistent across conditions and tasks in previous studies (Chvatal et al. 2011; Safavynia and Ting 2012; Torres-Oviedo and Ting 2007; 2010); thus, it is possible that trunk muscles may not be constrained in a SF muscle synergy structure. In contrast to more distal limb muscles however, trunk muscles span several joint segments and insert in a variety of locations on the axial skeleton with multiple functions. Thus, it is also likely that while coordination patterns exist and can be constrained in a SF muscle synergy organization, they cannot be identified simply via surface EMG at one location for each muscle.

4.4.4 General principles for motor control

Task-level control of SF muscle synergies may represent one general principle for motor control, reflecting a common hierarchical neural architecture for motor tasks. For example, in reaching tasks, SF muscle synergies have been identified and have been demonstrated to be modulated in response to task-variables such as target direction (d'Avella et al. 2008; d'Avella et al. 2006; d'Avella et al. 2011) and reaching speed (d'Avella et al. 2008). Accordingly, pyramidal neurons in motor cortex have been shown to respond to task-level variables such as endpoint force, velocity, movement direction,

and hand location (Georgopoulos et al. 1986; Sergio and Kalaska 1997). Moreover, limb

orientation can be encoded across the neuraxis, including reticular formation (Deliagina

et al. 2008), motor cortex (Scott and Kalaska 1997), and dorsal spinocerebellar tract

(Poppele et al. 2002). SF muscle synergies have also been identified in walking (Clark et

al. 2010; Gizzi et al. 2011) and postural control (Torres-Oviedo et al. 2006; Torres-

Oviedo and Ting 2007; 2010); moreover, it has been demonstrated that the same SF

muscle synergies are recruited in both walking and postural control to move the CoM

(Chvatal 2011). CoM can be represented by integrating proprioceptive, visual, and

vestibular information (Green et al. 2005; Horak and Macpherson 1996; Peterka 2002),

presumably in higher neural centers. Similarly, neurons in the reticular formation have

been shown to respond to task-level changes in postural equilibrium (Stapley and Drew

2009).

The recruitment and structure of SF muscle synergies may occur at multiple levels

of the neuraxis, consistent with hierarchical control. Muscle synergies identified from a

variety of tasks have been hypothesized to be encoded along the neuraxis, including

spinal cord for locomotion and primitive movements (Bizzi et al. 1991; Drew et al. 2008;

Kargo et al. 2010; Roh et al. 2011; Saltiel et al. 2001), brainstem for postural control

(Chvatal et al. 2011; Torres-Oviedo et al. 2006; Torres-Oviedo and Ting 2007), and

motor cortex for grasping (d'Avella et al. 2008; Overduin et al. 2008). Regardless of the

location of muscle synergies, they may be recruited from a variety of structures

throughout the neuraxis. For example, SF muscle synergies identified from natural

movements in the frog have been shown to be consistent following transections at rostral

midbrain or medulla (Roh et al. 2011), or at the pontomedullary junction (Hart and

Giszter 2004). However, the movement repertoire from such transections was not as rich as from the full system, suggesting that muscle synergies could be recruited from a variety of neural structures. Similarly, the same muscle synergies have been identified from walking and postural control (Chvatal 2011); however, they are likely to be recruited differently because locomotion requires feedforward control (McCrea 2001; Rossignol et al. 1996) while balance is primarily a feedback process (Kuo 1995; 2002; Lockhart and Ting 2007; Peterka 2002; Welch and Ting 2009; 2008). While SF muscle synergies have not been identified from reactive arm movements, it is likely that the same SF muscle synergies may be recruited during reactive versus voluntary arm movements, although with different control mechamisms. Thus, while muscle synergies may be distributed along multiple locations throughout the neuraxis, they may be hierarchically recruited at different levels of the neuraxis corresponding to the relevant task-variable.

CHAPTER 5:   CONCLUDING REMARKS

5.1   SUMMARY

Taken together, the studies in the previous chapters suggest that the nervous system is hierarchically organized to robustly produce functional motor outputs throughout human postural responses. By combining muscle synergy analysis with task-level feedback, I described a functional spatiotemporal organization of muscle activity throughout a postural task. I demonstrated that both spatial and temporal features of muscle activity are constrained by a low-dimensional structure. While the spatial features of muscle activity are defined by spatially-fixed (SF) muscle synergies, the temporal features of muscle activity can be described by hierarchical control of SF muscle synergy recruitment. As opposed to local-level joint feedback, I demonstrated task-level feedback of center of mass (CoM) is responsible for modulating the temporal features of muscle activity during postural responses to perturbations. Moreover, I showed that task-level feedback is a continuous process employed throughout the maintenance of standing balance.

The hierarchical recruitment of SF muscle synergies based on task-level goals provides one neural framework for understanding complex muscle activity and may reflect general principles of motor control. Previously, muscle synergies have been identified from a variety of voluntary and reactive movements in upper and lower limbs (Cheung et al. 2009; Clark et al. 2010; d'Avella et al. 2008; Gizzi et al. 2011; Hug et al. 2011; Saltiel et al. 2001; Torres-Oviedo et al. 2006; Torres-Oviedo and Ting 2007). In separate studies, task-level control of voluntary and reactive limb movements has been demonstrated (Kurtzer et al. 2008; Lockhart and Ting 2007; Marsden et al. 1981; Pruszynski et al. 2011; Welch and Ting 2009; 2008). In this work, I demonstrated that task-level control of SF muscle synergies could robustly reproduce muscle activity throughout a variety of postural tasks. Such a hierarchical structure reflects the structure of the central nervous system; neuronal populations have been identified that respond to task-level goals (Georgopoulos et al. 1992; Georgopoulos et al. 1986; Stapley and Drew 2009; Yakovenko et al. 2011), and hypothesized structures of SF muscle synergies mirror divergent interneuronal projections (Hart and Giszter 2010; Turton et al. 1993).

By understanding normal motor control in a hierarchical framework, it may be possible to functionally characterize abnormal patterns of muscular coordination exhibited in pathologic populations. Specifically, differences in the number, structure, and recruitment of SF muscle synergies may be indicative of the level of motor skill or impairment. Thus, one could perform SF muscle synergy analysis on a patient with motor deficits and evaluate changes in the number, structure, and recruitment of SF muscle synergies with respect to a healthy population. Such a functional characterization of

muscle activity could help discriminate between a variety of motor strategies and aid in diagnosis and rehabilitation of a variety of motor deficits.

5.2 A HIERARCHICAL FRAMEWORK FOR MOTOR CONTROL

Task-level control of SF muscle synergies may reflect a general principle for producing coordinated movements. In Chapter 2, I demonstrated that the temporal recruitment of SF muscle synergies could be described using task-level feedback in a postural task. In Chapter 3, I showed that delayed feedback of CoM robustly and continuously modulated muscle activity over long timescales, whereas local-level autogenic joint feedback could not reliably reproduce muscle activity. Lastly in Chapter 4, I extended these findings to show that SF muscle synergies recruited in postural tasks are continuously and predictably modulated with respect to the task-level goal of directing the CoM. It has been recently demonstrated that the same SF muscle synergies recruited in reactive postural tasks are recruited in voluntary locomotion (Chvatal 2011), suggesting that task-level control of SF muscle synergies can be utilized with different neural control schemes. In voluntary reaching, muscle synergies are modulated in response to task-level goals, such as reaching speed (d'Avella et al. 2008), target direction (d'Avella et al. 2006; d'Avella et al. 2011), or object manipulation (Yakovenko et al. 2011). Moreover, muscle synergies in grasping movements have been shown to be modulated with respect to the size of the object (Overduin et al. 2008).

I propose that SF muscle synergies represent the neural structure of motor outputs and that they are recruited by a variety of task-level goals. SF muscle synergies have been identified from a variety of tasks (Cheung et al. 2005; Clark et al. 2010; d'Avella and Bizzi 2005; Roh et al. 2011; Torres-Oviedo and Ting 2007), and the patterns of SF

muscle synergies reflect the activity of spinal interneurons (Hart and Giszter 2010). I demonstrated that SF muscle synergies could be predictably recruited by CoM motion in a particular direction throughout standing balance control; moreover, I demonstrated that SF muscle synergy recruitment could be inhibited by CoM motion in the opposite direction. Because neurons have been known to encode task-level variables (Bosco and Poppele 2001; Stapley and Drew 2009), it is possible that neurons tuned to a particular CoM direction activate a particular SF muscle synergy. Inhibition of SF muscle synergies could thus arise from inhibitory signals from populations of neurons tuned to opposite directions of CoM motion. Alternatively, reciprocal inhibition may exist from other SF muscle synergies with opposing actions, similar to reciprocal inhibition of flexor and extensor motor pools proposed in central pattern generation (CPG) models (McCrea and Rybak 2008). Moreover, I demonstrated that some SF muscle synergies were recruited in response to two directions of CoM motion. It is possible that these SF muscle synergies may be recruited by spatial summation of multiple CoM encoding neurons that are tuned to different directions. Alternatively, SF muscle synergies with two directions of tuning may not be recruited by task-level variables themselves but rather recruited by other muscle synergies that may require additional biomechanical functions to satisfy task-level goals. For example, models of muscle synergy recruitment in locomotion reveal that muscle synergies made up of quadriceps muscles act to stabilize the limb (Neptune et al. 2009); in our studies, SF muscle synergies with two directions of tuning were most often composed of quadriceps muscles. Thus, quadriceps SF muscle synergies may be recruited by a variety of other muscle synergies in order to stabilize the limb while controlling the CoM. The recruitment of such SF muscle synergies could exist from a variety of signals

at many levels of the neuraxis as well, as the same SF muscle synergies identified in voluntary tasks have been identified in reactive tasks that do not require cortical involvement (Chvatal 2011). Alternatively, the recruitment of SF muscle synergies can arise from distributed signals throughout the musculoskeletal system (Bunderson et al. 2008; Honeycutt and Nichols 2010a).

My results support the idea that muscle synergies are recruited to produce consistent biomechanical functions. Previous studies have demonstrated that SF muscle synergies produce consistent biomechanical outputs that are robust over tasks and limb configurations (Chvatal et al. 2011; McKay and Ting 2008; Ting and Macpherson 2005; Torres-Oviedo et al. 2006; Torres-Oviedo and Ting 2010). Thus, an SF muscle synergy organization is advantageous because task-level goals can be reliably transformed to complex motor outputs. Consistent with previous studies (Chvatal et al. 2011; Torres-Oviedo and Ting 2007; 2010), I identified intersubject variability in the structure of SF muscle synergies; such variability may be attributed to biomechanical differences across subjects. It is thus possible that the structure of SF muscle synergies is shaped as a result of learning appropriate motor patterns to reliably produce specific motor functions. When learning new tasks, existing SF muscle synergies may be modified to more precisely control relevant task variables, or new SF muscle synergies may be formed.

SF muscle synergies may exist in the nervous system as part of a hierarchical nested structure that modulates outputs to muscles. Due to muscular redundancy, there is large variability in spatial and temporal patterns of electromyographic (EMG) activity during movements (Ting 2007). A large amount (~90%) of EMG variability in complex motor tasks can be explained using a small number of SF muscle synergies. These

findings suggest an SF muscle synergy structure may underlie the neural activation of muscles. However, it is known there are other influences on muscle activity. In the intact limb, the response of any one muscle results from the convergence of a number of different pathways, including local reflexes (Liddell and Sherrington 1924; Schmidt 1983), heterogenic feedback (Lundberg 1979; Nichols 1999) and direct cortical control (Rathelot and Strick 2009). Thus, muscles may be activated by competing influences that may act at the level of the SF muscle synergy or at the level of the individual muscle. Such a nested hierarchical structure has been proposed to explain deletions during fictive locomotion (McCrea and Rybak 2008). Similarly, a nested structure may explain why only a few muscles were activated during continuous perturbations administered in Chapter 3.

In contrast to hierarchical control of SF muscle synergies via CoM feedback, the structure and recruitment of SF muscle synergies comprised of hip muscles may be explained by more distributed structures that may be recruited by a variety of task-level variables. One could explain the inconsistency of SF muscle synergies with actions at the hip in Chapters 2 and 4 as part of a nested, distributed structure where hip muscles are activated by more competing local and non-local influences than the distal limb musculature. Similarly, while the recruitment of SF muscle synergies comprised of distal musculature may be dominated by CoM feedback that can be derived from somatosensory signals, the recruitment of SF muscle synergies with actions at the hip may be dominated more by visual and/or vestibular signals. Models of sensory reweighting have been shown to predict shifts in postural responses from distal "ankle" strategies to more proximal "hip" strategies (Peterka 2002). In sinusoidal perturbations,

hip motion predominates at higher perturbation frequencies (Kuo 1995); moreover, postural strategies switch from intrinsic variables such as CoM control at low frequencies to extrinsic variables such as head stabilization at high frequencies (Buchanan and Horak 2001). However, the influence of implicit versus explicit variables has yet to be tested within an SF muscle synergy organization.

5.3   CLINICAL IMPLICATIONS OF MUSCLE SYNERGY ANALYSIS

Muscle synergy analysis may be a useful metric for the assessment of motor disorders, as changes in the number, structure, and recruitment of muscle synergies may be able to discriminate among a variety of pathological changes in the nervous system. Changes in muscle synergy number would affect the number of independent motor subtasks that can be independently recruited. For example, a smaller number of SF muscle synergies have been identified in hemiparetic stroke patients during forward walking compared to healthy controls; moreover, the reduced number of muscle synergies resembled merged versions of healthy SF muscle synergies (Clark et al. 2010). A reduction in the number of SF muscle synergies may be the result of reduced corticospinal drive, compromising the ability of the nervous system to recruit spinal locomotor muscle synergies in the paretic limb (Nielsen et al. 2008). Consequently, stroke patients may rely more heavily on alternative pathways (e.g., reticulospinal, bulbospinal) that could recruit the same spinal muscle synergies but with less individuation, causing abnormal joint and torque patterns (Dewald and Beer 2001; Lum et al. 2003). Depending on the task, muscle synergies have been hypothesized to be encoded at different levels of the central nervous system, including motor cortex for grasping (d'Avella et al. 2008; Overduin et al. 2008), brainstem for postural control

(Torres-Oviedo et al. 2006; Torres-Oviedo and Ting 2007), and spinal cord for

locomotion (Drew et al. 2008). Lesions to neural structures encoding the muscle

synergies could result in a reduced number of muscle synergies available for a given task

or changes in muscle synergy structure. Changes in muscle synergy structure would

affect the muscle coordination patterns themselves and could reflect changes in neural

connectivity or excitability (Dietz et al. 1984; Dietz and Sinkjaer 2007), such as in stroke,

spinal injury, multiple sclerosis, or traumatic brain injury. Even if the number and

structure of muscle synergies remains intact, changes in muscle synergy recruitment

could result in abnormal muscle patterns by affecting the timing and strength of normal

motor subtasks. It is possible that changes in muscle synergy recruitment could be seen in

motor disorders such as writer's cramp, a task-specific focal hand dystonia. These

patients can produce normal and complex hand postures in non-writing tasks, suggesting

that they have access to a full library of muscle synergies with normal structure; however,

abnormal contractions during writing may result from decreased surround inhibition at

the level of motor cortex (Sitburana and Jankovic 2008; Sohn and Hallett 2004), which

would cause abnormal recruitment of muscle synergies that are typically silent during

writing. In general, the number, structure, and recruitment of muscle synergies can

indicate whether motor subtasks are accessible, functional, or able to be appropriately

modulated, respectively. This information may be used for classifying differences across

patients within and across pathologies that would more precisely describe the nature of

impairment and better inform rehabilitation or treatment decisions.

I further propose that the number of muscle synergies may more generally reflect

motor skill level in healthy subjects, in which differences in the number and structure of

muscle synergies have been identified in both walking and balance tasks (Clark et al. 2010; Torres-Oviedo and Ting 2007). Across healthy subjects, many of the identified muscle synergies have similar structures for performing similar functions necessary for balance and locomotion. However, in some cases, muscle synergies with different muscular patterns but similar functional outcomes can be identified in a subpopulation. During balance control, some subjects use a knee-bending strategy, recruiting a muscle synergy specific to that strategy that is not identified in other subjects (Torres-Oviedo and Ting 2007). It is possible that new muscle synergies are formed during motor skill acquisition. For example, musicians have great muscular independence (Chen et al. 2006), and patterns of joint coordination elicited through transcranial magnetic stimulation (TMS) of the motor cortex of musicians cannot be reproduced in patterns of joint coordination elicited by TMS stimulation of motor cortex in nonmusicians (Gentner et al. 2010). These differences in muscle coordination are consistent with white matter changes seen in musicians with extensive training (Bengtsson et al. 2005). Other skilled populations, such as dancers (Gerbino et al. 2007) and tai chi practitioners (Tsang and Hui-Chan 2005), also exhibit fine motor control that improves with practice. This motor independence is likely to represent an increase of muscle synergies available to these groups. As motor training for as little as 6 weeks can induce changes in white matter (Scholz et al. 2009), motor training may encourage the development of new muscle synergies for new tasks, change the structure of existing muscle synergies, or change the manner in which existing muscle synergies are recruited.

Muscle synergy analysis may also be useful in evaluating the ability of rehabilitative therapies to promote a restitution of function following neural injury. As

opposed to endpoint performance based measures of motor function such as the Fugl-Meyer Scale (FMS) or the Wolf Motor Function Test (WMFT) (Fugl-Meyer 1980; Gladstone et al. 2002; Levin et al. 2009; Morris et al. 2001), muscle synergy analysis can reveal how muscles are coordinated to achieve certain tasks and does not rely on subjective assessments of motor performance. Because muscle synergies are hypothesized to reflect a neural organization of motor coordination, muscle synergy analysis may thus be used as a metric to assess rehabilitation interventions at the neuronal level. Therefore, with regular motor assessment using muscle synergies, it may be possible to differentiate a patient's response to a rehabilitation therapy and promote restitution of motor function versus motor compensation. Because compensation relies on using existing neural pathways to achieve tasks in novel ways, compensatory motor strategies would likely alter the recruitment of existing muscle synergies but not change the number or structure of muscle synergies. Alternatively, restitution of motor function reflects plasticity in the nervous system; therefore, restitution of motor function would be expected to alter the composition of muscle synergies, increase the number of muscle synergies (as patients learn new coordination patterns) as well as change the recruitment of muscle synergies. By increasing the number of muscle synergies and refining their composition, it is possible to expand the library of motor subtasks, thus increasing the number of recombinant muscle patterns and expanding the motor repertoire. Changes in muscle synergy number, structure, and recruitment may also help elucidate why different interventions work for certain patients and not for others, helping to develop prognostic indicators of rehabilitative treatments. Once therapies could be quantified using muscle synergy analysis, it may be possible to compare the efficacy of different therapies on an

individual basis and evaluating whether subjects have gained motor functions that generalize to activities of daily living. By regularly assessing a patient's muscle synergy profile, it may be possible to identify a patient's functional deficit, track rehabilitation results, and adjust treatments. Much like current approaches in genetics and molecular biology, a patient's muscle synergy profile could possibly allow clinicians to more effectively treat motor dysfunctions by organizing patients into subclasses and tailoring the treatment to the specific patient's deficit.

5.4   LIMITATIONS AND FUTURE WORK

While these studies have demonstrated that SF muscle synergies are robustly recruited during human standing balance by task-level feedback, the robustness of task-level recruitment of SF muscle synergies beyond postural control is purely speculative. Moreover, within balance tasks, only delayed feedback of CoM kinematics has been used to explain the recruitment SF muscle synergies. CoM is unlikely to be a task-variable in upper limb tasks, as control of reaching movements is more dependent on endpoint stabilization (van der Steen and Bongers 2011). Other complex tasks may rely on a variety of different task-level variables, such as maintaining constant angular momentum during turning movements (Laws 2002), or minimizing vertical force variance in hopping (Yen et al. 2009). Even within balance control, delayed feedback of CoM kinematics was unable to explain the recruitment of SF muscle synergies with actions at the hip. While task-level variables such as maintaining an upright orientation (Horak and Macpherson 1996; Kluzik et al. 2005) or head stabilization (Corna et al. 1999; De Nunzio et al. 2005) have been proposed to also be important for balance control, the relationship between alternative task-level goals and SF muscle synergy recruitment has not been tested. To

fully understand the effects of task-level variables on SF muscle synergy recruitment, it would be necessary to design specific tasks that exploit alternative task-level goals, and apply hierarchical models on SF muscle synergy recruitment. As a first step towards elucidating the role of alternative task-level variables on SF muscle synergy recruitment, I have developed continuous multidirectional perturbations ("star" perturbations) that result in head stabilization and much smaller deviations of CoM. Star perturbations could thus be used to examine the recruitment of SF muscle synergies in a condition where various task-level variables are independent.

Although it is assumed that task-level variables are integrated in higher neural centers, it is possible that some task-level variables may be encoded from local neural circuitry at the level of muscles and joints. CoM is unlikely to be locally encoded because CoM must be inferred from the position of all of the body segments; however, other task-level variables may not require global integration of signals. For example, muscle spindles have been hypothesized to encode muscle position and velocity (Cordo et al. 2002), and they are intrinsically history dependent, even without evoking fusimotor drive (Haftel et al. 2004; Nichols and Cope 2004). Fusimotor drive can change the dynamic response of muscle spindles throughout a task in response to task-level goals (Matthews 1981). Additionally, a variety of crossed-extension and heterogenic reflexes exist and can modulate muscle activity (Bonasera and Nichols 1996; Nichols 1989). Thus, it is possible that muscles can be activated in response to task-level goals from local signals alone (Bunderson et al. 2010; Honeycutt and Nichols 2010a). However, these more local signals still require integration of sensory inputs. Moreover, local circuits are essential to obtain information about the CoM. The question remains then whether integration of

task-level variables occurs within a hierarchical versus a distributed neural framework. Without detailed electrophysiological studies, it is impossible to know exactly where task-level variables may be encoded. As a result, the local versus non-local activation of muscles is part of an ongoing debate and is unlikely to be definitively answered for some time.

The fact that the musculoskeletal system can produce a variety of coordinated movements when individual muscles are activated raises the question: do muscle synergies really exist? The number of neural synapses greatly exceeds the number of motor units in the body. In fact, it may be argued that the musculoskeletal system reduces the dimension of neural outputs as opposed to the nervous system reducing the dimension of motor outputs. Indeed, the number of possible movements is greatly diminished when one considers the effects of inter-joint coupling (van Antwerp et al. 2007) and connective tissue (Stahl and Nichols 2011) in the musculoskeletal system. Although muscle synergies have been identified in a variety of tasks, the structure of muscle synergies may simply reflect biomechanical and/or task constraints (Tresch and Jarc 2009). Thus, simply identifying muscle synergies in tasks does not prove that they actually represent neural constraints. Moreover, studies examining variability in finger force production reveal that muscles can be independently controlled, challenging the muscle synergy hypothesis (Kutch et al. 2008; Valero-Cuevas et al. 2009). In order to demonstrate that muscle synergies represent preferred patterns of muscle coordination, one could investigate the learning of a new task. If muscle synergies truly reflect the inherent structure of the nervous system, then the nervous system would perform a new task using

existing muscle synergy constraints, even if the performance of such a task were suboptimal.

Although non-negative matrix factorization (NNMF) produces more physiologically relevant results for EMG than other components analyses such as principal component analysis (PCA), there are inherent limitations with the NNMF algorithm. Because PCA allows for components with negative values and negative weightings, muscle activation patterns can be reproduced by combining positive and negative signals (Lee and Seung 2001; Ting and Chvatal 2011). Whereas motoneurons receive both excitatory and inhibitory inputs, motoneurons themselves can only generate positive activations of muscles in an all-or-none response pattern (Latash 2008). Moreover, an inhibitory effect of motor output can only be seen if there is a sufficient amount of background activity (i.e. when motoneurons are not quiescent) (Ting and Chvatal 2011). As opposed to PCA, NNMF only allows for positive data and produces only positive components and weightings. Thus, NNMF is particularly suited to study muscle activation, as muscle actions are only positive. However, NNMF cannot reveal the neural inhibition of muscle activity due to non-negative constraints. While NNMF has still proven useful in studies of tasks with minimal inhibition including postural control (Chvatal et al. 2011; Torres-Oviedo and Ting 2007), locomotion (Chvatal 2011; Clark et al. 2010), and reaching movements (d'Avella et al. 2008; d'Avella et al. 2011), the fact that neural inhibition cannot be directly addressed may limit the generalization of NNMF to more complex motor tasks. Compared to PCA, the non-negative constraints of NNMF result in more intuitive, parts-based representations of data (Ting and Chvatal 2011). This fact has been demonstrated in reproducing images of faces (Lee and Seung 1999):

components identified by PCA resemble whole faces, some of which are difficult to recognize due to positive and negative values, whereas components identified by NNMF resemble only salient parts of faces (i.e. ears, noses, eyes, etc.). However, NNMF is not well suited for data with negative values, particularly kinetics and kinematics. For NNMF to be applied with kinetics and kinematics, the data need to be separated into positive and negative components, resulting in discontinuities at zero and an increased dimensionality of the data (Chvatal et al. 2011). In these cases, combinations of PCA with independent component analysis (ICA), another parts-based component algorithm, may be better suited to explaining variability among these variables (Tresch et al. 2006; Trumbower et al. 2010), although recent evidence suggests that component analyses on kinematic space are greatly dependent on the coordinate system used (Hogan and Sternad 2011).

While NNMF may be advantageous for identifying structure in muscle coordination, it may not completely reflect the hypothesized neural structures underlying muscle activity due to methodological limitations. In order to implement NNMF, the only assumptions are that linear combinations can reproduce the original dataset (Ting and Chvatal 2011; Tresch et al. 2006); there are thus no constraints on causality or normality. However unlike PCA, NNMF does not reveal a unique solution every time it is run because it starts with a random set of components and iteratively improves on them to minimize error (Ting and Chvatal 2011). While the components identified from NNMF are often similar after repeated runs, solutions that are observed with high frequency may not be the solution with the least error. This poses a problem with uniformity (Tangirala et al. 2007), and many different adaptations of NNMF are being used to improve performance of the algorithm in specific applications (Fevotte et al. 2009; O'Grady and

Pearlmutter 2008). While it has been shown that PCA and NNMF give similar muscular compositions of muscle synergies (Tresch et al. 2006), the fact that NNMF doesn't yield a unique solution may be a barrier in the future to accurately and precisely describing muscle coordination patterns.

Lastly, there are a number of practical barriers to the clinical application of muscle synergy analysis. First and foremost, it is necessary to demonstrate changes in muscle synergy number, structure, and/or recruitment in pathologic populations before muscle synergy analysis could become useful in a clinical setting. While some groups have already begun to investigate changes in muscle synergies in stroke (Cheung et al. 2009; Clark et al. 2010), there are a variety of motor disorders that these analyses could be applied to. Unfortunately, muscle synergy analysis requires a high degree of EMG variability, which is usually accomplished by having subjects perform many trials of a task. Because patients with motor deficits fatigue quicker than those without deficits, novel approaches may need to be developed to acquire EMG variability in smaller time frames. In addition to time constraints, clinicians face budget constraints and would be equally benefitted by administering tasks that do not require expensive equipment. Because I have demonstrated that SF muscle synergies can be consistently and continuously recruited in response to task-level goals, by designing an appropriate task, it may be possible to quickly and economically evaluate a patient's muscle synergy profile.

APPENDIX A: SUPPLEMENTAL FIGURES
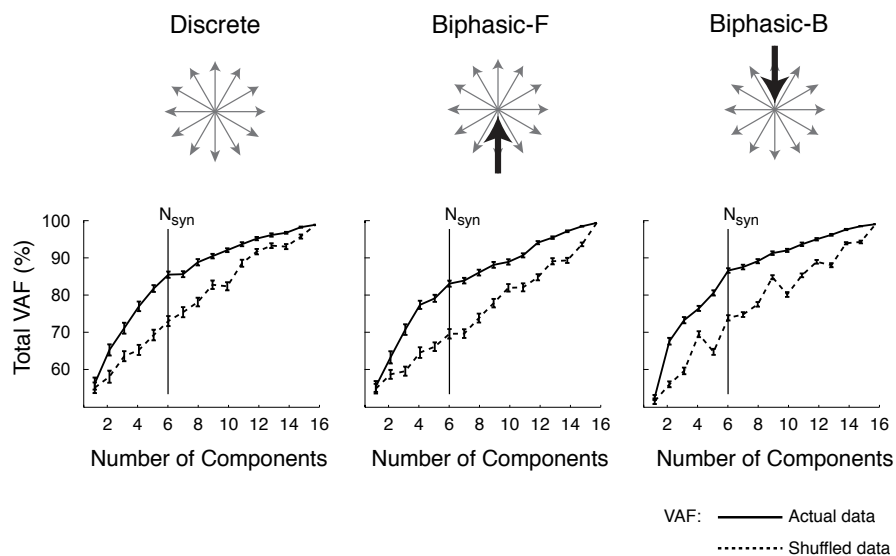
Figure A.1. Variability accounted for (VAF) of SF muscle synergies across perturbation types using actual versus shuffled data. Six SF muscle synergies were identified in all perturbation types. SF muscle synergy extractions from actual data accounted for significantly more variability than with SF muscle synergies extracted from shuffled data. On average, the lower limit of the 95% confidence interval (CI) for total VAF of SF muscle synergies extracted from actual data was 7.3 CIs higher than the upper limit of the 95% CI of SF muscle synergies extracted from shuffled data. Error bars represent the estimated 95% confidence interval of VAF.
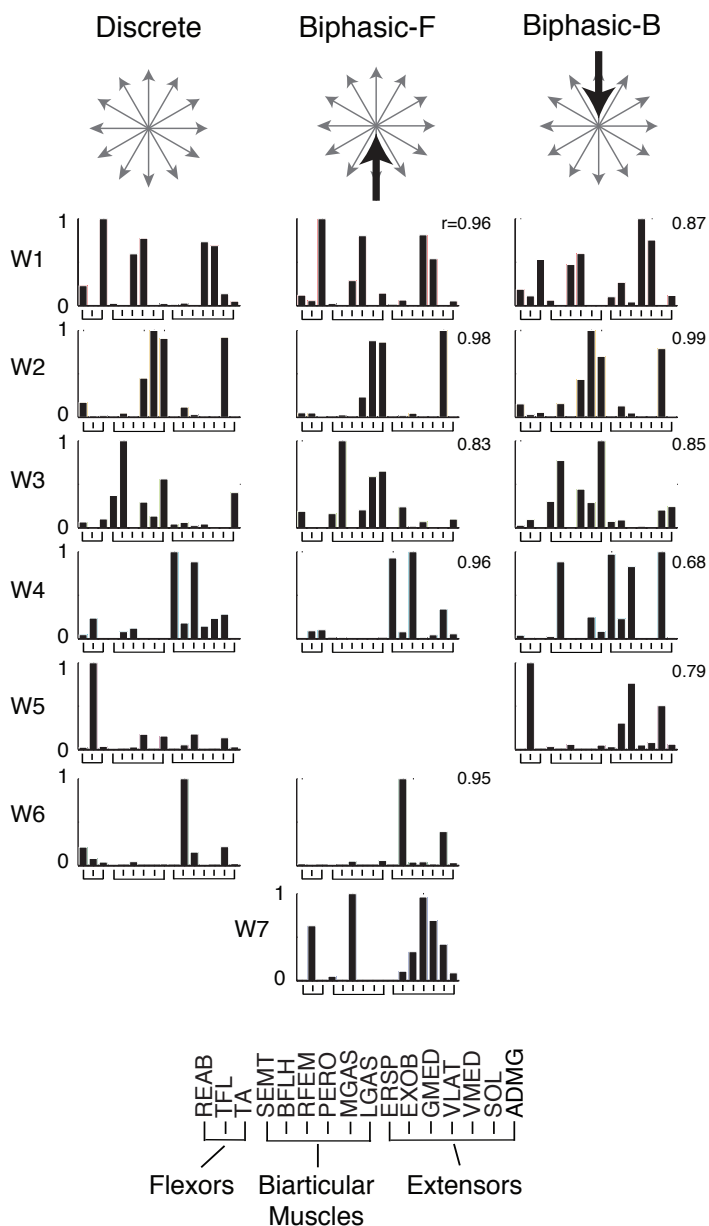
Figure A.2. Consistency of SF muscle synergy structure across perturbation types. Six SF muscle synergies were identified for a representative subject (subject 11) in discrete perturbations. Five of six SF muscle synergies identified in forward biphasic perturbations were similar to discrete perturbations. All SF muscle synergies identified in backward biphasic perturbations were similar to discrete perturbations. For each subject, 4-7 SF muscle synergies were consistent across perturbation types at p < 0.01 (0.65 ≤ r ≤ 0.99, r + 0.87 ± 0.10). Only 1-2 SF muscle synergies per subject were not consistent across perturbation epochs; these muscle synergies consisted mainly of muscles REAB, EXOB, GMEG and ERSP, all of which had actions at the trunk.
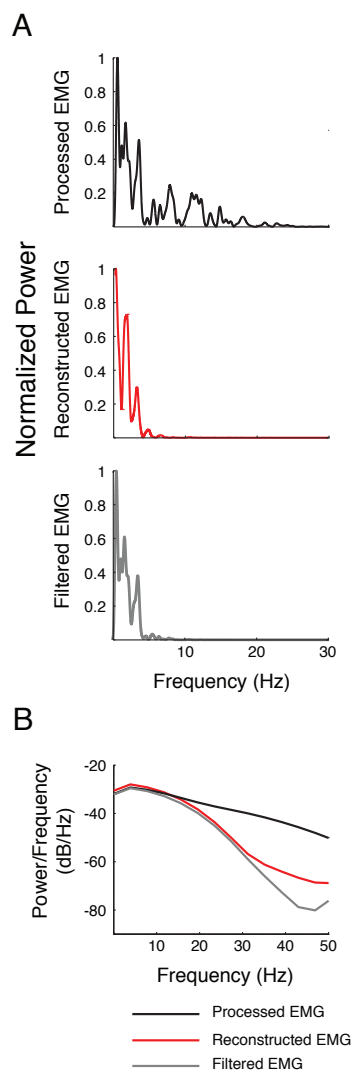
Figure A.3. Frequency content of recorded EMG, reconstructed EMG, and filtered EMG. A, power spectra for EMG signals. Power spectra were normalized to the power of the fundamental frequency. The power spectrum of reconstructed EMG (red) more closely matched the power spectrum of EMG low pass filtered at 20 Hz (grey) than the recorded EMG signal. **B,** power spectral density for EMG signals. For frequencies below 30 Hz, the spectral density of reconstructed EMG (red) was very similar to that of 20 Hz low pass filtered EMG.

REFERENCES

Alexandrov A, Frolov A, and Massion J. Axial synergies during human upper trunk bending. *Experimental Brain Research* 118: 210-220, 1998.

Allum JH, Carpenter MG, and Honegger F. Directional aspects of balance corrections in man. *IEEE Eng Med Biol Mag* 22: 37-47, 2003.

Bengtsson SL, Nagy Z, Skare S, Forsman L, Forssberg H, and Ullen F. Extensive piano practicing has regionally specific effects on white matter development. *Nat Neurosci* 8: 1148-1150, 2005.

Berg K, and Norman KE. Functional assessment of balance and gait. *Clin Geriatr Med* 12: 705-723, 1996.

Berg K, Wood-Dauphinee S, and Williams JI. The Balance Scale: reliability assessment with elderly residents and patients with an acute stroke. *Scand J Rehabil Med* 27: 27-36, 1995.

Berniker M, Jarc A, Bizzi E, and Tresch MC. Simplified and effective motor control based on muscle synergies to exploit musculoskeletal dynamics. *Proc Natl Acad Sci U S A* 106: 7601-7606, 2009.

Bernstein N. *The Coordination and Regulation of Movements*. New York: Pergamon Press, 1967.

Bingham JT, Choi JT, and Ting LH. Stability in a frontal plane model of balance requires coupled changes to postural configuration and neural feedback control. *J Neurophysiol* 106: 437-448, 2011.

Bizzi E, Mussa-Ivaldi FA, and Giszter SF. Computations Underlying the Execution of Movement: A biological Perspective. 287-291, 1991.

Bonasera SJ, and Nichols TR. Mechanical actions of heterogenic reflexes among ankle stabilizers and their interactions with plantarflexors of the cat hindlimb. *J Neurophysiol* 75: 2050-2070, 1996.

Bosco G, and Poppele RE. Proprioception from a spinocerebellar perspective. *Physiol Rev* 81: 539-568, 2001.

Bosco G, Rankin AM, and Poppele RE. Representation of passive hindlimb postures in cat spinocerebellar activity. *J Neurophysiol* 76: 715-726, 1996.

Bourbonnais D, Vandennoven S, Carey KM, and Rymer WZ. Abnormal Spatial Patterns of Elbow Muscle Activation in Hemiparetic Human-Subjects. *Brain* 112: 85-102, 1989.

Brown G. On the nature of the fundamental activity of the nervous centres; together with an analysis of the conditioning of rhythmic activity in progression, and a theory of the evolution of function in the nervous system. *J Physiol* 24-46, 1914.

Brown LA, Jensen JL, Korff T, and Woollacott MH. The translating platform paradigm: perturbation displacement waveform alters the postural response. *Gait Posture* 14: 256-263, 2001.

Buchanan JJ, and Horak FB. Transitions in a postural task: do the recruitment and suppression of degrees of freedom stabilize posture? *Experimental Brain Research* 139: 482-494, 2001.

Bunderson NE, Burkholder TJ, and Ting LH. Reduction of neuromuscular redundancy for postural force generation using an intrinsic stability criterion. *J Biomech* 2008.

Bunderson NE, McKay JL, Ting LH, and Burkholder TJ. Directional constraint of endpoint force emerges from hindlimb anatomy. *J Exp Biol* 213: 2131-2141, 2010.

Burleigh AL, Horak FB, and Malouin F. Modification of postural responses and step initiation: evidence for goal-directed postural interactions. *J Neurophysiol* 72: 2892-2902, 1994.

Camicioli R, Panzer VP, and Kaye J. Balance in the healthy elderly: posturography and clinical assessment. *Arch Neurol* 54: 976-981, 1997.

Campbell KS, and Moss RL. History-dependent mechanical properties of permeabilized rat soleus muscle fibers. *Biophys J* 82: 929-943, 2002.

Campbell KS, and Moss RL. A thixotropic effect in contracting rabbit psoas muscle: prior movement reduces the initial tension response to stretch. *J Physiol* 525 Pt 2: 531-548, 2000.

Cappellini G, Ivanenko YP, Poppele RE, and Lacquaniti F. Motor patterns in human walking and running. *Journal of Neurophysiology* 95: 3426-3437, 2006.

Carpenter MG, Allum JHJ, and Honegger F. Directional sensitivity of stretch reflexes and balance corrections for normal subjects in the roll and pitch planes. *Experimental Brain Research* 129: 93-113, 1999.

Carpenter MG, Thorstensson A, and Cresswell AG. Deceleration affects anticipatory and reactive components of triggered postural responses. *Exp Brain Res* 167: 433-445, 2005.

Cattaneo D, De Nuzzo C, Fascia T, Macalli M, Pisoni I, and Cardini R. Risks of falls in subjects with multiple sclerosis. *Arch Phys Med Rehabil* 83: 864-867, 2002.

CDC. Injury Prevention and Control: Data & Statistics (WISQARS) http://www.cdc.gov/injury/wisqars/index.html.

Chen J, Woollacott M, and Pologe S. Accuracy and underlying mechanisms of shifting movements in cellists. *Exp Brain Res* 174: 467-476, 2006.

Cheung VC, d'Avella A, Tresch MC, and Bizzi E. Central and sensory contributions to the activation and organization of muscle synergies during natural motor behaviors. *J Neurosci* 25: 6419-6434, 2005.

Cheung VC, Piron L, Agostini M, Silvoni S, Turolla A, and Bizzi E. Stability of muscle synergies for voluntary actions after cortical stroke in humans. *Proc Natl Acad Sci U S A* 106: 19563-19568, 2009.

Chvatal SA. Muscle synergies for directional control of center of mass in various postural strategies. In: *Wallace H Coulter Department of Biomedical Engineering*. Atlanta: Georgia Institute of Technology, 2011, p. 223.

Chvatal SA, Torres-Oviedo G, Safavynia SA, and Ting LH. Common muscle synergies for control of center of mass and force in non-stepping and stepping postural behaviors. *J Neurophysiol* 106: 999-1015, 2011.

Clark DJ, Ting LH, Zajac FE, Neptune RR, and Kautz SA. Merging of healthy motor modules predicts reduced locomotor performance and muscle coordination complexity post-stroke. *J Neurophysiol* 103: 844-857, 2010.

Collins JJ, and De Luca CJ. Open-loop and closed-loop control of posture: a random-walk analysis of center-of-pressure trajectories. *Exp Brain Res* 95: 308-318, 1993.

Collins JJ, and De Luca CJ. Random walking during quiet standing. *Physical Review Letters* 73: 764-767, 1994.

Cordo PJ, Flores-Vieira C, Verschueren SM, Inglis JT, and Gurfinkel V. Position sensitivity of human muscle spindles: single afferent and population representations. *J Neurophysiol* 87: 1186-1195, 2002.

Corna S, Tarantola J, Nardone A, Giordano A, and Schieppati M. Standing on a continuously moving platform: is body inertia counteracted or exploited? *Exp Brain Res* 124: 331-341, 1999.

Crago PE, Houk JC, and Hasan Z. Regulatory actions of human stretch reflex. *J Neurophysiol* 39: 925-935, 1976.

Creath R, Kiemel T, Horak F, Peterka R, and Jeka J. A unified view of quiet and perturbed stance: simultaneous co-existing excitable modes. *Neurosci Lett* 377: 75-80, 2005.

Cruz TH, and Dhaher YY. Evidence of abnormal lower-limb torque coupling after stroke: an isometric study. *Stroke* 39: 139-147, 2008.

d'Avella A, and Bizzi E. Shared and specific muscle synergies in natural motor behaviors. *Proc Natl Acad Sci U S A* 102: 3076-3081, 2005.

d'Avella A, Fernandez L, Portone A, and Lacquaniti F. Modulation of phasic and tonic muscle synergies with reaching direction and speed. *J Neurophysiol* 100: 1433-1454, 2008.

d'Avella A, Portone A, Fernandez L, and Lacquaniti F. Control of fast-reaching movements by muscle synergy combinations. *J Neurosci* 26: 7791-7810, 2006.

d'Avella A, Portone A, and Lacquaniti F. Superposition and modulation of muscle synergies for reaching in response to a change in target location. *J Neurophysiol* 106: 2796-2812, 2011.

De Nunzio AM, Nardone A, and Schieppati M. Head stabilization on a continuously oscillating platform: the effect of a proprioceptive disturbance on the balancing strategy. *Exp Brain Res* 165: 261-272, 2005.

Deliagina TG, Beloozerova IN, Zelenin PV, and Orlovsky GN. Spinal and supraspinal postural networks. *Brain Res Rev* 57: 212-221, 2008.

Dewald JP, and Beer RF. Abnormal joint torque patterns in the paretic upper limb of subjects with hemiparesis. *Muscle Nerve* 24: 273-283, 2001.

Dewald JP, Pope PS, Given JD, Buchanan TS, and Rymer WZ. Abnormal muscle coactivation patterns during isometric torque generation at the elbow and shoulder in hemiparetic subjects. *Brain* 118 (Pt 2): 495-510, 1995.

Diener HC, Bootz F, Dichgans J, and Bruzek W. Variability of postural "reflexes" in humans. *Exp Brain Res* 52: 423-428, 1983.

Diener HC, and Dichgans J. On the role of vestibular, visual and somatosensory information for dynamic postural control in humans. *Prog Brain Res* 76: 253-262, 1988.

Diener HC, Dichgans J, Bootz F, and Bacher M. Early stabilization of human posture after a sudden disturbance: influence of rate and amplitude of displacement. *Exp Brain Res* 56: 126-134, 1984.

Dietz V, Quintern J, and Berger W. Corrective reactions to stumbling in man: functional significance of spinal and transcortical reflexes. *Neurosci Lett* 44: 131-135, 1984.

Dietz V, and Sinkjaer T. Spastic movement disorder: impaired reflex function and altered muscle mechanics. *Lancet Neurol* 6: 725-733, 2007.

Drew T, Kalaska J, and Krouchev N. Muscle synergies during locomotion in the cat: a model for motor cortex control. *J Physiol* 586: 1239-1245, 2008.

Eccles JC. The inhibitory control of spinal reflex action. *Electroen Clin Neuro* Suppl 25:20-34, 1967.

Fevotte C, Bertin N, and Durrieu JL. Nonnegative matrix factorization with the Itakura-Saito divergence: with application to music analysis. *Neural Comput* 21: 793-830, 2009.

Fugl-Meyer AR. Post-stroke hemiplegia assessment of physical properties. *Scandinavian journal of rehabilitation medicine Supplement* 7: 85-93, 1980.

Gentner R, Gorges S, Weise D, aufm Kampe K, Buttmann M, and Classen J. Encoding of motor skill in the corticomuscular system of musicians. *Curr Biol* 20: 1869-1874, 2010.

Georgopoulos AP, Ashe J, Smyrnis N, and Taira M. The motor cortex and the coding of force. *Science* 256: 1692-1695, 1992.

Georgopoulos AP, Kalaska JF, Caminiti R, and Massey JT. On the Relations between the Direction of Two-Dimensional Arm Movements and Cell Discharge in Primate Motor Cortex. *Journal of Neuroscience* 2: 1527-1537, 1982.

Georgopoulos AP, Schwartz AB, and Kettner RE. Neuronal population coding of movement direction. *Science* 233: 1416-1419, 1986.

Gerbino PG, Griffin ED, and Zurakowski D. Comparison of standing balance between female collegiate dancers and soccer players. *Gait Posture* 26: 501-507, 2007.

Getz EB, Cooke R, and Lehman SL. Phase transition in force during ramp stretches of skeletal muscle. *Biophys J* 75: 2971-2983, 1998.

Gill J, Allum JH, Carpenter MG, Held-Ziolkowska M, Adkin AL, Honegger F, and Pierchala K. Trunk sway measures of postural stability during clinical balance tests: effects of age. *J Gerontol A Biol Sci Med Sci* 56: M438-447, 2001.

Giszter SF, Mussa-Ivaldi FA, and Bizzi E. Convergent force fields organized in the frog's spinal cord. *J Neurosci* 13: 467-491, 1993.

Gizzi L, Nielsen JF, Felici F, Ivanenko YP, and Farina D. Impulses of activation but not motor modules are preserved in the locomotion of subacute stroke patients. *J Neurophysiol* 106: 202-210, 2011.

Gladstone DJ, Danells CJ, and Black SE. The fugl-meyer assessment of motor recovery after stroke: a critical review of its measurement properties. *Neurorehabil Neural Repair* 16: 232-240, 2002.

Gollhofer A, Horstmann GA, Berger W, and Dietz V. Compensation of translational and rotational perturbations in human posture: stabilization of the centre of gravity. *Neurosci Lett* 105: 73-78, 1989.

Gottlieb GL, Chen CH, and Corcos DM. Relations between joint torque, motion, and electromyographic patterns at the human elbow. *Exp Brain Res* 103: 164-167, 1995.

Green AM, Shaikh AG, and Angelaki DE. Sensory vestibular contributions to constructing internal models of self-motion. *J Neural Eng* 2: S164-179, 2005.

Haftel VK, Bichler EK, Nichols TR, Pinter MJ, and Cope TC. Movement reduces the dynamic response of muscle spindle afferents and motoneuron synaptic potentials in rat. *J Neurophysiol* 91: 2164-2171, 2004.

Hart CB, and Giszter SF. Modular Premotor Drives and Unit Bursts as Primitives for Frog Motor Behaviors. *J Neurosci* 24: 5269-5282, 2004.

Hart CB, and Giszter SF. A neural basis for motor primitives in the spinal cord. *J Neurosci* 30: 1322-1336, 2010.

Henry SM, Fung J, and Horak FB. EMG responses to maintain stance during multidirectional surface translations. *Journal of Neurophysiology* 80: 1939-1950, 1998.

Hillman CH, Rosengren KS, and Smith DP. Emotion and motivated behavior: postural adjustments to affective picture viewing. *Biol Psychol* 66: 51-62, 2004.

Hogan N, and Sternad D. Identifying task-dependent synergies with coordinate-free methods. In: *Society for Neuroscience*. Washington, D.C.: Society for Neursocience, 2011.

Honeycutt CF, and Nichols TR. The decerebrate cat generates the essential features of the force constraint strategy. *J Neurophysiol* 103: 3266-3273, 2010a.

Honeycutt CF, and Nichols TR. Disruption of cutaneous feedback alters magnitude but not direction of muscle responses to postural perturbations in the decerebrate cat. *Exp Brain Res* 203: 765-771, 2010b.

Horak F, and Moore SP. The effect of prior leaning on human postural responses. *Gait Posture* 1: 203-210, 1993.

Horak FB, Diener HC, and Nashner LM. Influence of central set on human postural responses. *J Neurophysiol* 62: 841-853, 1989.

Horak FB, Earhart GM, and Dietz V. Postural responses to combinations of head and body displacements: vestibular-somatosensory interactions. *Exp Brain Res* 141: 410-414, 2001.

Horak FB, Henry SM, and Shumway-Cook A. Postural perturbations: new insights for treatment of balance disorders. *Phys Ther* 77: 517-533, 1997.

Horak FB, and Macpherson JM. Postural orientation and equilibrium. In: *Handbook of Physiology, Section 12*. New York: American Physiological Society, 1996, p. 255-292.

Hubel DH, and Wiesel TN. Receptive fields, binocular interaction and functional architecture in the cat's visual cortex. *J Physiol* 160: 106-154, 1962.

Hug F, Turpin NA, Couturier A, and Dorel S. Consistency of muscle synergies during pedaling across different mechanical constraints. *J Neurophysiol* 106: 91-103, 2011.

Hwang EJ, Donchin O, Smith MA, and Shadmehr R. A gain-field encoding of limb position and velocity in the internal model of arm dynamics. *Plos Biol* 1: E25, 2003.

Ivanenko YP, Cappellini G, Dominici N, Poppele RE, and Lacquaniti F. Coordination of locomotion with voluntary movements in humans. *J Neurosci* 25: 7238-7253, 2005.

Ivanenko YP, Grasso R, Zago M, Molinari M, Scivoletto G, Castellano V, Macellari V, and Lacquaniti F. Temporal components of the motor patterns expressed by the human spinal cord reflect foot kinematics. *Journal of Neurophysiology* 90: 3555-3565, 2003.

Ivanenko YP, Poppele RE, and Lacquaniti E. Five basic muscle activation patterns account for muscle activity during human locomotion. *Journal of Physiology-London* 556: 267-282, 2004.

Jackson JH. On the comparative study of diseases of the nervous system. *The British Medical Journal* 2: 355-362, 1889.

Jacobs JV, and Horak FB. Cortical control of postural responses. *J Neural Transm* 114: 1339-1348, 2007.

Jacobs R, and Macpherson JM. Two functional muscle groupings during postural equilibrium tasks in standing cats. *Journal Of Neurophysiology* 76: 2402-2411, 1996.

Jankowska E. Interneuronal relay in spinal pathways from proprioceptors. *Prog Neurobiol* 38: 335-378, 1992.

Kargo WJ, and Giszter SF. Rapid correction of aimed movements by summation of force-field primitives. *J Neurosci* 20: 409-426, 2000.

Kargo WJ, Ramakrishnan A, Hart CB, Rome LC, and Giszter SF. A simple experimentally based model using proprioceptive regulation of motor primitives captures adjusted trajectory formation in spinal frogs. *J Neurophysiol* 103: 573-590, 2010.

Keshner EA, Allum JH, and Pfaltz CR. Postural coactivation and adaptation in the sway stabilizing responses of normals and patients with bilateral vestibular deficit. *Exp Brain Res* 69: 77-92, 1987.

Kluzik J, Horak FB, and Peterka RJ. Differences in preferred reference frames for postural orientation shown by after-effects of stance on an inclined surface. *Exp Brain Res* 162: 474-489, 2005.

Krishnamoorthy V, Latash ML, Scholz JP, and Zatsiorsky VM. Muscle modes during shifts of the center of pressure by standing persons: effect of instability and additional support. *Experimental Brain Research* 157: 18-31, 2004.

Krishnamoorthy V, Latash ML, Scholz JP, and Zatsiorsky VM. Muscle synergies during shifts of the center of pressure by standing persons. *Experimental Brain Research* 152: 281-292, 2003.

Krouchev N, Kalaska JF, and Drew T. Sequential activation of muscle synergies during locomotion in the intact cat as revealed by cluster analysis and direct decomposition. *J Neurophysiol* 96: 1991-2010, 2006.

Kung UM, Horlings CG, Honegger F, Duysens JE, and Allum JH. Control of roll and pitch motion during multi-directional balance perturbations. *Exp Brain Res* 194: 631-645, 2009.

Kuo AD. An optimal control model for analyzing human postural balance. *IEEE Trans Biomed Eng* 42: 87-101, 1995.

Kuo AD. The relative roles of feedforward and feedback in the control of rhythmic movements. *Motor Control* 6: 129-145, 2002.

Kuo AD, and Zajac FE. A biomechanical analysis of muscle strength as a limiting factor in standing posture. *J Biomech* 26 Suppl 1: 137-150, 1993.

Kurtzer I, Pruszynski JA, Herter TM, and Scott SH. Primate upper limb muscles exhibit activity patterns that differ from their anatomical action during a postural task. *J Neurophysiol* 95: 493-504, 2006.

Kurtzer IL, Pruszynski JA, and Scott SH. Long-latency reflexes of the human arm reflect an internal model of limb dynamics. *Curr Biol* 18: 449-453, 2008.

Kutch JJ, Kuo AD, Bloch AM, and Rymer WZ. Endpoint force fluctuations reveal flexible rather than synergistic patterns of muscle cooperation. *J Neurophysiol* 100: 2455-2471, 2008.

Kwakkel G. Towards integrative neurorehabilitation science. *Physiother Res Int* 14: 137-146, 2009.

Lam T, Anderschitz M, and Dietz V. Contribution of feedback and feedforward strategies to locomotor adaptations. *J Neurophysiol* 95: 766-773, 2006.

Latash ML. *Neurophysiological basis of movement*. Urbana, IL: Human Kinetics, 2008.

Latash ML, Scholz JF, Danion F, and Schoner G. Finger coordination during discrete and oscillatory force production tasks. *Exp Brain Res* 146: 419-432, 2002.

Laws K. *Physics and the Art of Dance: Understanding Movement*. New York: Oxford, 2002.

Lee DD, and Seung HS. Algorithms for non-negative matrix factorization. *Adv Neural Info Proc Syst* 13: 556-562, 2001.

Lee DD, and Seung HS. Learning the parts of objects by non-negative matrix factorization. *Nature* 401: 788-791, 1999.

Levin MF, Kleim JA, and Wolf SL. What do motor "recovery" and "compensation" mean in patients following stroke? *Neurorehabil Neural Repair* 23: 313-319, 2009.

Liddell EGT, and Sherrington C. Reflexes in response to stretch (myotatic reflexes). *Proc R Soc Lond B* 96: 212-242, 1924.

Lockhart DB, and Ting LH. Optimal sensorimotor transformations for balance. *Nat Neurosci* 10: 1329-1336, 2007.

Loeb GE, Brown IE, and Cheng EJ. A hierarchical foundation for models of sensorimotor control. *Experimental Brain Research* 126: 1-18, 1999.

Lum P, Burgar CG, and Shor PC. Evidence for strength imbalances as a significant contributor to abnormal synergies in hemiparetic subjects. *Muscle & Nerve* 27: 211-221, 2003.

Lundberg A. Multisensory control of spinal reflex pathways. *Prog Brain Res* 50: 11-28, 1979.

Macpherson JM. Strategies that simplify the control of quadrupedal stance. II. Electromyographic activity. *J Neurophysiol* 60: 218-231, 1988.

Macpherson JM, Fung J, and Jacobs R. Postural orientation, equilibrium, and the spinal cord. *Adv Neurol* 72: 227-232, 1997.

Macpherson JM, Horak FB, Dunbar DC, and Dow RS. Stance dependence of automatic postural adjustments in humans. *Exp Brain Res* 78: 557-566, 1989.

Marsden CD, Merton PA, and Morton HB. Human postural responses. *Brain* 104: 513-534, 1981.

Massion J. Postural control system. *Curr Opin Neurobiol* 4: 877-887, 1994.

Matthews PB. Evolving views on the internal operation and functional role of the muscle spindle. *J Physiol* 320: 1-30, 1981.

McCrea DA. Spinal circuitry of sensorimotor control of locomotion. *Journal of Physiology-London* 533: 41-50, 2001.

McCrea DA, and Rybak IA. Organization of mammalian locomotor rhythm and pattern generation. *Brain Res Rev* 57: 134-146, 2008.

McIlroy WE, and Maki BE. The 'deceleration response' to transient perturbation of upright stance. *Neurosci Lett* 175: 13-16, 1994.

McKay JL, and Ting LH. Functional muscle synergies constrain force production during postural tasks. *J Biomech* 41: 299-306, 2008.

Mergner T. A neurological view on reactive human stance control. *Annual Reviews in Control* 34: 177-198, 2010.

Metz GA, Antonow-Schlorke I, and Witte OW. Motor improvements after focal cortical ischemia in adult rats are mediated by compensatory mechanisms. *Behav Brain Res* 162: 71-82, 2005.

Monaco V, Ghionzoli A, and Micera S. Age-related modifications of muscle synergies and spinal cord activity during locomotion. *J Neurophysiol* 104: 2092-2102, 2010.

Moroz A, Bogey RA, Bryant PR, Geis CC, and O'Neill BJ. Stroke and neurodegenerative disorders. 2. Stroke: comorbidities and complications. *Arch Phys Med Rehabil* 85: S11-14, 2004.

Morris S, Morris ME, and Iansek R. Reliability of measurements obtained with the Timed "Up & Go" test in people with Parkinson disease. *Phys Ther* 81: 810-818, 2001.

Muceli S, Boye AT, d'Avella A, and Farina D. Identifying representative synergy matrices for describing muscular activation patterns during multidirectional reaching in the horizontal plane. *J Neurophysiol* 103: 1532-1542, 2010.

Nardone A, Giordano A, Corra T, and Schieppati M. Responses of leg muscles in humans displaced while standing. Effects of types of perturbation and of postural set. *Brain* 113 (Pt 1): 65-84, 1990.

Nashner LM. Adapting reflexes controlling the human posture. *Exp Brain Res* 26: 59-72, 1976.

Nashner LM. Fixed patterns of rapid postural responses among leg muscles during stance. *Exp Brain Res* 30: 13-24, 1977.

Neptune RR, Clark DJ, and Kautz Sa. Modular control of human walking: a simulation study. *Journal of Biomechanics* 42: 1282-1287, 2009.

Nevitt MC, Cummings SR, Kidd S, and Black D. Risk factors for recurrent nonsyncopal falls. A prospective study. *JAMA* 261: 2663-2668, 1989.

Nichols TR. The organization of heterogenic reflexes among muscles crossing the ankle joint in the decerebrate cat. *J Physiol* 410: 463-477, 1989.

Nichols TR. Receptor mechanisms underlying heterogenic reflexes among the triceps surae muscles of the cat. *J Neurophysiol* 81: 467-478, 1999.

Nichols TR, and Cope TC. Cross-bridge mechanisms underlying the history-dependent properties of muscle spindles and stretch reflexes. *Can J Physiol Pharmacol* 82: 569-576, 2004.

Nichols TR, and Houk JC. Improvement in linearity and regulation of stiffness that results from actions of stretch reflex. *J Neurophysiol* 39: 119-142, 1976.

Nielsen JB, Brittain JS, Halliday DM, Marchand-Pauvert V, Mazevet D, and Conway BA. Reduction of common motoneuronal drive on the affected side during walking in hemiplegic stroke patients. *Clin Neurophysiol* 119: 2813-2818, 2008.

Nilsson J, Thorstensson A, and Halbertsma J. Changes in leg movements and muscle activity with speed of locomotion and mode of progression in humans. *Acta Physiol Scand* 123: 457-475, 1985.

Norris JA, Marsh AP, Smith IJ, Kohut RI, and Miller ME. Ability of static and statistical mechanics posturographic measures to distinguish between age and fall risk. *J Biomech* 38: 1263-1272, 2005.

O'Grady PD, and Pearlmutter BA. Discovering speech pnones using convolutive non-negative matrix factorisation with a sparseness constraint. *Neurocomputing* 72: 88-101, 2008.

Overduin SA, d'Avella A, Roh J, and Bizzi E. Modulation of Muscle Synergy Recruitment in Primate Grasping. *J Neurosci* 28: 880-892, 2008.

Pai YC, and Patton J. Center of mass velocity-position predictions for balance control. *J Biomech* 30: 347-354, 1997.

Pai YC, Rogers MW, Patton J, Cain TD, and Hanke TA. Static versus dynamic predictions of protective stepping following waist-pull perturbations in young and older adults. *Journal of biomechanics* 31: 1111-1118, 1998.

Park S, Horak FB, and Kuo AD. Postural feedback responses scale with biomechanical constraints in human standing. *Exp Brain Res* 154: 417-427, 2004.

Pearson KG, and Collins DF. Reversal of the influence of group Ib afferents from plantaris on activity in medial gastrocnemius muscle during locomotor activity. *J Neurophysiol* 70: 1009-1017, 1993.

Peterka RJ. Postural control model interpretation of stabilogram diffusion analysis. *Biol Cybern* 82: 335-343, 2000.

Peterka RJ. Sensorimotor integration in human postural control. *J Neurophysiol* 88: 1097-1118, 2002.

Poppele RE, Bosco G, and Rankin AM. Independent representations of limb axis length and orientation in spinocerebellar response components. *J Neurophysiol* 87: 409-422, 2002.

Poppele RE, Rankin A, and Eian J. Dorsal spinocerebellar tract neurons respond to contralateral limb stepping. *Exp Brain Res* 149: 361-370, 2003.

Prochazka A. Chapter 3: Proprioceptive Feedback and Movement Regulation. In: *Handbook of Physiology*1996.

Pruszynski JA, Kurtzer I, and Scott SH. The long-latency reflex is composed of at least two functionally independent processes. *J Neurophysiol* 106: 449-459, 2011.

Raghavan P, Santello M, Gordon AM, and Krakauer JW. Compensatory motor control after stroke: an alternative joint strategy for object-dependent shaping of hand posture. *J Neurophysiol* 103: 3034-3043, 2010.

Rathelot JA, and Strick PL. Subdivisions of primary motor cortex based on cortico-motoneuronal cells. *Proc Natl Acad Sci U S A* 106: 918-923, 2009.

Reisman DS, Block HJ, and Bastian AJ. Interlimb coordination during locomotion: what can be adapted and stored? *J Neurophysiol* 94: 2403-2415, 2005.

Richardson JK, and Hurvitz EA. Peripheral neuropathy: a true risk factor for falls. *J Gerontol A Biol Sci Med Sci* 50: M211-215, 1995.

Roh J, Cheung VC, and Bizzi E. Modules in the brain stem and spinal cord underlying motor behaviors. *J Neurophysiol* 106: 1363-1378, 2011.

Rossignol S, Chau C, Brustein E, Belanger M, Barbeau H, and Drew T. Locomotor capacities after complete and partial lesions of the spinal cord. *Acta Neurobiol Exp (Wars)* 56: 449-463, 1996.

Runge CF, Shupert CL, Horak FB, and Zajac FE. Ankle and hip postural strategies defined by joint torques. *Gait Posture* 10: 161-170, 1999.

Safavynia SA, and Ting LH. A common feedabck model can explain long-latency reflexes of the human leg throughout discrete and continuous perturbations. in prep.

Safavynia SA, and Ting LH. Task-level feedback can explain temporal recruitment of spatially-fixed muscle synergies throughout postural perturbations. *J Neurophysiol* 107: 159-177, 2012.

Saltiel P, Wyler-Duda K, D'Avella A, Tresch MC, and Bizzi E. Muscle synergies encoded within the spinal cord: evidence from focal intraspinal NMDA iontophoresis in the frog. *J Neurophysiol* 85: 605-619, 2001.

Schepens B, Stapley P, and Drew T. Neurons in the pontomedullary reticular formation signal posture and movement both as an integrated behavior and independently. *J Neurophysiol* 100: 2235-2253, 2008.

Schmidt RF. Motor systems. In: *Human Physiology*, edited by Schmidt RF, and Thews G. Berlin: Springer, 1983, p. 81-110.

Scholz J, Klein MC, Behrens TE, and Johansen-Berg H. Training induces changes in white-matter architecture. *Nat Neurosci* 12: 1370-1371, 2009.

Scholz JP, and Schoner G. The uncontrolled manifold concept: identifying control variables for a functional task. *Exp Brain Res* 126: 289-306, 1999.

Scott SH. Optimal feedback control and the neural basis of volitional motor control. *Nature Reviews Neuroscience* 5: 534-546, 2004.

Scott SH, and Kalaska JF. Reaching movements with similar hand paths but different arm orientations. I. Activity of individual cells in motor cortex. *J Neurophysiol* 77: 826-852, 1997.

Sergio LE, and Kalaska JF. Systematic changes in directional tuning of motor cortex cell activity with hand location in the workspace during generation of static isometric forces in constant spatial directions. *J Neurophysiol* 78: 1170-1174, 1997.

Shumway-Cook A, and Woollacott M. Attentional demands and postural control: the effect of sensory context. *J Gerontol A Biol Sci Med Sci* 55: M10-16, 2000.

Sinkjaer T, Andersen JB, and Larsen B. Soleus stretch reflex modulation during gait in humans. *J Neurophysiol* 76: 1112-1120, 1996.

Sitburana O, and Jankovic J. Focal hand dystonia, mirror dystonia and motor overflow. *J Neurol Sci* 266: 31-33, 2008.

Sohn YH, and Hallett M. Disturbed surround inhibition in focal hand dystonia. *Ann Neurol* 56: 595-599, 2004.

Stahl VA, and Nichols TR. Short-term effects of muscular denervation and fasciotomy on global limb variables during locomotion in the decerebrate cat. *Cells Tissues Organs* 193: 325-335, 2011.

Stapley PJ, and Drew T. The pontomedullary reticular formation contributes to the compensatory postural responses observed following removal of the support surface in the standing cat. *J Neurophysiol* 101: 1334-1350, 2009.

Stapley PJ, Ting LH, Hulliger M, and Macpherson JM. Automatic postural responses are delayed by pyridoxine-induced somatosensory loss. *J Neurosci* 22: 5803-5807, 2002.

Stapley PJ, Ting LH, Kuifu C, Everaert DG, and Macpherson JM. Bilateral vestibular loss leads to active destabilization of balance during voluntary head turns in the standing cat. *J Neurophysiol* 95: 3783-3797, 2006.

Stevens JA. Falls among older adults--risk factors and prevention strategies. *J Safety Res* 36: 409-411, 2005.

Szturm T, and Fallang B. Effects of varying acceleration of platform translation and toes-up rotations on the pattern and magnitude of balance reactions in humans. *J Vestib Res* 8: 381-397, 1998.

Tangirala AK, Kanodia J, and Shah SL. Applications of non-negative matrix factorization to plant-wide oscillation detection and diagnosis. *Industrial and Engineering Chemistry Research* 46: 801-817, 2007.

Taube W, Schubert M, Gruber M, Beck S, Faist M, and Gollhofer A. Direct corticospinal pathways contribute to neuromuscular control of perturbed stance. *Journal of Applied Physiology* 01447.02005, 2006.

Tinetti ME. Clinical practice. Preventing falls in elderly persons. *N Engl J Med* 348: 42-49, 2003.

Ting LH. Dimensional reduction in sensorimotor systems: a framework for understanding muscle coordination of posture. *Prog Brain Res* 165: 299-321, 2007.

Ting LH, and Chvatal SA. Decomposing muscle activity in motor tasks: methods and interpretation. In: *Motor control: theories, experiments, and applications*, edited by Danion F, and Latash MLOxford, 2011, p. 102-138.

Ting LH, and Macpherson JM. A limited set of muscle synergies for force control during a postural task. *J Neurophysiol* 93: 609-613, 2005.

Ting LH, and Macpherson JM. Ratio of shear to load ground-reaction force may underlie the directional tuning of the automatic postural response to rotation and translation. *J Neurophysiol* 92: 808-823, 2004.

Ting LH, and McKay JL. Neuromechanics of muscle synergies for posture and movement. *Curr Opin Neurobiol* 17: 622-628, 2007.

Todorov E. Optimality principles in sensorimotor control. *Nat Neurosci* 7: 907-915, 2004.

Torres-Oviedo G, Macpherson JM, and Ting LH. Muscle synergy organization is robust across a variety of postural perturbations. *J Neurophysiol* 96: 1530-1546, 2006.

Torres-Oviedo G, and Ting LH. Muscle synergies characterizing human postural responses. *J Neurophysiol* 98: 2144-2156, 2007.

Torres-Oviedo G, and Ting LH. Subject-specific muscle synergies in human balance control are consistent across different biomechanical contexts. *J Neurophysiol* 103: 3084-3098, 2010.

Tresch MC, and Bizzi E. Responses to spinal microstimulation in the chronically spinalized rat and their relationship to spinal systems activated by low threshold cutaneous stimulation. *Experimental Brain Research* 129: 401-416, 1999.

Tresch MC, Cheung VC, and d'Avella A. Matrix factorization algorithms for the identification of muscle synergies: evaluation on simulated and experimental data sets. *J Neurophysiol* 95: 2199-2212, 2006.

Tresch MC, and Jarc A. The case for and against muscle synergies. *Curr Opin Neurobiol* 19: 601-607, 2009.

Tresch MC, Saltiel P, and Bizzi E. The construction of movement by the spinal cord. *Nat Neurosci* 2: 162-167, 1999.

Trivedi H, Leonard JA, Ting LH, and Stapley PJ. Postural responses to unexpected perturbations of balance during reaching. *Exp Brain Res* 202: 485-491, 2010.

Trumbower RD, Ravichandran VJ, Krutky MA, and Perreault EJ. Contributions of altered stretch reflex coordination to arm impairments following stroke. *J Neurophysiol* 104: 3612-3624, 2010.

Tsang WW, and Hui-Chan CW. Comparison of muscle torque, balance, and confidence in older tai chi and healthy adults. *Med Sci Sports Exerc* 37: 280-289, 2005.

Turton A, Fraser C, Flament D, Werner W, Bennett KMB, and Lemon RN. Organization of cortico-motoneuronal projections from the primary motor cortex: evidence for task-related function in monkey and man. In: *Spasticity - Mechanisms and Management*, edited by Thilmann A, Burke DJ, and W.Z. R. Berlin, Heidelberg: Springer-Verlag, 1993, p. 8-24.

Valero-Cuevas FJ, Venkadesan M, and Todorov E. Structured variability of muscle activations supports the minimal intervention principle of motor control. *J Neurophysiol* 102: 59-68, 2009.

van Antwerp KW, Burkholder TJ, and Ting LH. Inter-joint coupling effects on muscle contributions to endpoint force and acceleration in a musculoskeletal model of the cat hindlimb. *J Biomech* 40: 3570-3579, 2007.

Van de Warrenburg BP, Bakker M, Kremer BP, Bloem BR, and Allum JH. Trunk sway in patients with spinocerebellar ataxia. *Mov Disord* 20: 1006-1013, 2005.

van der Kooij H, and de Vlugt E. Postural Responses Evoked by Platform Pertubations Are Dominated by Continuous Feedback. *J Neurophysiol* 98: 730-743, 2007.

van der Steen MM, and Bongers RM. Joint angle variability and co-variation in a reaching with a rod task. *Exp Brain Res* 208: 411-422, 2011.

Weber DJ, Stein RB, Everaert DG, and Prochazka A. Limb-state feedback from ensembles of simultaneously recorded dorsal root ganglion neurons. *J Neural Eng* 4: S168-180, 2007.

Weinstein JM, Balaban CD, and VerHoeve JN. Directional tuning of the human presaccadic spike potential. *Brain Res* 543: 243-250, 1991.

Welch TD, and Ting LH. A feedback model explains the differential scaling of human postural responses to perturbation acceleration and velocity. *J Neurophysiol* 101: 3294-3309, 2009.

Welch TD, and Ting LH. A feedback model reproduces muscle activity during human postural responses to support-surface translations. *J Neurophysiol* 99: 1032-1038, 2008.

Winter DA. *Biomechanics and Motor Control of Human Movement*. Hoboken: John Wiley & Sons, 2005.

Winter DA, and Yack HJ. EMG profiles during normal human walking: stride-to-stride and inter-subject variability. *Electroencephalogr Clin Neurophysiol* 67: 402-411, 1987.

Wolf SL, Barnhart HX, Kutner NG, McNeely E, Coogler C, and Xu T. Reducing frailty and falls in older persons: an investigation of Tai Chi and computerized balance training. Atlanta FICSIT Group. Frailty and Injuries: Cooperative Studies of Intervention Techniques. *J Am Geriatr Soc* 44: 489-497, 1996.

Woodbury ML, Howland DR, McGuirk TE, Davis SB, Senesac CR, Kautz S, and Richards LG. Effects of trunk restraint combined with intensive task practice on poststroke upper extremity reach and function: a pilot study. *Neurorehabil Neural Repair* 23: 78-91, 2009.

Woollacott M, and Shumway-Cook A. Attention and the control of posture and gait: a review of an emerging area of research. *Gait Posture* 16: 1-14, 2002.

Yakovenko S, Krouchev N, and Drew T. Sequential activation of motor cortical neurons contributes to intralimb coordination during reaching in the cat by modulating muscle synergies. *J Neurophysiol* 105: 388-409, 2011.

Yen JT, Auyang AG, and Chang YH. Joint-level kinetic redundancy is exploited to control limb-level forces during human hopping. *Exp Brain Res* 196: 439-451, 2009.

Zajac FE, and Gordon ME. Determining muscle's force and action in multi-articular movement. *Exerc Sport Sci Rev* 17: 187-230, 1989.

Zar JH. *Biostatistical Analysis*. Upper Saddle River, NJ: Prentice-Hall, 1999, p. 663.